TION TOP AND BOTTOM

	UNCLASSIFIED		CONFIDENTIAL		SECRET

OFFICIAL ROUTING SLIP

TO	NAME AND ADDRESS	DATE	INITIALS
1	[redacted]		STAT
2			
3			
4			
5			
6			

	ACTION		DIRECT REPLY		PREPARE REPLY
	APPROVAL		DISPATCH		RECOMMENDATION
	COMMENT		FILE		RETURN
	CONCURRENCE	/	INFORMATION		SIGNATURE

Remarks:

CORNING CONTRACT ENDED 6/30/70. ATTACHED FINAL REPORT RECEIVED IN EARLY SEPTEMBER. DELAY DUE TO CORNING INTERNAL ADMINISTRATIVE PROCEDURES — HOME OFFICE MUST APPROVE ALL FINAL REPORTS.

FOLD HERE TO RETURN TO SENDER

FROM: NAME, ADDRESS AND PHONE NO.	DATE
[redacted]	10/19 STAT

	UNCLASSIFIED		CONFIDENTIAL		SECRET

GPO : 1968 O - 297-542

FINAL TECHNICAL REPORT

IMPROVED SCREEN FOR
REAR-PROJECTION VIEWERS

JULY 17, 1970

Electronics Research

File copy
99706-5

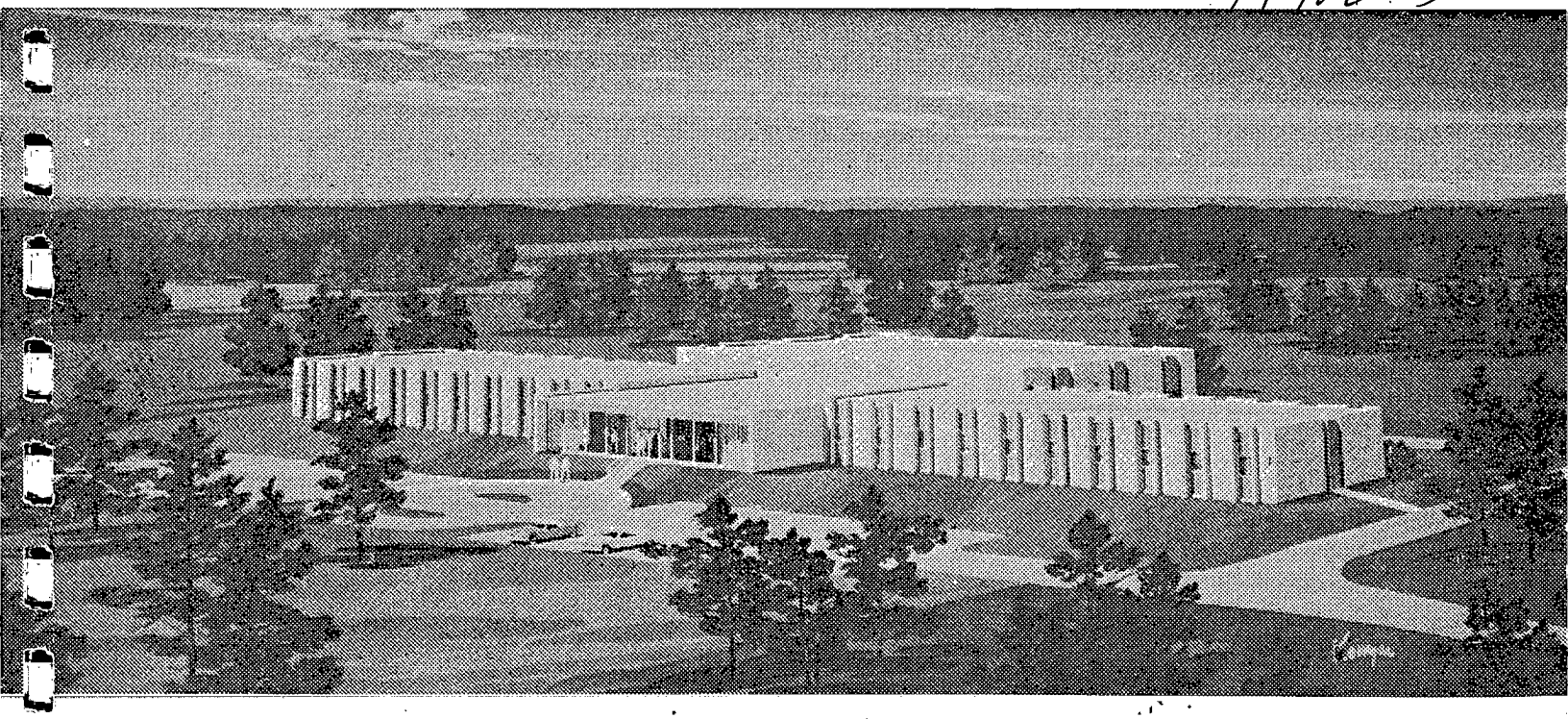

CORNING
ELECTRONICS
A DIVISION OF CORNING GLASS WORKS
RALEIGH, NORTH CAROLINA

J-44-P
REV. 2/63

CORNING GLASS WORKS

CORNING

CORNING, NEW YORK

RESEARCH AND DEVELOPMENT LABORATORY

TECHNICAL STAFFS DIVISION

TITLE: Improved Screen for Rear-Projection Viewers
Final Technical Report

REPORT NO. P-19-53, 54, 55, and 56.

PRINT NOS.

PROJECT NO. 997065

NO. OF PGS. 97

NO. OF FIGS. 40

DATE July 17, 1970

STAT

ABSTRACT: The objective was to design high quality rear-projection screens which could ultimately be made in a 30" by 30" size. A careful review of the parameters required for high quality screens was made with the result that appreciably more brightness variation could be allowed than originally specified. To verify previous work on scattering particle screens and to further investigate parameters significant to high quality screens a group of experimental 12" by 15" scattering screens was fabricated and judged for quality. High screen brightness was shown to be very desirable although the advantage of substrate absorption, at the expense of brightness, is noticeable for low contrast images. The best Corning scattering particle screens and the best commercial screens are substantially equivalent.

Lenticular screens, conceptually, offer better performance possibilities but are difficult to fabricate, particularly with the small lenticules required for high resolution. A lenticular design, based on crossed cylindrical plastic lenses and a photographic masking technique, was conceived and an operating 6-1/2" by 6-1/2" sample made. A ruling engine was used to make a master from which the mold to cast the 2 mil lenticules was made. The sample screen is approximately 2.6 times as bright as the nearest comparable scattering screen. In addition the lenticular screen maintains contrast in the presence of high ambient light levels much better than the scattering screen. The resolution of both types of screens are almost identical. The regularity and small size of the lenticules causes an undesirable diffraction effect, as the analysis and photographs in Appendix A shows. Suppression of the diffraction effect by randomizing the vertex positions of the lenticules is analyzed in Appendix B.

STAT

CORNING GLASS WORKS
ELECTRO-OPTICS DEPARTMENT
RALEIGH, NORTH CAROLINA

IMPROVED SCREEN FOR REAR-PROJECTION VIEWERS

TECHNICAL REPORTS NOS. — P-19-53, 54, 55,
AND FINAL TECHNICAL REPORT P-19-56

Date — July 17, 1970

Periods Covered — March 27, to April 24, 1970
April 24, to May 22, 1970
May 22, to June 19, 1970
June 19, to July 17, 1970

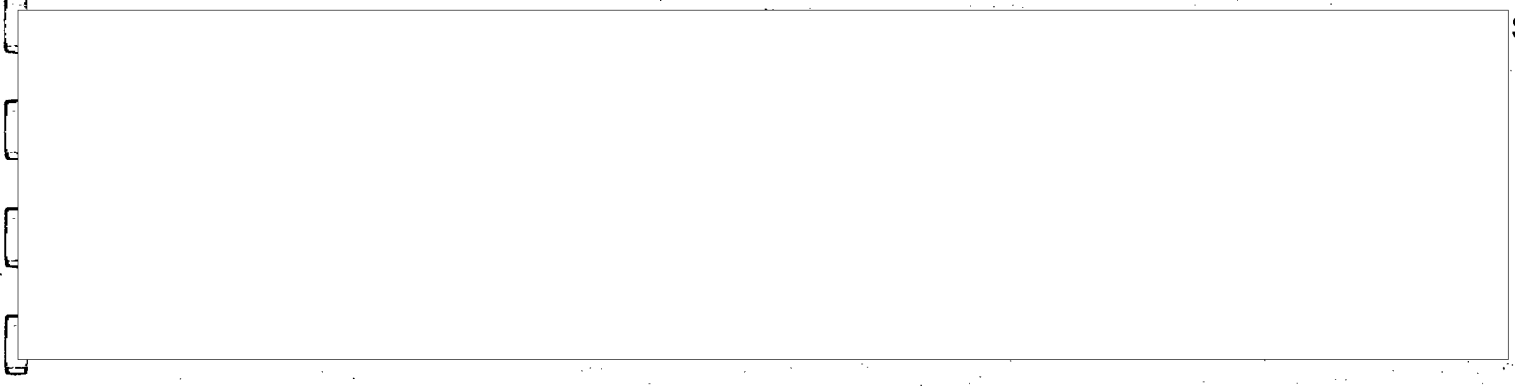

STAT

ABSTRACT

The objective was to design high quality rear-projection screens which could ultimately be made in a 30" by 30" size. A careful review of the parameters required for high quality screens was made with the result that appreciably more brightness variation could be allowed than originally specified. To verify previous work on scattering particle screens and to further investigate parameters significant to high quality screens, a group of experimental 12" by 15" scattering screens was fabricated and judged for quality. High screen brightness was shown to be very desirable although the advantage of substrate absorption, at the expense of brightness, is noticeable for low contrast images. The best Corning scattering particle screens and the best commercial screens are substantially equivalent.

Lenticular screens, conceptually, offer better performance possibilities but are difficult to fabricate, particularly with the small lenticules required for high resolution. A lenticular design, based on crossed cylindrical plastic lenses and a photographic masking technique, was conceived and an operating 6½" by 6½" feasibility sample made. A ruling engine was used to make a master from which the mold to cast the 2 mil lenticules was made. The sample screen is approximately 2.6 times as bright as the nearest comparable scattering screen. In addition, the lenticular screen maintains contrast in the presence of high ambient light levels much better than the scattering screen. The resolution of both types of screens are almost identical. The regularity and small size of the lenticules causes an undesirable diffraction effect, as the analysis and photographs in Appendix A show. Suppression of the diffraction effect by randomizing the vertex positions of the lenticules is analyzed in Appendix B.

Considerable potential exists for further improvement towards an ideal screen. At least two possibilities exist for extending the size to 30" x 30". However, to maximize the desirable characteristics it is essential to investigate the feasibility of fabricating glass lenticular screens.

TABLE OF CONTENTS

LIST OF ILLUSTRATIONS

Appendix A

Appendix B

LIST OF TABLES

I. INTRODUCTION

The principal objectives of this work were a review of rear-projection screen performance requirements, optimization of diffusing-type screens, and construction of a practical, high-performance, lenticular screen. Emphasis was to be placed on the lenticular approach, and subsequent evaluation of a group of diffusing test screens further strengthened our conviction that a large performance improvement could come only by use of the lenticular concept.

II. REVIEW OF PERFORMANCE REQUIREMENTS

A. Requirements from Previous Contract

The screen performance objectives outlined in the previous contract were essentially for an ideal screen. These requirements, as stated on page 19 of P-19-30,[1] are reproduced here in Table I. Brightness Variation was defined as

$$V = \pm \frac{B_{max} - B_{min}}{B_{max} + B_{min}}$$

where B_{max} is the maximum and B_{min} the minimum brightness within a specified range of viewing angles. A value of $V = \pm 0.33$, e.g., is equivalent to the brightness falling to half its maximum value. Efficiency T_{45} was defined as the diffuse transmittance into a $\pm 45^{\circ}$ half-angle cone centered on the normal to the screen. Similarly T_d was the Diffuse transmittance into such a $\pm 90^{\circ}$ half-angle cone. Since T_{spec} is negligible compared with T_d for practical screens, T_d and T_{90} were used interchangeably.

B. Revised Requirements

As a first step in the production of usable rear-projection screens in actual projectors we undertook a review of these specifications. Since the suitability

Table I. Screen Performance Requirements for Previous Contract

Screen Property	Screen Performance Requirement
Resolution	
Initial Goal	MTF ≥ 0.9 at 10 cycles/mm
Final Goal	MTF ≥ 0.9 at 20 cycles/mm
Diffuse Reflectance (R_d)	Equivalent to that of black velvet.
Brightness Variation (V)	*± 15% within a ± 45° viewing angle.
Efficiency (T_{45})	100%
Diffuse Transmittance (T_d)	100%
Specular Transmittance (T_{spec})	0
Color Fidelity	Minimum color contribution.
Size	≥ 30" x 30"

*Relaxed to ± 30% - ± 40% at end of contract.

of a screen must finally be judged by the user on a subjective basis, both objective and subjective criteria were considered. The list of properties and specifications, taken from P-19-32,[4] appears here in Table II. The important properties are listed along with qualitative, or subjective, specifications, where applicable. These are followed by what we considered to be reasonable and attainable quantitative, or objective, specifications. In some cases the values for lenticular screens differ from those for diffusing screens.

These specifications were written for a viewing distance of no less than 14". It was assumed that the screen would be used for scanning of imagery and that for close scrutiny the screen would be bypassed by use of an auxiliary magnifier. Hence it was possible to ease the MTF requirement. Even though ambient light was expected to be well controlled, front reflection was minimized in order to preserve contrast in dim areas of the imagery. Diffuse reflectance R_D referred to the scattering layer alone and the rather hopeful value of 5% was chosen because such low values, consistent with moderate brightness variation, had been previously measured in some Corning materials.

The brightness variation gradient of 2% per inch was added to take care of "hot spots" associated either with excessive gain dropoff, specular transmission, or possible gain variations with angle in lenticular screens.

For a scattering screen meeting the brightness variation requirement and also having sufficient substrate absorption (about 50%) to reduce the effective

Table II. Screen Performance Requirements as Revised During First Stage of Current Contract

Property	Requirement	
	Qualitative	Quantitative
1. Resolution	Screen should not appear to limit resolution.	MTF ≥ 0.7 at 10 mm^{-1}
2. Front reflection		
Specular	Reflected images should not be distracting.	< 0.5% at all viewing angles.
Diffuse	Should not unduly restrict ambient light level.	R_D < 5% for scattering screens. Less for lenticular screens.
3. Brightness Variation	Should not force operator to change head position.	No more than ± 25% over the screen.
	No "hot spot"	No more than 2% per inch gradient.
4. Efficiency (T_{45})	———	20%-30% for scattering. 60%-80% for lenticular.
5. Color Effects	Should not be strong enough to be a distraction.	
Screen transmittance spectrum.		
Color variation with bend angle.		
Diffraction Spectra		
Scintillation		
6. Trapped Light (α_T)	Contrast should be maintained adjacent to bright areas of imagery.	$\alpha_T \leq 0.1$

diffuse reflectance and the trapped light, the efficiency is, even theoretically, no greater than 20 - 30%. Lenticular screens can in principle be made 100% efficient, but practical considerations suggested the somewhat lower goal indicated.

Color variation with bend angle, non-uniform spectral transmittance, and colored sparkle or scintillation have all been observed in scattering screens. In lenticular screens we expected in addition to observe diffraction colors under some conditions. A possible quantitative limit on these color variations was suggested based on Mac Adam's data on just noticeable differences in chromaticity discrimination for different positions on the chromaticity diagram.[2] These data imply that the addition of approximately 1% of monochromatic blue or red light to a white background is just detectable, while about 0.3% of monochromatic blue-green is just detectable.

Except for item 6 these requirements were discussed in more detail in P-19-32.[4] The trapped light ratio α_T was explained in P-19-39.[4] This is a measurable screen parameter defined as

$$\alpha_T = B_T/B_D \qquad (1)$$

where B_D is the directly transmitted screen brightness and B_T is the spurious additional brightness due to trapped projector light. It can be related to observed contrast by

$$\frac{M}{M_0} = \frac{1}{1 + N\,\alpha_T} \quad , \qquad (2)$$

which shows how the observed contrast M, as a fraction of contrast M_0 presented to the screen, is reduced in the presence of trapped light when the average screen brightness is N times greater than the brightness of the local area being observed.

C. Current Screen Performance Requirements

The current performance objectives are based jointly on somewhat different viewing conditions (i.e. 26" viewing distance and 100" minimum projector-to—screen distance) and the experience we have gained with a particular lenticular screen design. The new objectives are listed in Table III.

The brightness variation requirement is quite stringent. For example, the Polacoat LS-60 screen has $\theta_{3:1} = 30^{\circ}$ and for our sample lenticular screens $\theta_{3:1} = 22 - 25^{\circ}$. However, with proper tailoring of lenticule shape and material it may be possible to attain such a broad, flat angular coverage. If so, the axial gain will necessarily be lower than for a narrower distribution. This tradeoff needs to be considered carefully. Whatever distribution is chosen, however, the efficiency with which light is transmitted into the useful viewing volume will be 2 or 3 times greater than for an equivalent diffusing screen.

Because of the discrete periodic nature of the array of lenticules, the MTF in principle depends on the angular as well as the translational position of the sine wave target with respect to the lenticules. As the spatial frequency is increased until the period of the sine wave is of the same order as the lenticule spacing the MTF becomes less and less well defined. Therefore instead of MTF, we use the terms sine wave and square wave modulation which can be measured in such a way as to approximate the eye's averaging over the lenticular sampling points and yield a nearly unique result at 5 mm^{-1} though perhaps not at 10 mm^{-1}.

Ideally, the contrast presented to the rear of the screen by the projector should be presented to the

Table III. Current Screen Performance Requirements

Property	Requirements	
	Qualitative	Quantitative
1. Brightness Variation	Edges of screen should not appear dark.	Horiz. $\theta_{3:1} \geq 39^{o}$ Vert. $\theta_{3:1} \geq 39^{o}$ Diag. $\theta_{3:1} \geq 51^{o}$ (Brightness falls to 1/3 peak value at bend angle $\theta_{3:1}$)
Gradient	No "hot spot"	≤ 2% per inch gradient
2. Efficiency		$T_p \geq 80\%$ Transmittance into pyramidal solid angle of vertical and horizontal half angle $\theta_{3:1}$
3. Resolution	Screen should not appear to limit resolution.	Sine-wave and/or square-wave modulation ≥ 0.90 @ 5 mm^{-1}.
4. Contrast Retention	Contrast should not be degraded by trapped or ambient light.	
Specular Reflectance	Reflected images should not be distracting.	$R_{spec} \leq 2\%$
Diffuse Reflectance		$R_D \leq 3\%$
Trapped Light		$\alpha_T \leq 0.3\%$ small area $\leq 0.1\%$ large area
5. Color Fidelity	Color effects should not be strong enough to be distracting and colored imagery should be faithfully reproduced.	
Screen transmittance spectrum.		
Color variation with bend angle.		
6. Spurious Effects	Not visible under conditions of projection.	
Diffraction Spectra (Includes Specular Transmittance)		
Scintillation		

viewer. Retention of contrast is affected by diffuse and specular reflectance and by trapped light. (Specular reflection is also objectionable because of its distracting effect.) The masked lenticular screen inherently preserves contrast well. The configuration in which the second set of cylindrical lenticules faces the observer presents a unique set of reflection properties. The true specular reflectance may be identified with the zeroth order of the reflected diffraction pattern and is much smaller than the reflectance of a flat plate. The remainder of the total reflectance, which we have called diffuse reflectance, is not truly diffuse but has strong directional properties which make ambient light control measures even more effective. In the case of isotropic ambient light, the value of R_D obtained by the usual integrating sphere method is an accurate measure of the effect. An antireflection coating is needed to maintain $R_D \leq 3\%$.

The trapped light ratio α_T is a partially arbitrary parameter in the sense that it depends on the illuminated screen area, the blacked out area, and the detector acceptance angle. But if these conditions are standardized a valid comparison of diffusing and lenticular screens can be made and the results can be related to the visual situation.

Color fidelity is assured if the screen material transmittance spectrum is flat, the spectral transmittance of the screen does not vary with bend angle, there are no visible diffraction spectra and no scintillation. If necessary the material transmittance spectrum can be compensated at the source, and it does not vary with bend angle. Color dispersion occurs, however, producing a color variation with bend angle

which shows up as color fringes at large angles where the intensity is dropping rapidly. The diffraction pattern can be rendered invisible by sufficient randomization of the lenticules and adjustment of projector aperture. (See Appendices A and B.) Specular transmittance may be represented by the zeroth order of this diffraction pattern and successful cancellation of the diffraction pattern implies no observable specular transmittance. Scintillation is minimized by attaining high optical quality throughout the screen. These color effects have been identified and means formulated for remedying them, but it remains to set quantitative limits.

III. DIFFUSING SCREENS

A. Purpose of Program

Useful sized diffusing type screens were to be optimized with respect to the property requirements of Table II above. The effects of substrate darkening and antireflection coating in particular were to be investigated with these screens. Objective and subjective testing programs were to be carried out on the screens and comparison made with available commercial screens.

B. Fabrication and Description of Screens

A diffusing screen fabrication process was developed by the Electronic Products Division of Corning Glass Works, and adapted to our needs. A film of glass particles in an organic binder was knife-cast onto a gray plate glass substrate. A second glass plate was antireflection coated and bonded to the first plate producing an optically continuous substrate with scattering layer on one side and antireflection coating on the other. The transmittances of the plates were selected to give four different resultant substrate transmittance values.

A large number of small sample screens were cast, with scattering layer thickness as a variable. Test results on these screens gave the empirical curves of brightness variation, efficiency, and diffuse reflectance, as functions of axial gain, shown as solid curves in Figs. 1 through 4. From these empirical curves, we made a selection of axial gain values to cover a range of screen property values near what was expected to be optimum. Eight full-size 12-1/8" x 15-1/8" screens were cast having the selected axial gain values and were then intensively tested. The individual points on Figs. 1 through 4 represent data on these full-size screens. Table IV lists the samples and the values of the parameters which were independently varied. Two types of scattering layer were represented, distinguished by the glass volume to binder volume ratio. Three levels of scattering layer axial gain were chosen and four values of substrate transmittance. Screens AL-4 and AL-5 had somewhat less favorable properties than the AQ and AR series, as can be seen in Figs. 1 through 4.

C. Objective Testing

Objective test results for the eight large screens and a sample of Polacoat LS60G1/4 then currently in use by government personnel appear in Table V. The axial gain, brightness variation, efficiency, and diffuse reflectance of the scattering layer alone were measured by the methods described in preceding Final Report P-19-30.[1]

The square-wave modulation measurements were made with a square-wave mask in contact with the scattering layer on the illumination side of the screen. The illuminated portion of the screen was projected onto a viewing plane containing a narrow slit oriented parallel

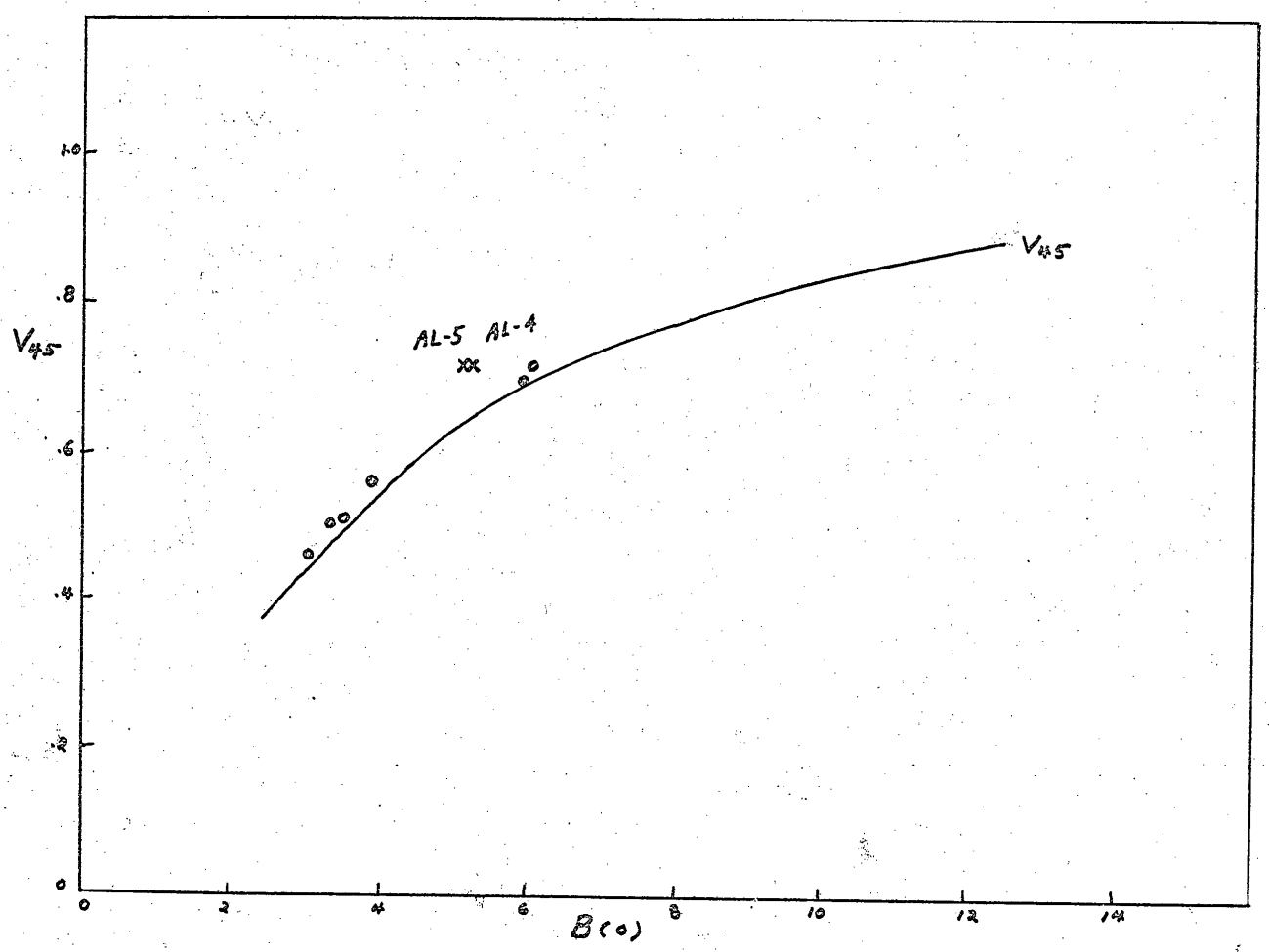

Figure 1. Brightness variation V_{45} versus axial gain for the AQ and AR Series screens. Solid curves represent the average of the data from many screens. Individual points represent data for candidate screens of Table IV.

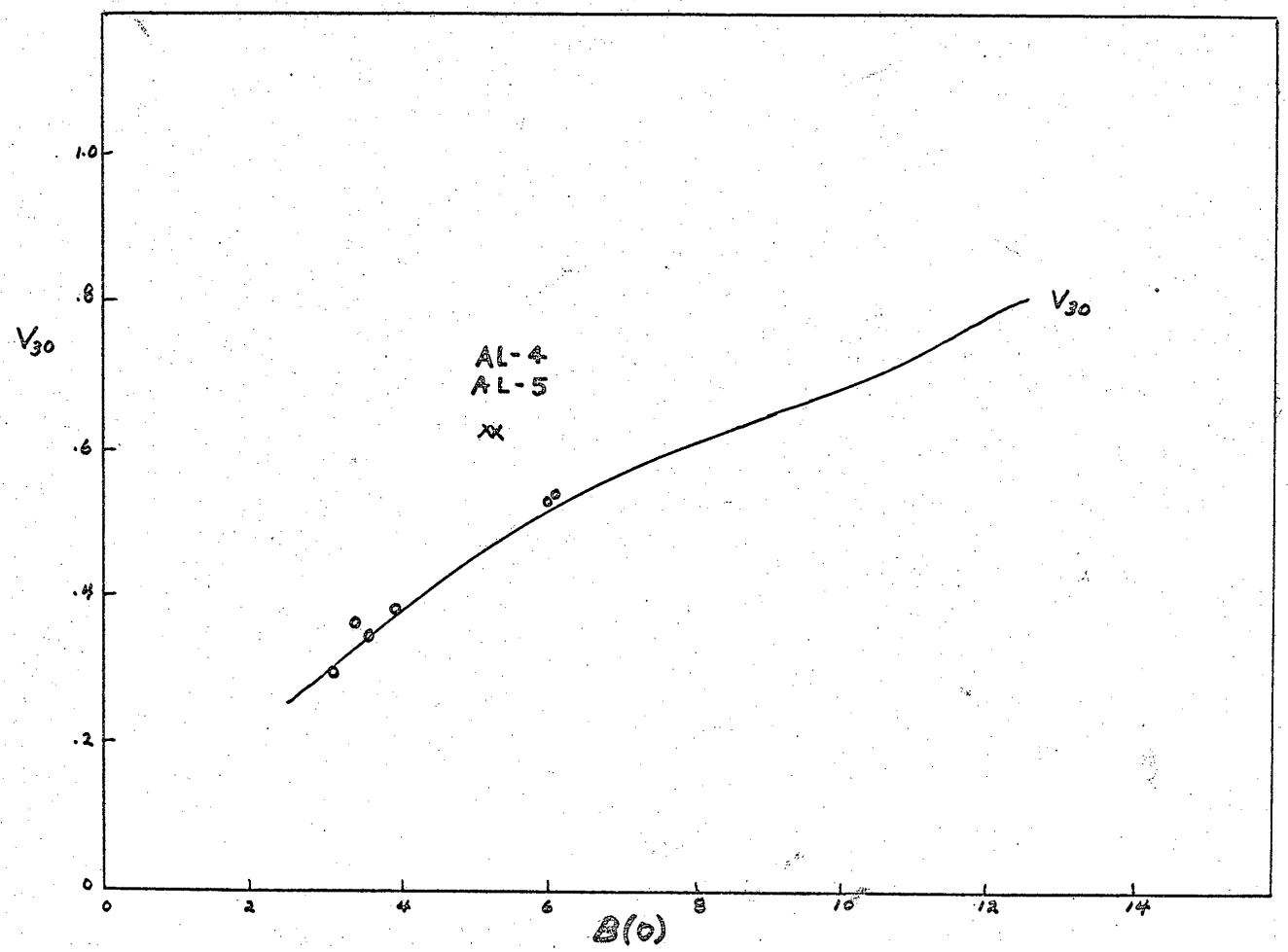

Figure 2. Brightness variation V_{30} versus axial gain for the AQ and AR Series screens. Solid curves represent the average of the data from many screens. Individual points represent data for candidate screens of Table IV.

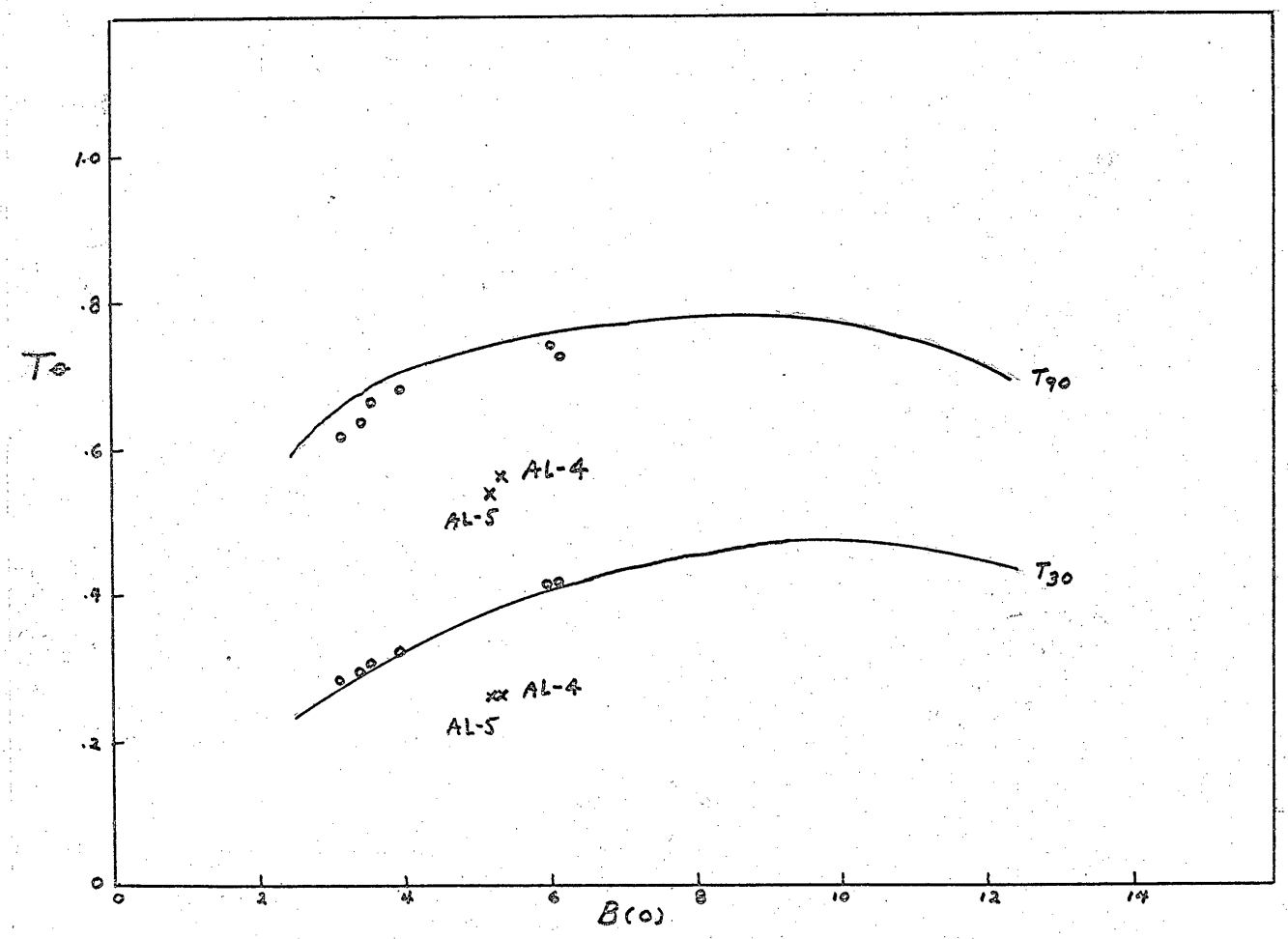

Figure 3. Diffuse transmittance T_{90} into the forward hemisphere and diffuse transmittance T_{30} into the forward 30 degrees half-angle cone for the AQ and AR Series screens. Solid curves represent the average of the data from many screens. Individual points represent data for candidate screens of Table IV.

P-19-53, 54, 55 and 56
July 17, 1970

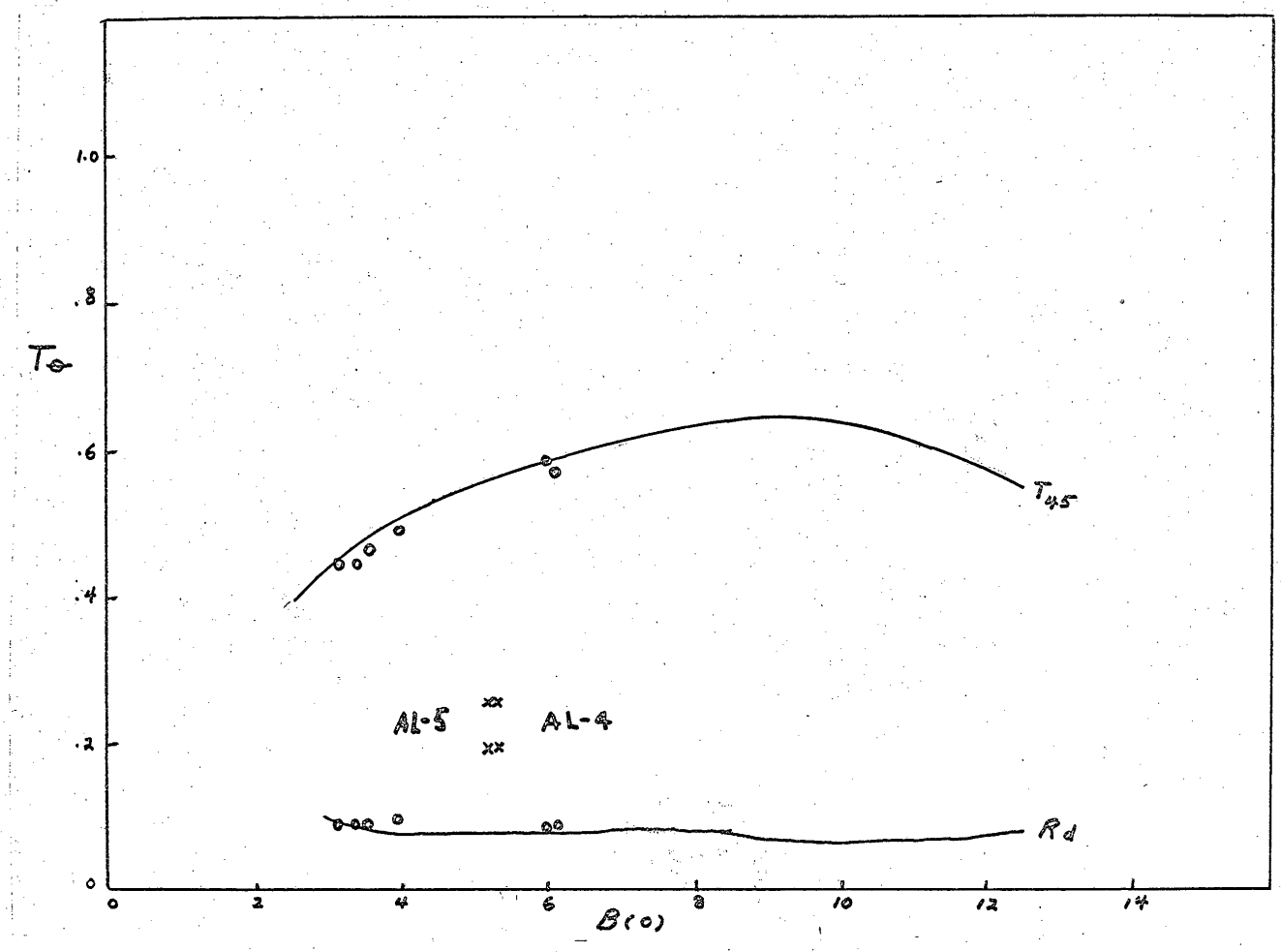

Figure 4. Diffuse transmittance T_{45} into the forward 45° half-angle cone and diffuse reflectance R_D for the AQ and AR Series Screens, versus axial gain. Solid curves represent the average of the data from many screens. Individual

P-19-53, 54, 55 and 56
July 17, 1970

Table IV

Values of the independent variables, glass-binder volume ratio, axial gain, and substrate transmittance, for the eight screens submitted for subjective testing.

Sample	Scatter Layer		Substrate Trans. T_s
	glass vol. / binder vol.	Axial Gain B(0)	
AQ-18	0.57	3.54	69
AQ-11	0.57	3.96	46
AQ-17	0.57	3.39	33
AQ-20	0.57	3.12	22
AR-28	0.57	6.14	69
AR-27	0.57	6.07	46
AL-4	1.0	5.3	69
AL-5	1.0	5.19	46

Table V

Objective Test Data on Eight Corning, and One Commercial, 12-1/8" x 15-1/8" Screens

Sample	Scattering Layer Only							Complete Rear-View Screen					
	B(0)	$V_{\%45}$	$V_{\%30}$	$T_{\%90}$	$T_{\%45}$	$T_{\%30}$	$R_{\%D}$	$T_{\%s}$	$B(0)T_s$	$T_{\%45}T_s$	$T_{\%30}T_s$	$R_{D\%}T_s^2$	$\alpha_{\%T}$
AQ-18	3.54	51	34	66	47	30	9.5	69	2.45	32	21	4.5	0.63
AQ-11	3.96	56	38	68	49	32	10.7	46	1.82	23	15	2.3	0.133
AQ-17	3.39	50	36	64	45	29	9.5	33	1.12	15	10	1.03	0.081
AQ-20	3.12	46	29	62	45	28	9.5	22	0.69	10	6	0.46	0.062
AR-28	6.14	72	54	73	57	41	9.5	69	4.23	39	28	4.5	0.24
AR-27	6.07	70	53	74	59	41	9.5	46	2.78	27	19	2.0	0.086
AL-4	5.30	72	62	56	39	26	20	69	3.66	27	18	9.5	0.74
AL-5	5.19	72	62	54	38	26	20	46	2.39	17	12	4.2	0.135
LS-60	-	73	51	-	-	-	-	-	4.35	43	30	2.0	0.11

Table V (Cont.)

Sample	SCATTERING LAYER ONLY				
	Thickness (microns)	Square Wave Modulation			
		0 mm^{-1}	5 mm^{-1}	10 mm^{-1}	15 mm^{-1}
AQ-18	82	1	0.970	0.867	0.716
AQ-11	74	1	0.974	0.908	0.788
AQ-17	80	1	0.976	0.888	0.700
AQ-20	89	1	0.961	0.819	0.653
AR-28	72	1	0.971	0.943	0.844
AR-27	78	1	0.985	0.920	0.820
AL-4	32	1	0.975	0.934	
AL-5	22	1	0.985	0.895	
LS-60	76	1	0.959	0.924	0.550

to the alternating clear and dark bars of the square-wave mask. The mask contained sets of bars at various spatial frequencies. Mask and screen were clamped together and translated slowly across the projection lens focal plane, producing maximum and minimum output voltages from a detector placed behind the slit. The modulation of the optical system, including the 1/4" glass substrate of the screen, was independently measured and taken into account. Furthermore, the illuminated area of the screen was kept small enough to preclude degradation of contrast by trapped light. The quantity we have measured is thus a characteristic of the scattering layer only, independent of the substrate thickness or transmittance. The spectral region for the measurement was 480 - 580 mμ. We avoid the term MTF and call this result square-wave modulation because it may not be rigorously equivalent to any of the transfer functions of linear systems theory. However, it does form an objective basis for comparison of resolution performance.

Parameters applicable to the assembled screens were calculated from substrate transmittance T_s and the scattering layer data, except for the trapped light ratio α_T. This was measured on the completed screens by a method described in P-19-39.[4]

The normalized curves of brightness gain versus angle are given in Figs. 5 through 8. Figure 9 shows the effectiveness of the antireflection coating.

D. Subjective Testing

The eight experimental scattering-type screens and one commercial scattering-type screen were evaluated in terms of observed resolution and judged quality by the Aerospace Group of the Boeing Company. Their final report is included in P-19-47 and 48[4] as an appendix.

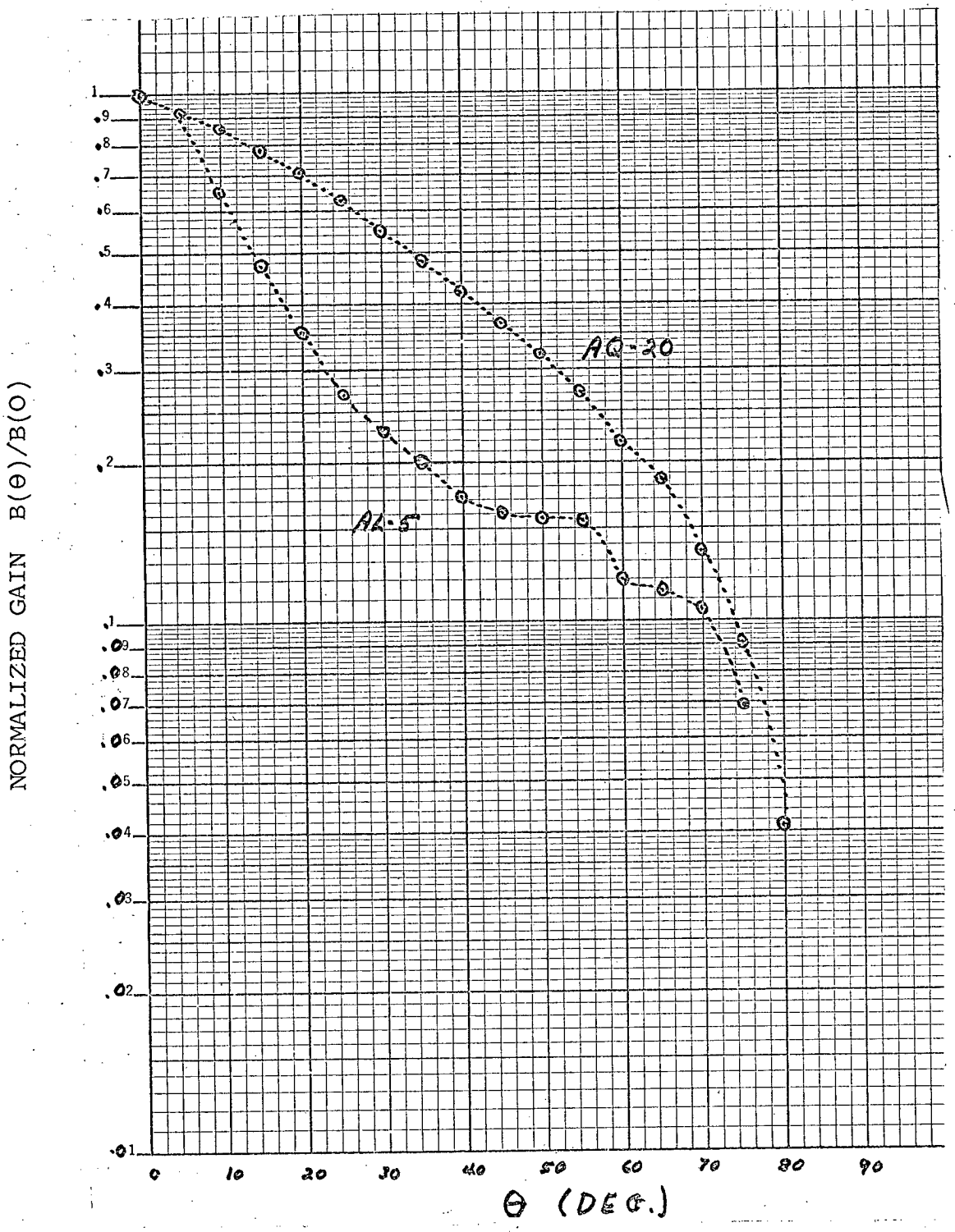

Figure 5. Normalized gain versus angle for candidate screens AQ-20 and AL-5.

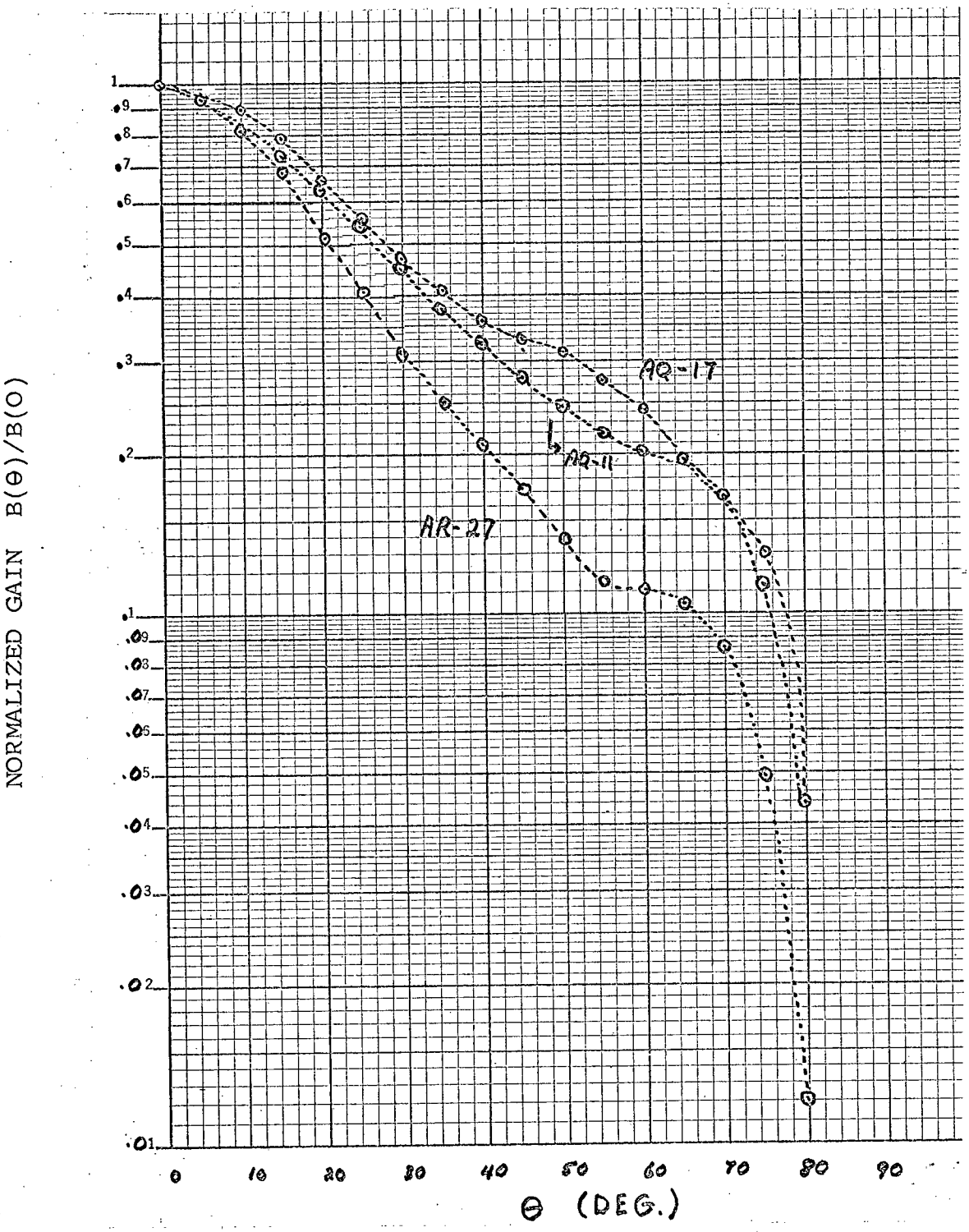

Figure 6: Normalized gain versus angle for candidate screens AQ-17, AQ-11 and AR-27.

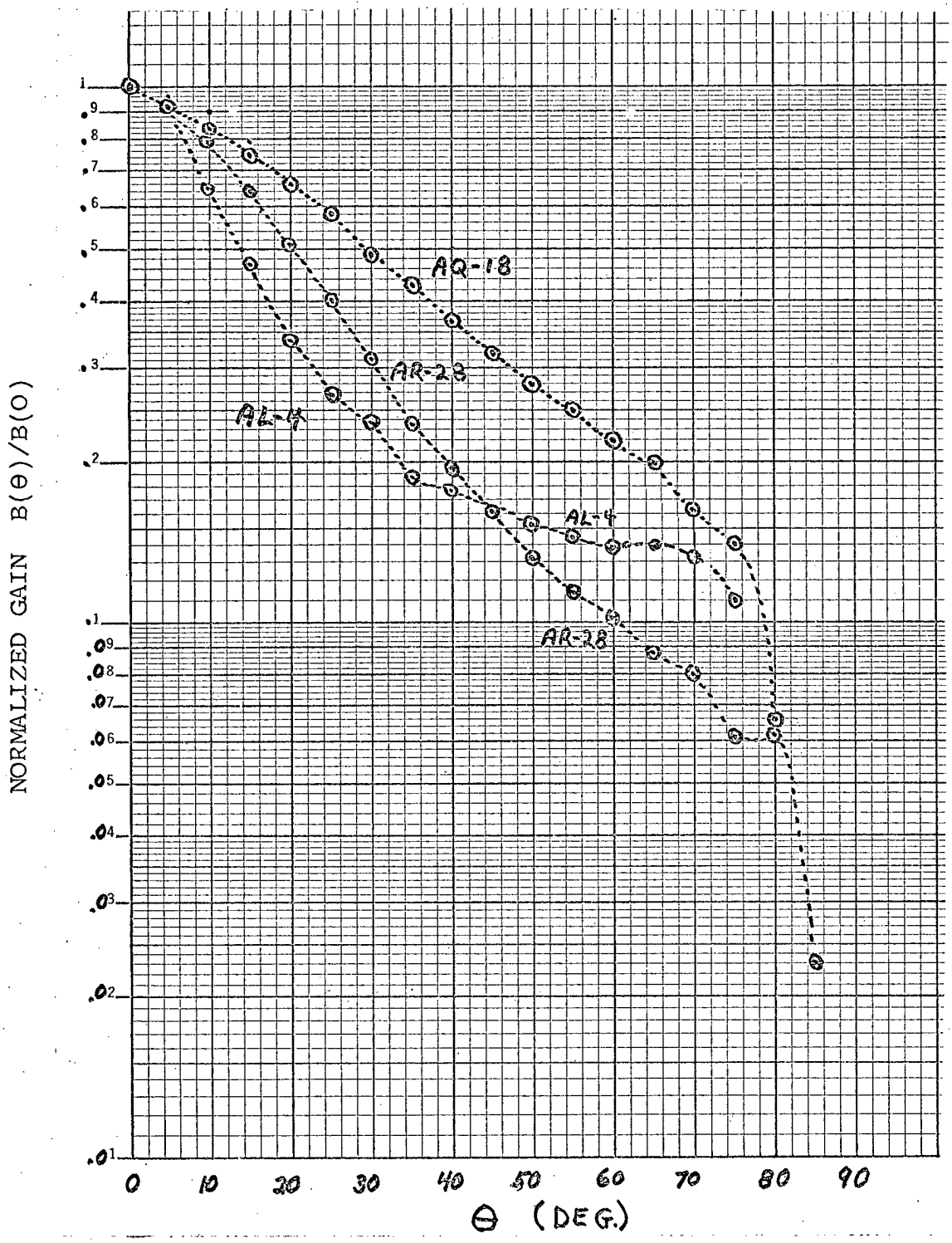

Figure 7. Normalized gain versus angle for candidate screens AQ-18, AR-28 and AL-4.

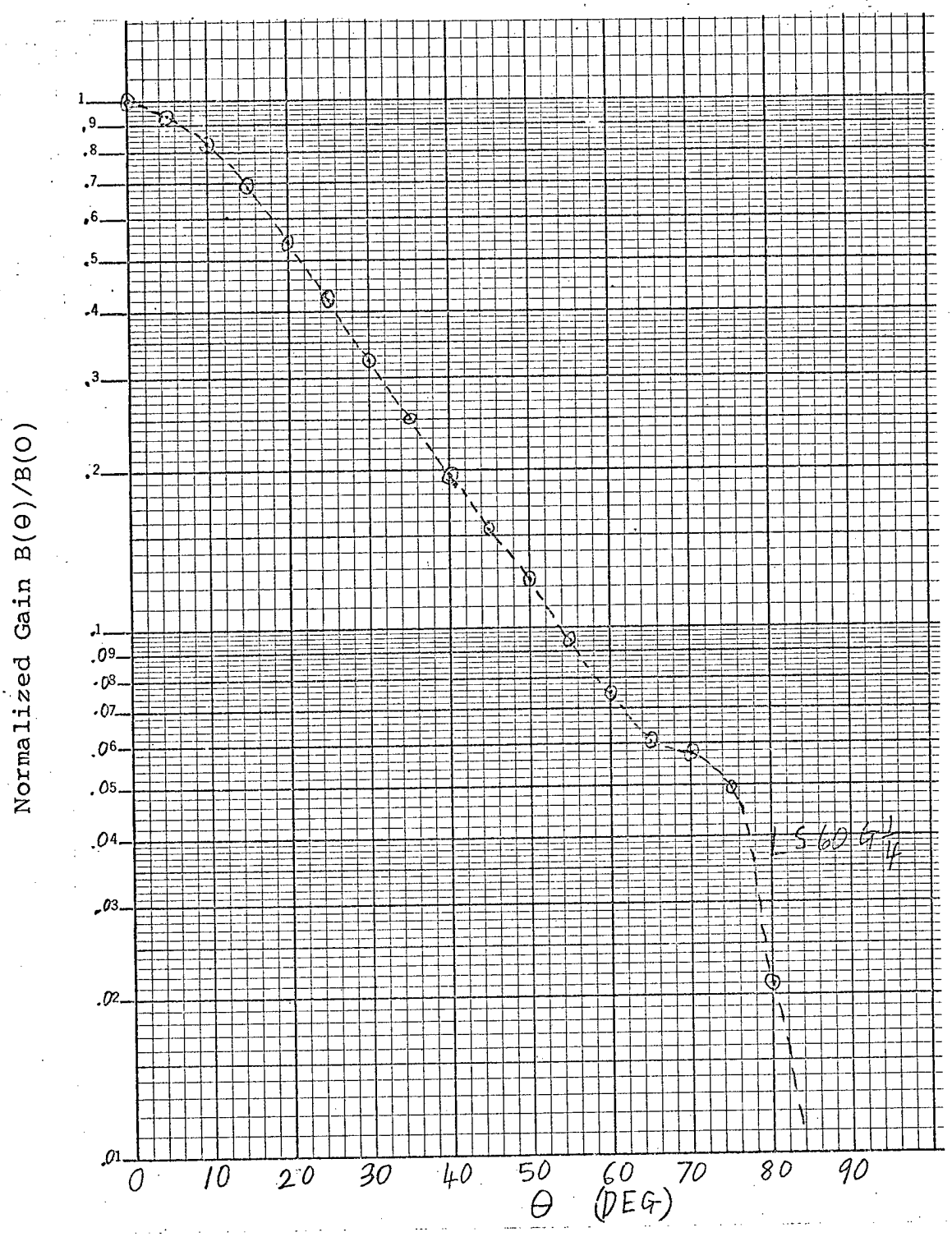

Figure 8. Normalized gain versus angle for Polacoat screen LS60-G.

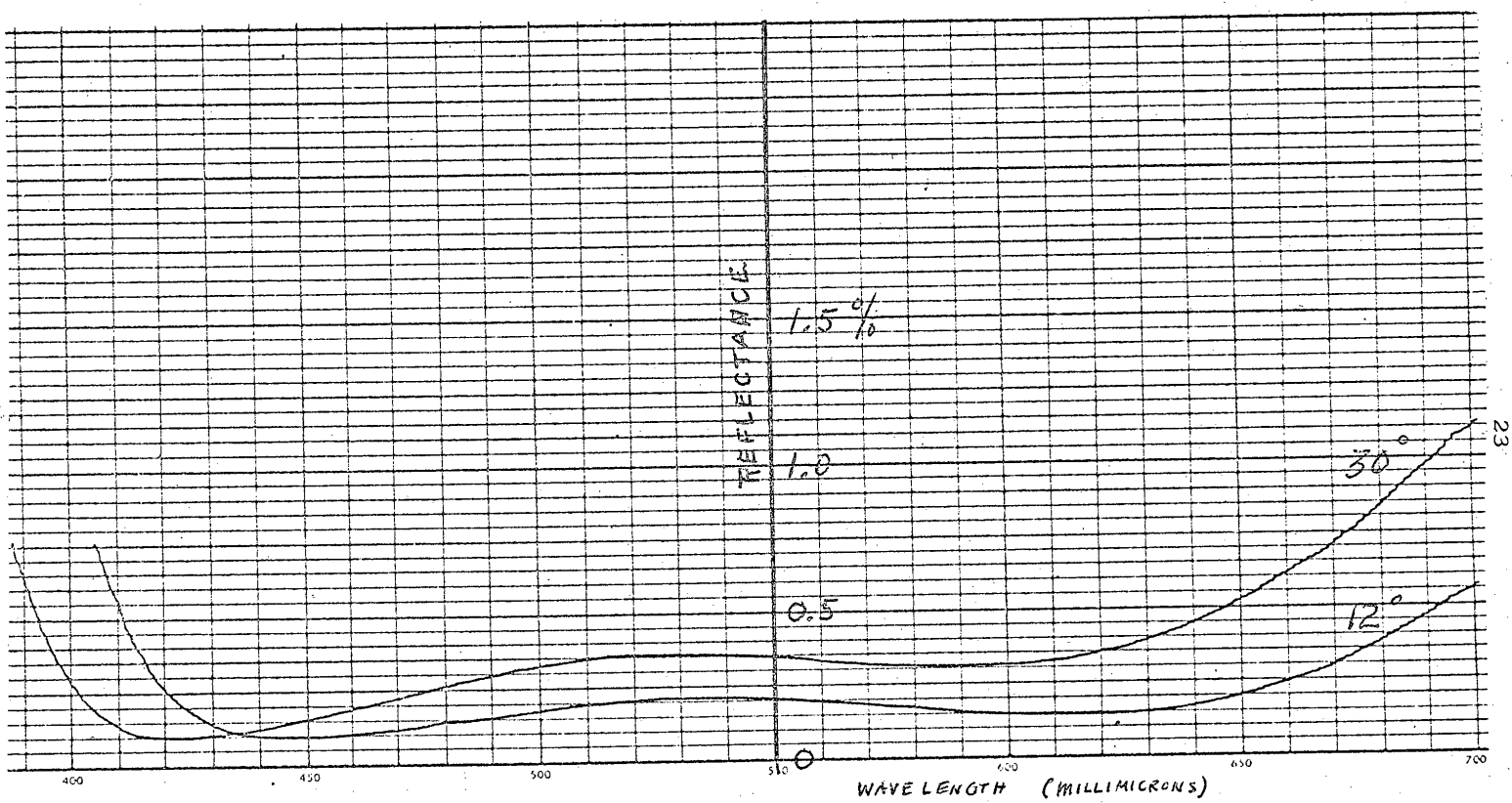

Figure 9. Typical reflection spectrum for antireflection coatings applied to observer side of screens submitted for subjective testing. Lower curve is for 12° angle of incidence, upper curve for 30°.

P-19-53, 54, 55 and 56
July 17, 1970

In the quality tests, each of the 12" x 15" screens was compared side by side with every other screen in a projector using standard imagery. Observations were made by several experienced photointerpreters and a quality scale factor Z was determined for each screen depending on how many times it was chosen as the better screen. For the resolution tests, a standard USAF tri-bar resolution charge was projected onto the screens and the photointerpreters recorded the highest resolvable spatial frequencies. The correlation of these quality and resolution judgments with measured screen properties such as axial gain, brightness variations, substrate transmittance, etc., was then investigated. In general, the differences among screens were found to be small both in judged quality and in judged resolution.

Some of the principal results are displayed in Figures 10 through 12 reproduced from the Boeing report.[4] In quality test I, projector output was constant and screen luminance varied from 10 fL to 107 fL, depending on the screen gain. In quality test II, the screen luminance was kept constant at 10 fL for all screens. In quality test III, screen luminance was adjusted to 30 fL for all except screen AQ-20, for which it was 14 fL. A positive value of Z means higher than average quality. Imagery of normal contrast and of low contrast was included in the tests. Resolution tests also were conducted under constant projector output ("normal luminance") conditions and under constant screen luminance ("controlled luminance") conditions.

E. Conclusions

The following conclusions are based on the remainder of the observational data and detailed discussion reported in P-19-47 and 48.[4]

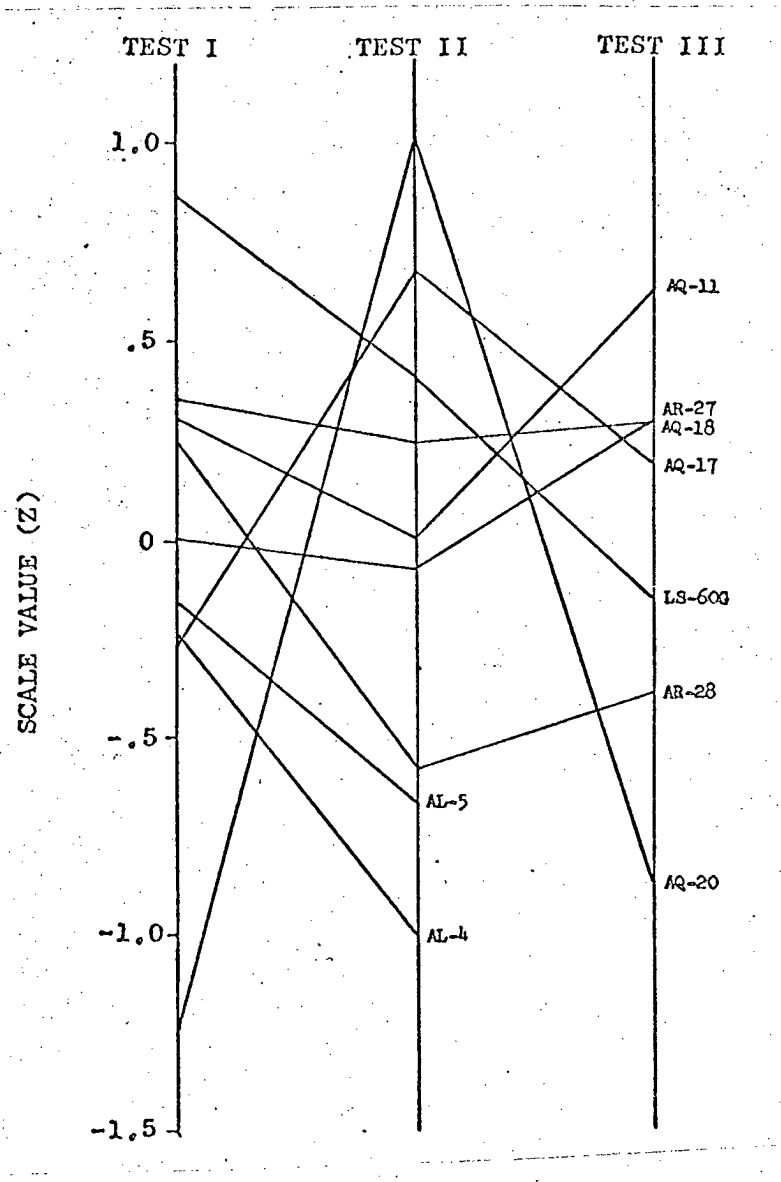

Figure 10. Screen quality scale values in each test.

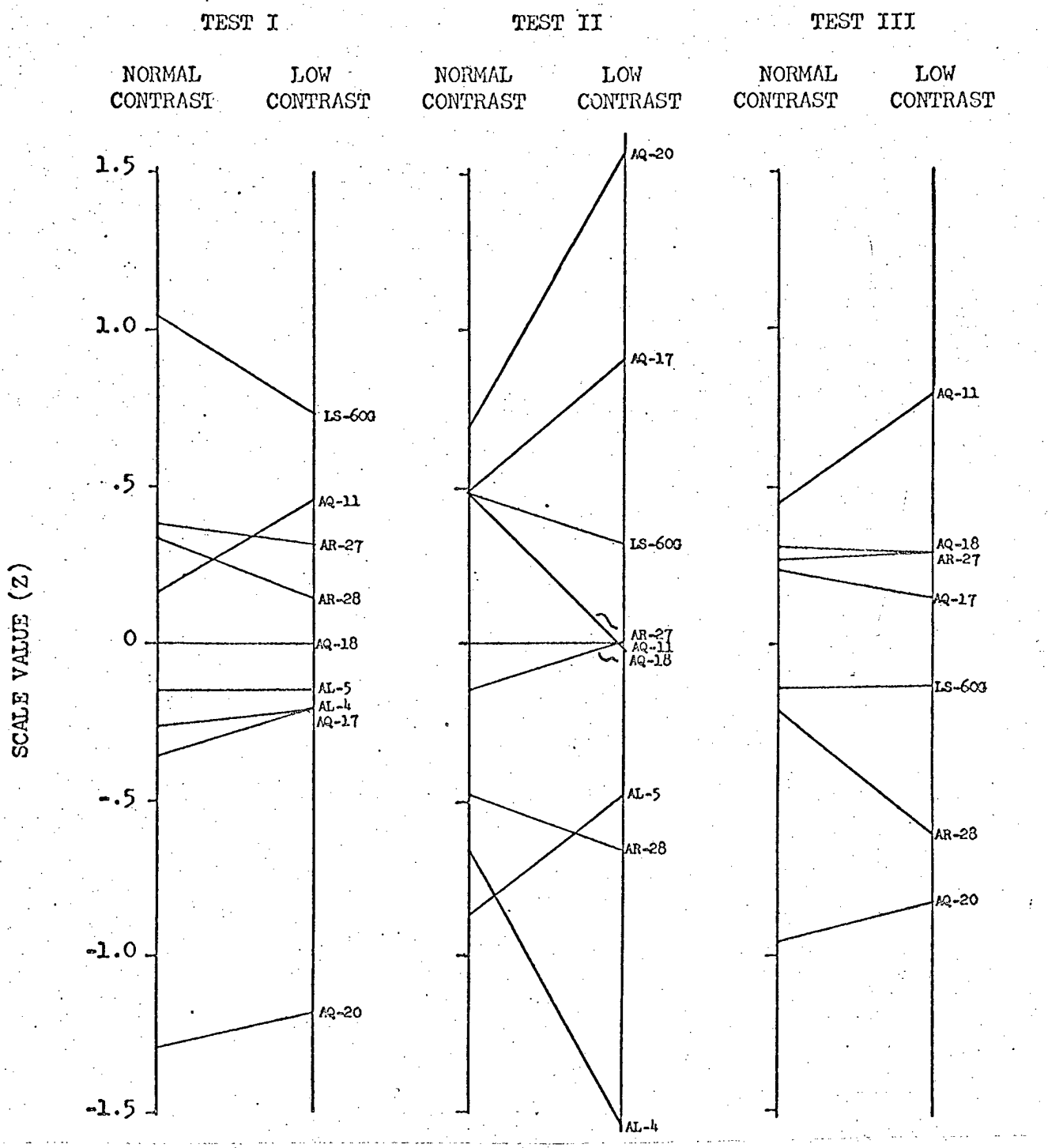

Figure 11. Effect of imagery contrast on screen quality scale values in each test.

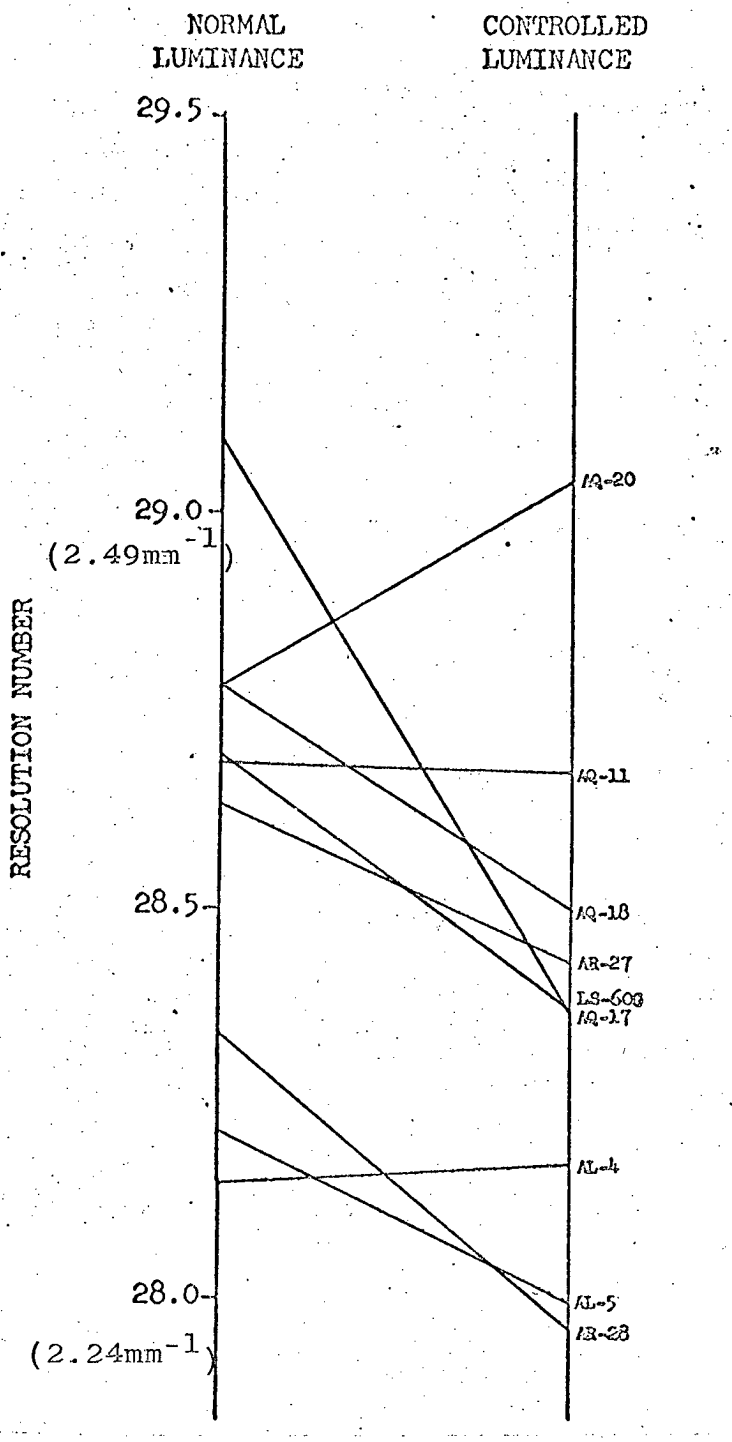

Figure 12. Resolution for each screen under each luminance condition for observers 2 and 3.

1. No one screen was judged superior in quality or resolution under all conditions. Screens AL-4 and AL-5, which had inferior objective test results, also performed poorly in the subjective tests.

2. The differences among screens under subjective testing were found to be small both in judged quality and in judged resolution. It was possible to deduce from the data that contrast loss in the projector and insufficient projector brightness limited the resolution of all screens, thus reducing observed differences.

3. Substrate absorption is effective in discriminating against ambient light. For example, in quality test II, where ambient light was an important factor, there was extremely good correlation between quality and $R_D T_s^2$, as shown in Fig. 13. In addition, darker screens appeared to perform better for low contrast resolution targets.

IV. LENTICULAR SCREENS

A. Introduction

Some work on lenticular screens was performed under the previous contract and reported in P-19-30.[1] It was recognized then that lenticular light-spreading devices are not subject to the same limitations as scattering screens. Conceptually, lenticular screens can simultaneously idealize many screen parameters. Fabrication difficulties, however, have prevented the wide use of lenticular rear-projection screens. Therefore, in order to prove the feasibility of the concept, we sought to fabricate a working high-resolution lenticular screen using whatever technology appeared easiest and capable of extension to large size screens. A 6-1/2" x 6-1/2"

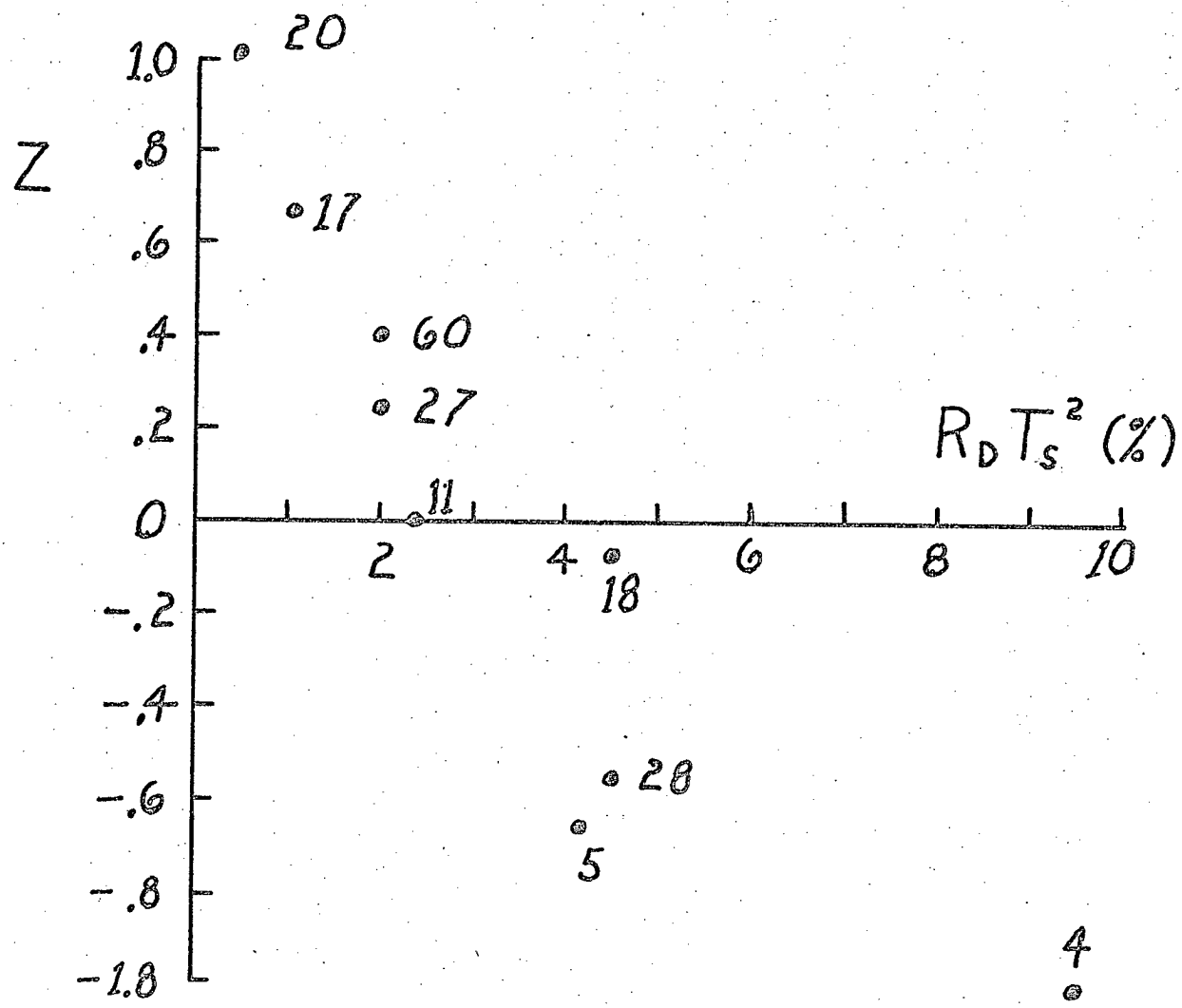

Figure 13. Quality scale factor Z versus $R_D T_S^2$ for Quality Test II.

sample screen was produced, evaluated, and delivered to the sponsoring agency. This screen exhibits the major advantages of the lenticular concept and holds promise of further improvement and size extension.

B. Design

The crossed cylindrical lenticule scheme illustrated in Fig. 14 has two important advantages over other possible configurations. One is the economy of effort which results from the fact that 2n cylindrical lenticules, each formed by a single rectilinear operation, produces an array of n^2 effectively spherical lenticules. Second, the resulting square array of lenticules is close-packed, wasting no space. The configuration which we have pursued, which has the second set of lenticules facing the observer, is easiest to fabricate because all components can be bonded together into a continuous solid sheet. If the second set is reversed so that both sets face the projector, more effective masking becomes possible at the expense of difficulty in fabrication; i.e., the two sets of lenticules must be separated by a low index material, ideally air.

Consideration of ray paths in Figure 14 together with pupil sizes and diffraction effects show that the image perceived by the eye consists of an array of small zone samples of the projected image. One zone occurs at each crossing of a lenticule from the first set with one from the second set. These zones are small compared to the lenticule size. The thickness of the substrate, which serves for mechanical support only, causes an astigmatic effect by separating the planes in which vertical and horizontal light spreading occur. The depth of focus of the eye, together

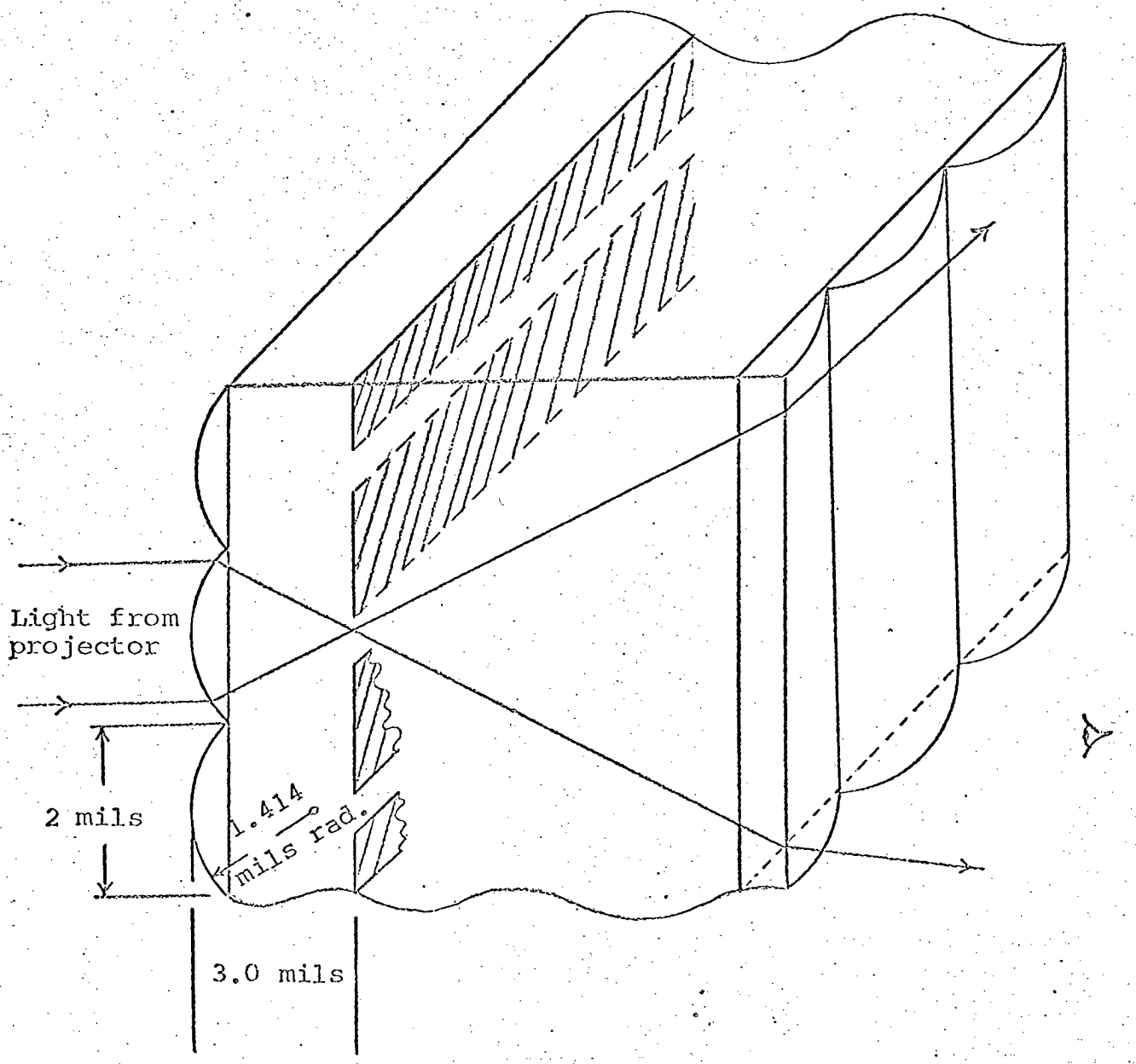

Figure 14. Schematic diagram of masked lenticular screen.

with the relatively thin substrate thickness of 1/16" prevents degradation of the projected image due to astigmatism.

The First Set of Lenticules

For an arbitrary convex cylindrical surface, the dependence of light spreading on refractive index and geometry can be calculated by reference to Fig. 15. The entering ray, essentially normal to the plane of the screen, strikes the first cylindrical surface at an angle θ_1, with respect to the surface normal, and is refracted at an angle θ_2. A second refraction occurs at the second surface yielding a spread angle θ_3. For the plane of incidence normal to the axis of the cylinder, the angle θ_3 lies in the same plane as θ_1 and θ_2 and the spread angle is given by

$$\sin \theta_3 = \frac{n}{n_0} \left[\sin \theta_1 - \arcsin \left(\frac{n_0}{n} \sin \theta_1 \right) \right], \quad (3)$$

where n_0 is the refractive index of the surrounding medium and n is the refractive index of the lenticule material. Figure 16 shows θ_3 calculated from this expression plotted versus θ_1 for $n/n_0 = 1.5$ and $n/n_0 = 1.6$. From these curves it can be seen that for a given θ_1 the spread angle is increased by increasing the relative refractive index n/n_0. If we require a spread angle $\theta_3 = 45^\circ$, and if we select n/n_0 as high as is practicable, then the maximum required θ_1 is determined. It is desirable to keep the maximum value of θ_1 small in order to minimize reflection and to minimize the difficulty of producing the required lenticule shape. The lenticule spacing w is given by

$$w = 2R \sin \theta_1 , \quad (4)$$

where R is the radius of curvature of the cylinder at the point in question. For a circular cylinder and

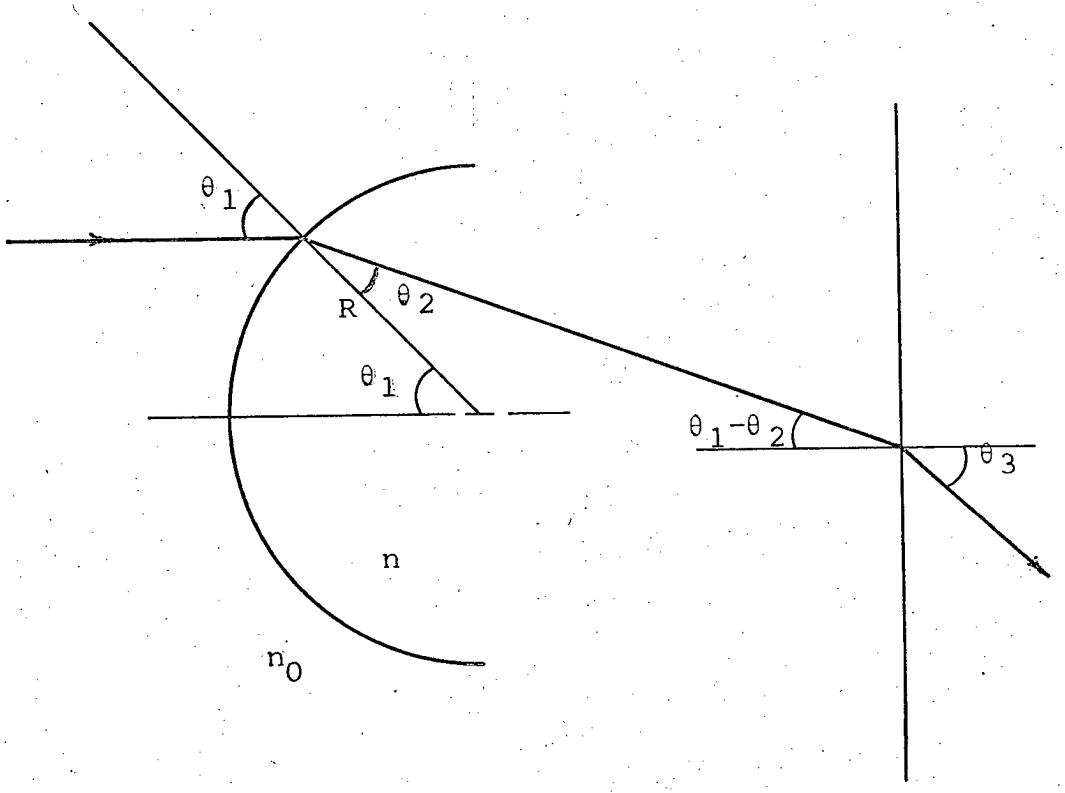

Figure 15. Ray diagram illustrating light spreading by cylindrical lenticule.

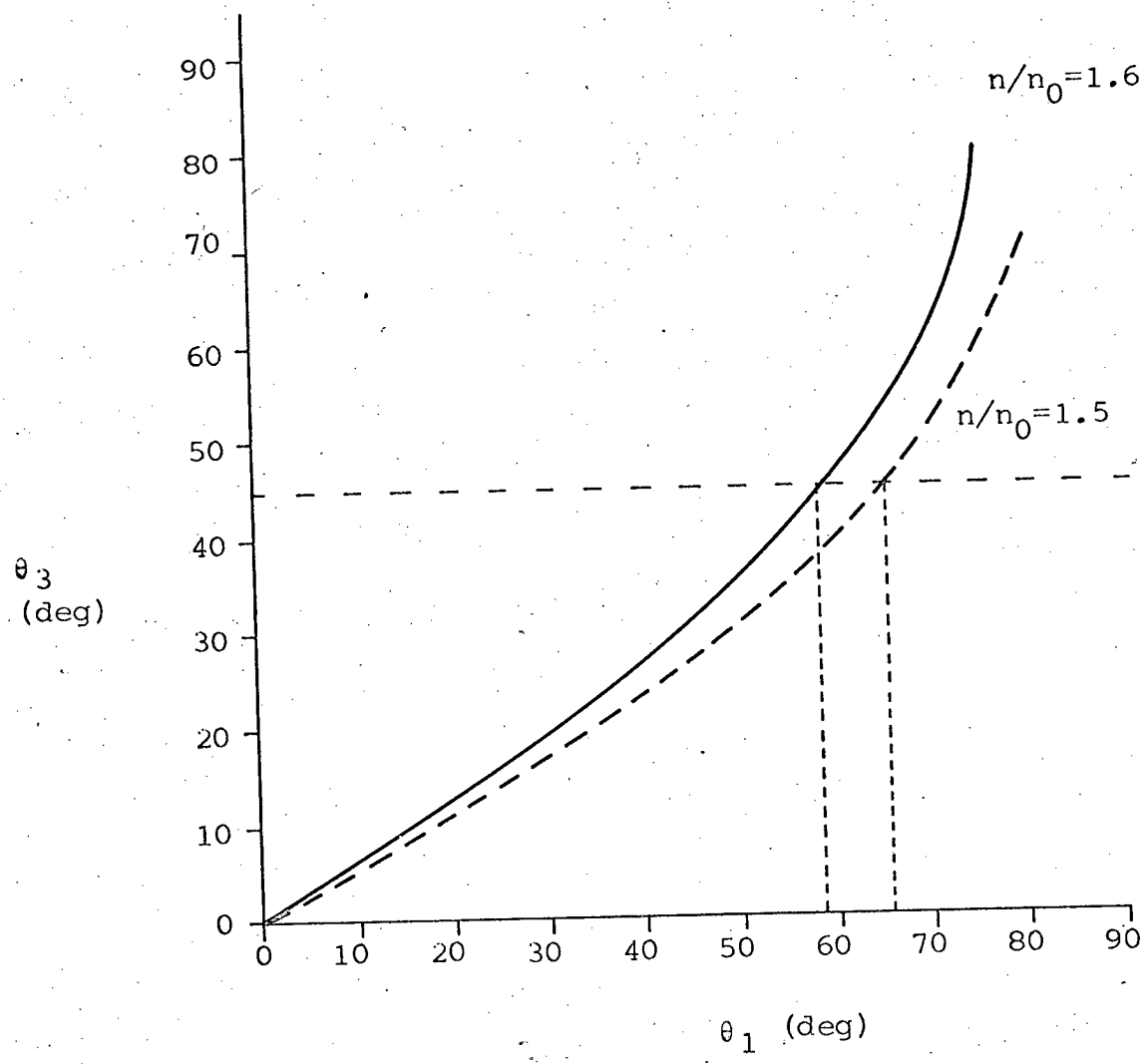

Figure 16. Spread angle θ_3 versus angle θ_1 of incidence onto curved surface of lenticule.

sufficiently small values of θ_1, the focal length is

$$f = \left(\frac{n_0}{n-n_0}\right) R = \left(\frac{n_0}{n-n_0}\right) \frac{w}{2 \sin \theta_1} \quad . \qquad (5)$$

This is sufficiently good approximation for present purposes. Since we wish to place a mask at the focal plane of the first set of lenticules, the total thickness of the first lenticular sheet is given by eq. (5). The first lenticular sheet was thus designed as in Fig. 17, with

Relative refractive index $\frac{n}{n_0} = 1.5$

Half-angle of cylinder $\theta_1 = 45^o$

Maximum angular spread $\theta_3 = 25^o$

Lenticule width $w = 0.002$ inch

Lenticule height $h = 0.000414$ inch

Lenticule radius $R = 0.001414$ inch

Focal length $f = 0.002828$ inch

Thickness, excluding masking $d = f - 0.00025$ inch
$= 0.002428$ inch.

The Second Set of Lenticules

When the light passes through the same lenticules in the reverse direction, the light spreading is different. (See Fig. 18). The maximum spread half-angle is 90^o minus the critical angle. $\theta_c = 41.8^o$ for an index of 1.5 giving a maximum spreading half angle of 48.2^o. For θ_1 between 41.8^o and 45^o, the light is totally internally reflected, thus wasted and contributing to trapped light. This defect was accepted, however, in order to get maximum spreading by the first set and yet use the same design for the second set.

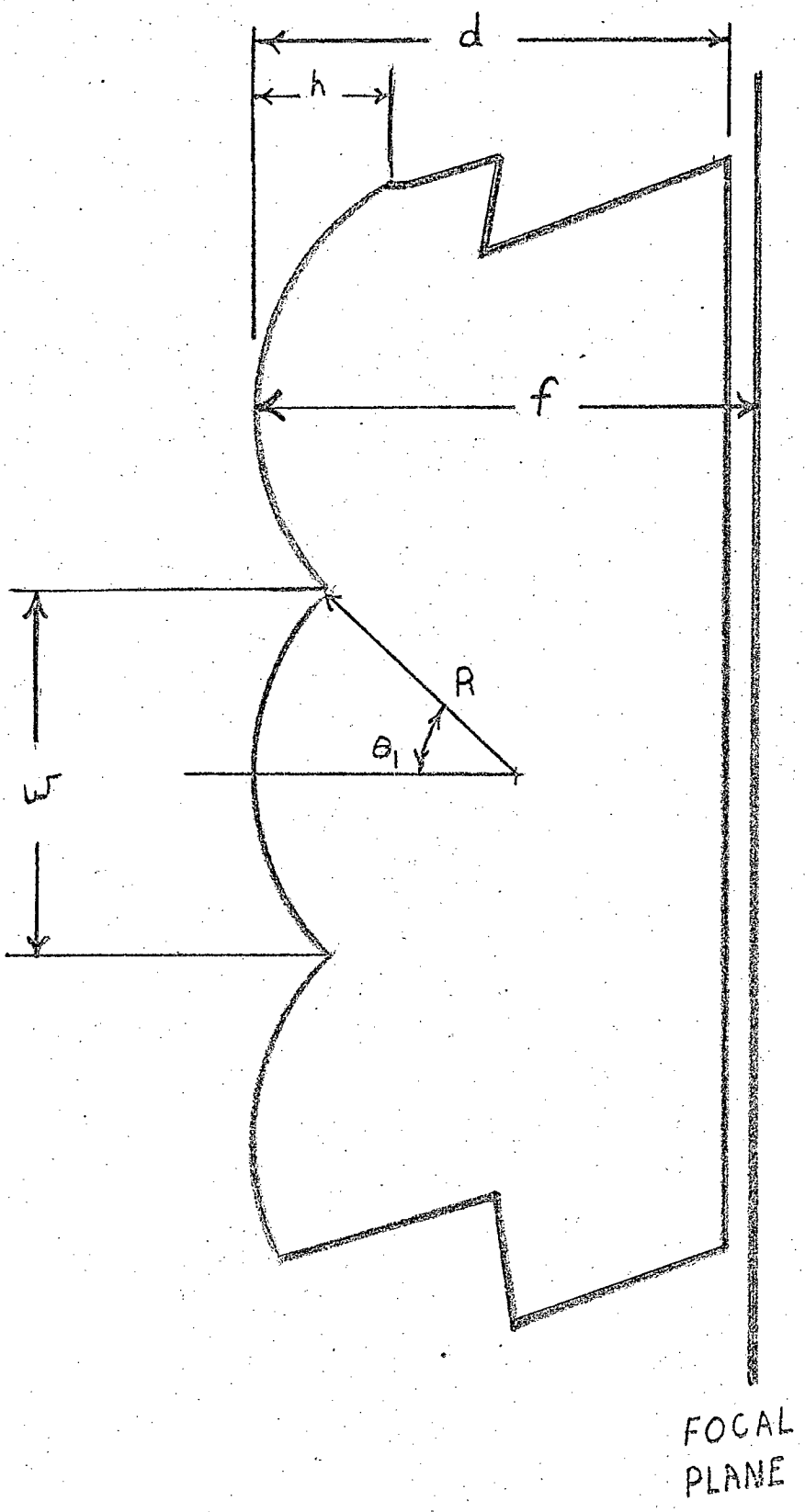

Figure 17. Cross section of first lenticule set.

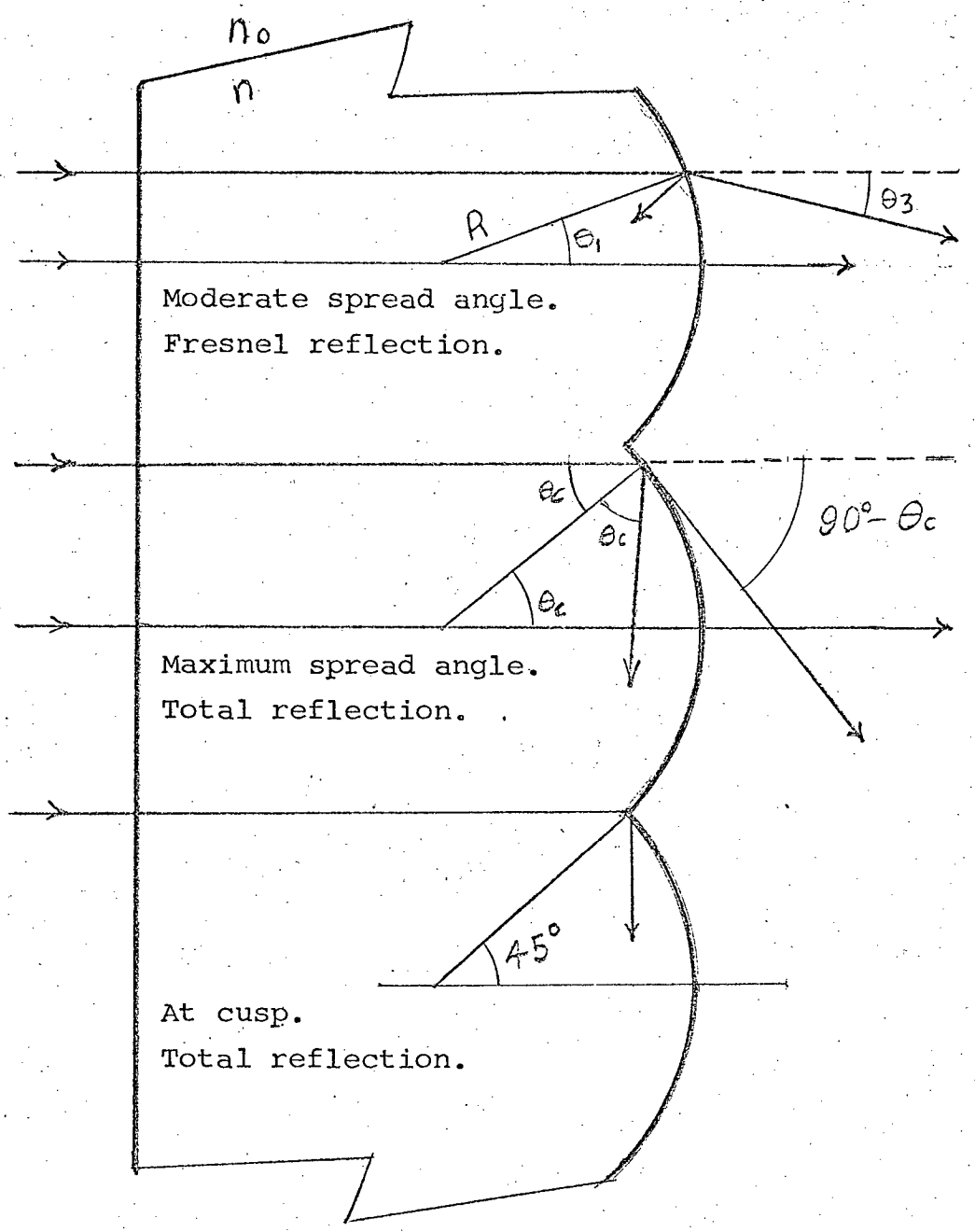

Figure 18. Optical paths through second set of lenticules.

$$\sin (\theta_3 + \theta_1) = \frac{n}{n_o} \sin \theta_1$$

C. Fabrication

The present method of construction is based on casting epoxy lenticule caps on either a film substrate for the masked lenticule set or a Plexiglas® acrylic substrate for the unmasked lenticule set. The film lenticule set is exposed through the lenticules in a geometry approximately simulating the projector. The film is then developed and reversed to give clear windows at the lenticule foci with dark spaces between. An unmasked and a masked lenticule set are then cemented together, at 90° to each other with lenticules outward to form the finished screen.

Fabrication of the mold for casting the epoxy lenticule caps is an important step in the process. A master, consisting of cylindrical furrows, is ruled into aluminum with a cylindrical diamond tool. The ruling removes metal, due to the large size of the furrows compared to normal grating grooves, rather than burnishing the grooves into the metal. Metal was removed in small increments so that the last cut was small to give a good surface. A reversed copy of the master, having cylindrical ridges, is then made in nickel by the electroform process. The nickel secondary is used as a mold to make a polypropylene replica of the original ruling. The mold is made in a heated platen molding machine, operating at 375°F in the pressure range 50 to 100 pounds per square inch. Many nickel replicas can be made from one master ruling and many polypropylene replicas can be made from each nickel replica.

The polypropylene mold is used to cast the lenticule caps onto substrates. Epoxy (Emerson and Cumins Stycast # 1266) with 25% excess hardener is used for room temperature setting and to lower the viscosity before setting. No parting agent is used and the polypropylene mold can be used about ten times before the epoxy begins adhering to the mold. The design of the masked lenticule set, see Fig. 19, requires that the cusps of the mold virtually touch the film to ensure that the lenticule focus is in the emulsion. Thus, careful squeezing out of the excess epoxy from between the mold and film is required. In addition, bubbles must also be squeezed out. Currently bubbles are squeezed out successfully but there is normally up to 0.0005" of epoxy left between the mold cusps and the film.

The film used for masking provides the mask, acts as a spacer between lenticule caps and the mask, and has surfaces compatible with adhesives. The film is a 2.5 mil thick Estar® base with 649GH emulsion and no dye in the reverse side. The reverse side is coated with clear gelatin. The emulsion and gelatin are bonded to the Estar® base during film manufacture. In screen fabrication the developed emulsion and gelatin adhere well to the epoxy used for bonding the screen components together and for the lenticules. Many different substrates and coatings and even mechanical roughening were tried before successful bonding was accomplished. It is now suspected that sticking of the epoxy in the mold caused much of this difficulty and the epoxy may not be as selective as had been thought.

The exposure scheme used to form the windows is shown in Fig. 20. A fluorescent lamp provides a uniform extended light source with the end baffles being used

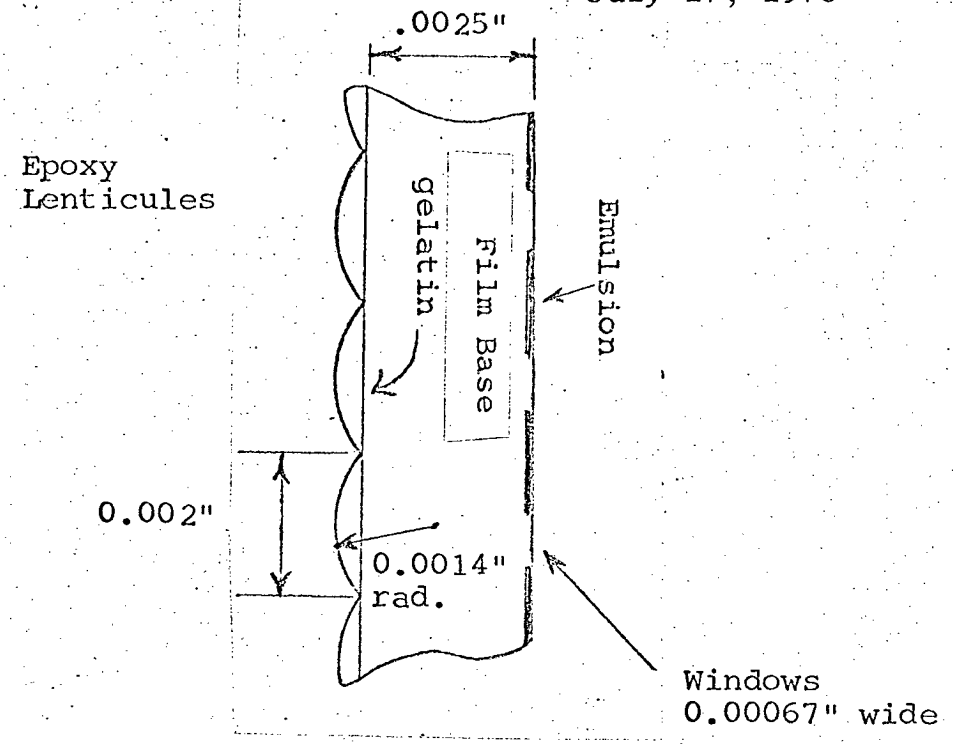

Figure 19. Masked lenticule set design.

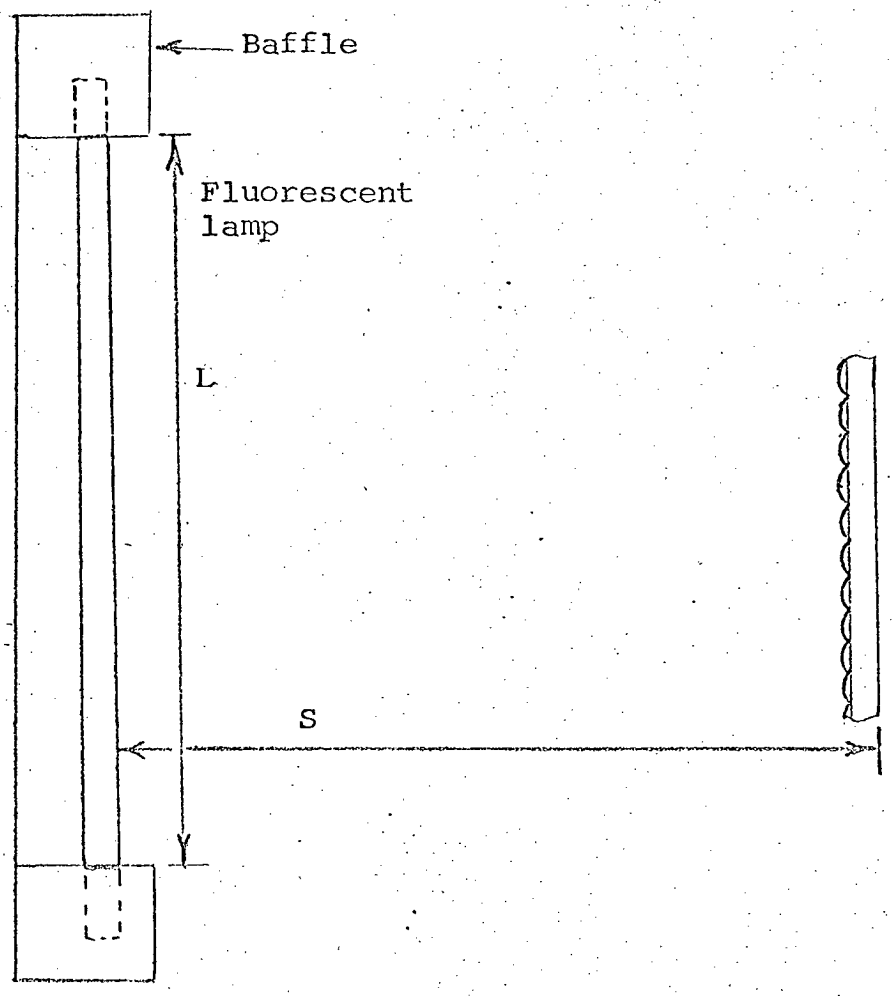

Figure 20. Exposure scheme for masked lenticules.

to determine the length L actually used. The distance S determines the size of the image of L formed at each lenticule focus. To allow for variable geometry between the projection lens and the screen, and for fabrication tolerances causing defocusing at the emulsion plane, a window size of one-third the pitch of the lenticule was chosen. Thus S was chosen so that the image of L in the lenticule window is 0.00067 inches. The actual geometry used is L = 5", S = 20". The film is developed and reversed to give the required masking pattern. The 649GH is very slow and insensitive and can be handled in red light easing lenticule casting and film processing problems.

The masked lenticule set is bonded to the plane side of an unmasked lenticule set to give the assembly shown in Fig. 14. Experimentation with a large number of bonding materials led to the choice of either Eastman 910 adhesive or Summer Laboratories' Lensbond optical cement for the bonding of photographic emulsions to polyester sheet or to glass. The Eastman 910 adhesive was found to produce a stronger bond but more distortion of the interface upon setting. The Lensbond optical cement produced a uniform, but only moderately strong, bond and less distortion. There was much less distortion when the thin polyester sheet or the emulsion were bonded to a glass plate. Subsequently, Scotch-Weld® 3520B/A Structural Adhesive was also found to be suitable. Currently, we are using the same epoxy for this purpose as for casting of lenticules.

D. Performance

To date ten lenticular screens have been assembled, three of which are the full 6-1/2" x 6-1/2" in size.

Two of these are sufficiently uniform and blemish free to be considered as good test samples. One of them, which will be called S-5 here, has undergone intensive subjective and objective testing, especially in comparison with the Polacoat LS60 screen previously tested by us and reported on in III-C above. S-5 is to be delivered to the government along with this report.

1. Subjective Testing

A high quality projection arrangement was set up as in Fig. 21. Magnification was 10X. The small Xenon source was effectively enlarged to fill a 1.5" aperture at the projection lens by use of the diffuser shown. The lenticular screen S-5 and the Polacoat LS60 were mounted in a slide so that each in turn could be placed at the center of the field where the imagery was located. The screen displays were photographed on Polaroid 3000 speed film. Figures 22 and 23 show the superior performance of S-5. Photographs A and B of Fig. 22 show the brightness advantage when equal illumination is supplied to each screen from the projector. (Room lights out.) Measurements show the lenticular screen 2.6 times brighter than the Polacoat screen. Photographs C and D of Figure 22 show the improved rejection of directional ambient light. The light intensity from the projector was adjusted to give equal viewed brightness (7.5 fL) for both screens. Directional ambient illumination of 125 fc was applied to both screens. Preliminary measurements show 7:1 contrast for the lenticular screen and 1.18:1 contrast for the Polacoat LS60. The direction was chosen so that surface reflections were not measured. The same Air Force target, ranging from $1mm^{-1}$ to $228mm^{-1}$, was used for all tests in Figs. 22 and 23. Thus, it can be seen from Fig. 22 that although some small loss of contrast is shown in photograph C (compared to A) the loss is much less than in

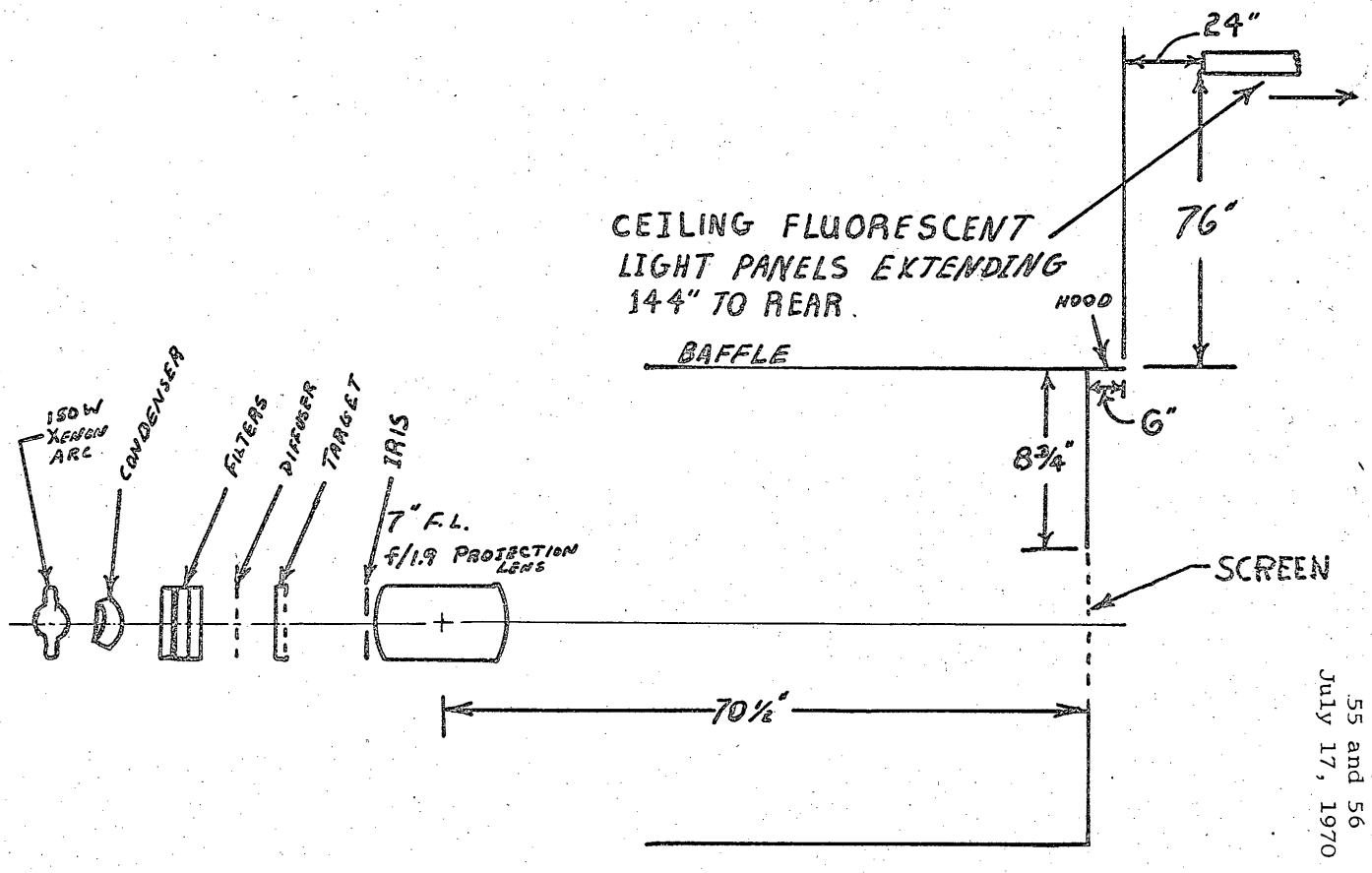

Figure 21. Projection Arrangement for Subjective Testing.

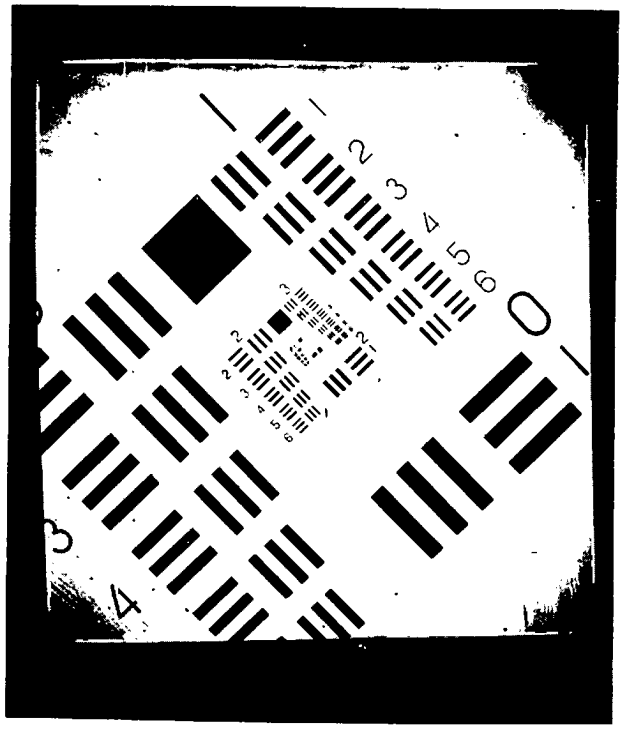

A. Lenticular Screen
(Corning Glass Works)

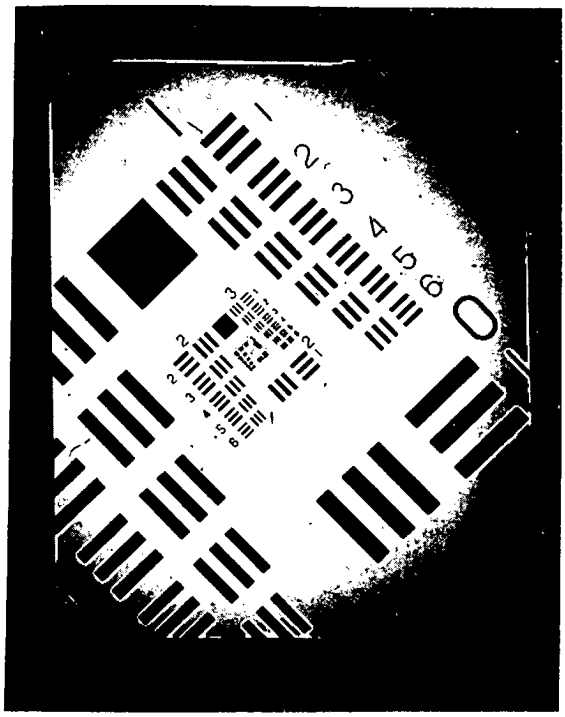

B. Scattering Screen
(Polacoat LS60)

Brightness comparison with
equal projector illumination.

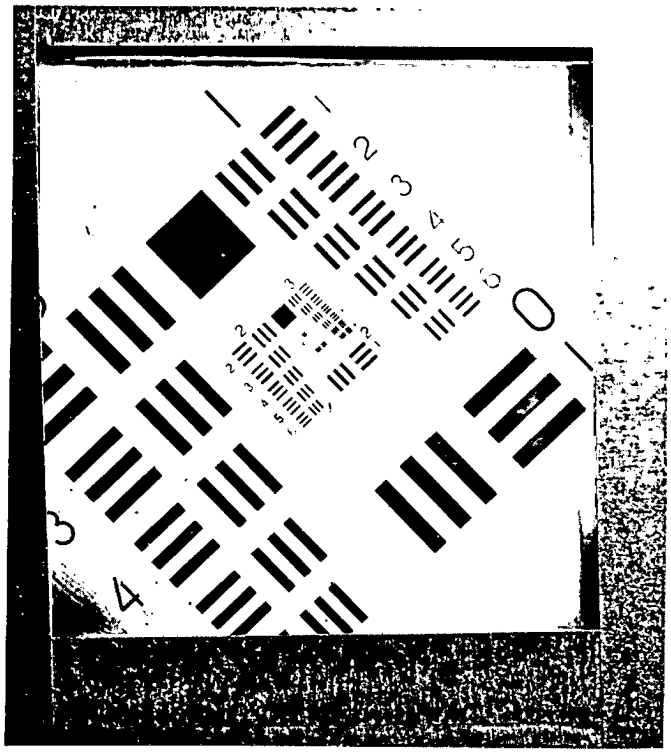

C. Lenticular Screen
(Corning Glass Works)

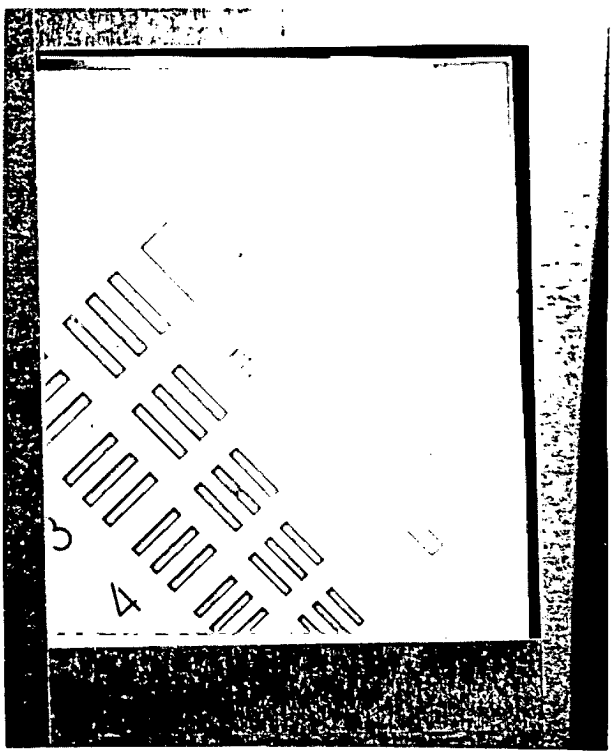

D. Scattering Screen
(Polacoat LS60)

Ambient light rejection with equal viewed
brightness, 7.5 fL. Directional ambient
illumination 125 fc.

Figure 22:

Comparison of brightness and
ambient light rejection

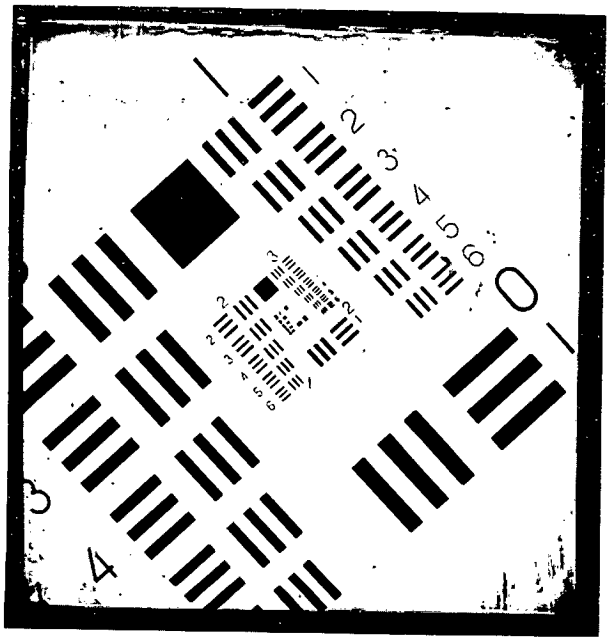

A. Lenticular Screen
(Corning Glass Works)

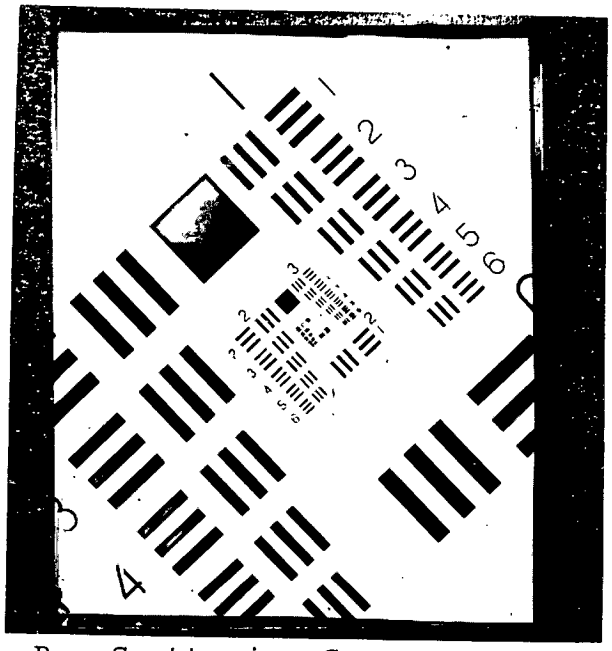

B. Scattering Screen
(Polacoat LS60)

Ambient light rejection with equal viewed brightness, 7.5 fL, and ordinary room illumination, 25 fc.

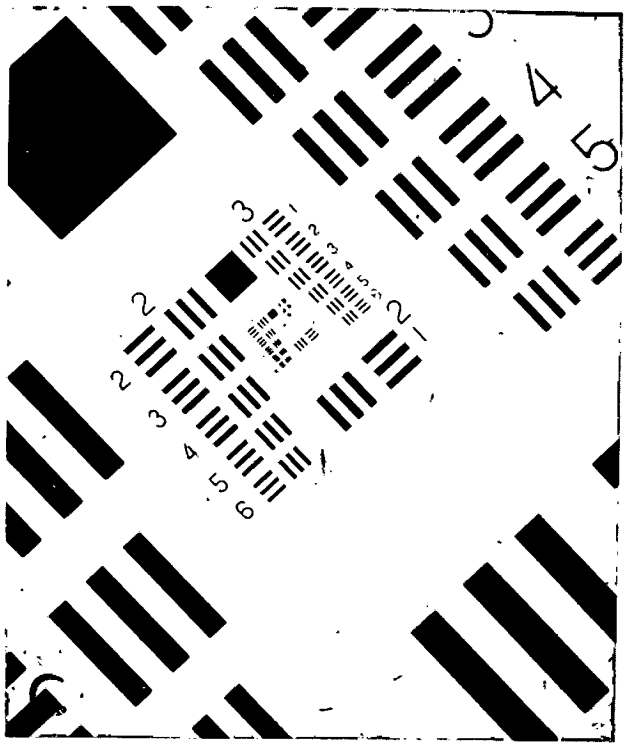

C. Lenticular Screen
(Corning Glass Works)

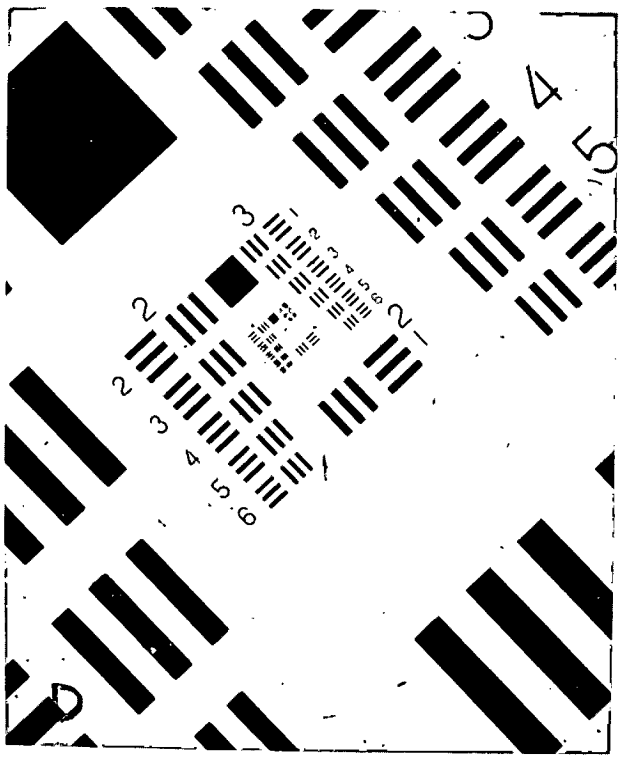

D. Scattering Screen
(Polacoat LS60)

Resolution with equal viewed brightness. Projector magnification 10X, camera magnification 1X.

Figure 23:

Ambient light rejection and resolution.

photograph D of the scattering particle screen. Figure 23 A and B illustrates the retention of contrast under ordinary room ambient light. Projector illumination was adjusted to make the viewed brightness of both screens about equal at 7.5 fL. The room illumination was 25 fc. Figures 23 C and D are actual size photographs of projected images, at equal viewed brightness and without ambient light, to show the resolving power of the screens. Unfortunately, the various reproduction stages mask the small difference in resolution detectable by direct inspection. Averaging the limiting Air Force target resolution as read by four observers with their unaided eyes gave 4.8 lines per millimeter for the lenticular screen compared with 4.3 lines per millimeter for the scattering particle screen. The use of a high f number 10X magnifier gave 9.05 and 9.2 lines per millimeter for the lenticular and scattering screens respectively. Lateral motion of the screens at some 3 to 4 inches per second gave 16.5 and 16.1 lines per millimeter for the lenticular and scattering screens respectively.

2. Summary of Objective Test Results

Table VI summarizes the objective test results for the lenticular screen S-5 and the Polacoat LS-60 sample. Table III may be consulted for corresponding recommended values. Except as otherwise indicated, all measurements were performed using 3 Corning C.S. 3-71 color filter, one C.S. 1-69 color filter, a detector with S-11 response, and a high pressure Xenon arc source. The product of filter transmittance and detector response is compared with the photopic eye response curve in Fig. 24. The Xenon arc spectrum weights the total system spectral

Table VI. Summary of Objective Test Results

Property		Test Result S-5	Test Result LS-60
1. Brightness Variation			
$\theta_{3:1}$	horiz.	± 22°	± 30°
	vert.	± 24°	± 30°
	diag.	± 19.5°	± 30°
Gradient (at 26 in)		45%/in	6%/in
2. Efficiency			
T_{90}		79.5%	49%
T_{45}		79%	40%
T_{30}		66%	29%
T_P		53%	24%
Maximum Gain			
Based on two-sided diffuser		9.8	3.4
Based on one-sided diffuser		4.9	1.7
3. Resolution			
Sq. Wave Modulation	0 mm^{-1}	1	1
	5 mm^{-1}	≥ 0.91	0.98
	10 mm^{-1}	≥ 0.85	0.98
4. Contrast Retention			
R_{spec}		≤ 0.037%	4.6%
R_D		7%	2%
α_T	small area	0.2%	0.63%
	large area	0.004%	0.12%
5. Color Fidelity			
Trans. Spectrum (Variation, 450 - 650 mμ)		6%	6%
Color Var. with bend angle		See Fig. 38	
6. Spurious Effects			
Diffraction Pattern		See Fig. 39 and Appendices A and B.	
$T_{spec.}$		Negligible	Negligible
Scintillation		Not measured	

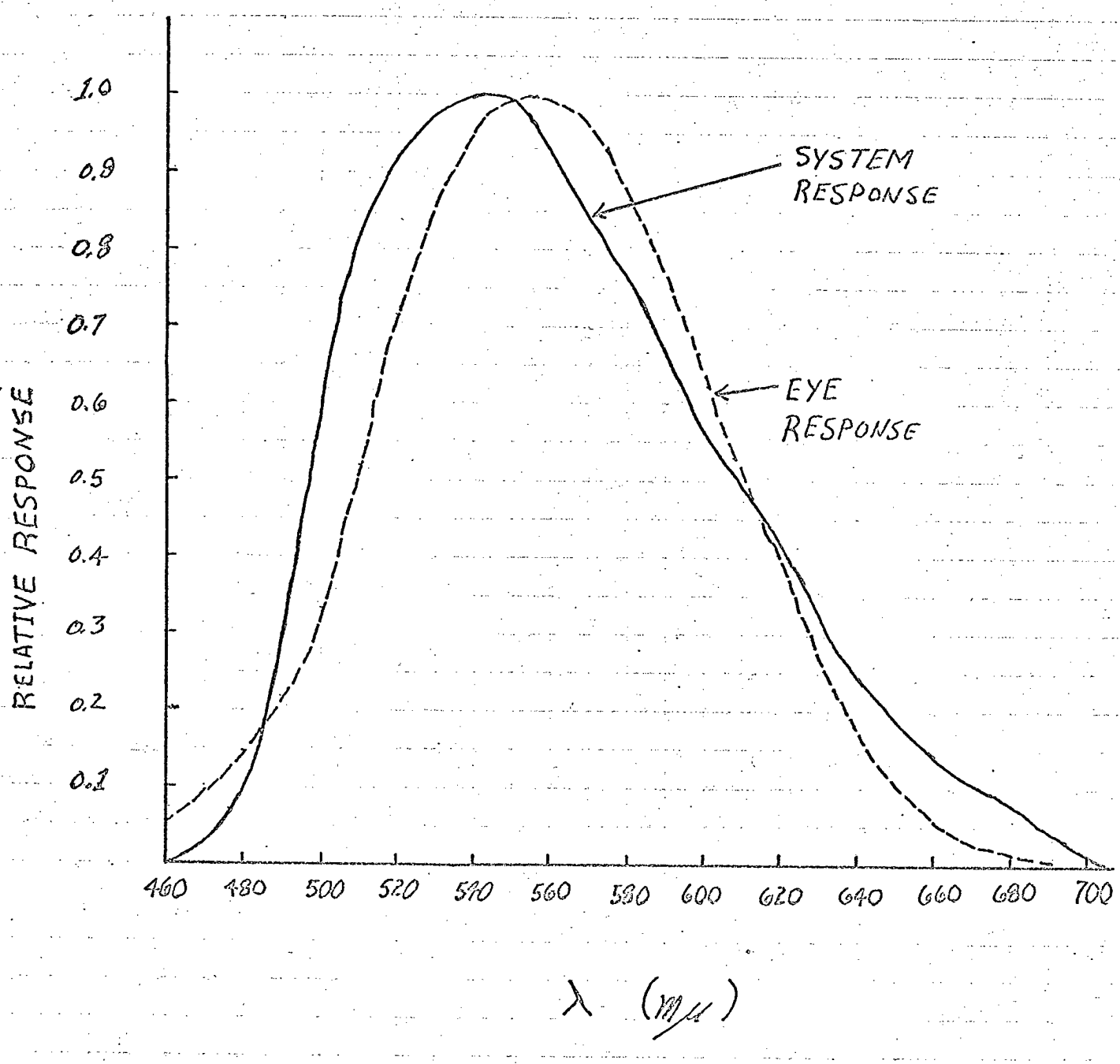

Figure 24. Spectral response of filter-detector system used in optical property measurements.

response somewhat towards the blue. The measurements are discussed in detail in the following sections.

3. Brightness Variation

The angular distribution of brightness was measured on the goniophotometer described in P-19-30,[1] with slight modifications. Spectral response was as given by Fig. 24. The cone of light falling on the sample converged at f/24. The detector optics were arranged to observe an 0.3 mm diameter spot of the screen, with an angular resolution of 0.6°.

In the following description of measurements the screen is assumed to remain fixed in the orientation in which it was designed to be used, i.e. with the masked horizontal lenticules facing the source. Goniophotometer scans were made and various projector angles were simulated in the horizontal, vertical, and diagonal planes. Figure 25 illustrates the geometry used. The goniophotometer was arranged to scan viewing angles θ_V from -45° to $+45^{\circ}$ with respect to the screen normal. The projector angle θ_P could be varied independently in the same plane as the detector scan. In this case the bend angle $\theta_B = \theta_V + \theta_P$.

Figure 26 is the horizontal scan about the center of the screen with zero projector angle. The brightness nearly falls to zero at $\pm 45^{\circ}$ as it should. The maxima and minima are supposed to be produced by very slight deviations of the lenticule curvature. This angular distribution of brightness has been found to be characteristic of all areas of the screen and has been observed on a single lenticule. Scanning electron microscope examination

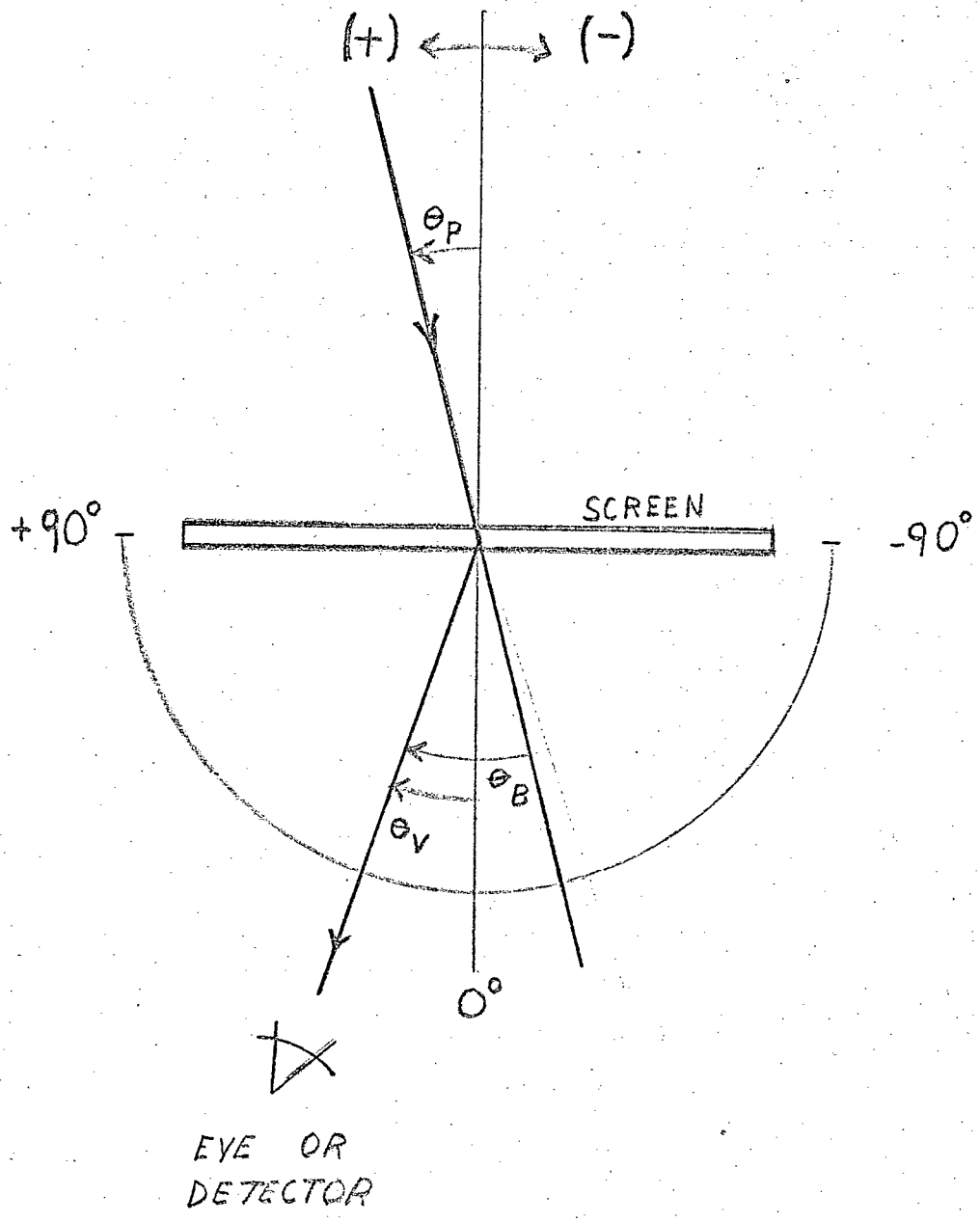

Figure 25. Goniophotometer scanning geometry,

$$\theta_B = \theta_V + \theta_P$$

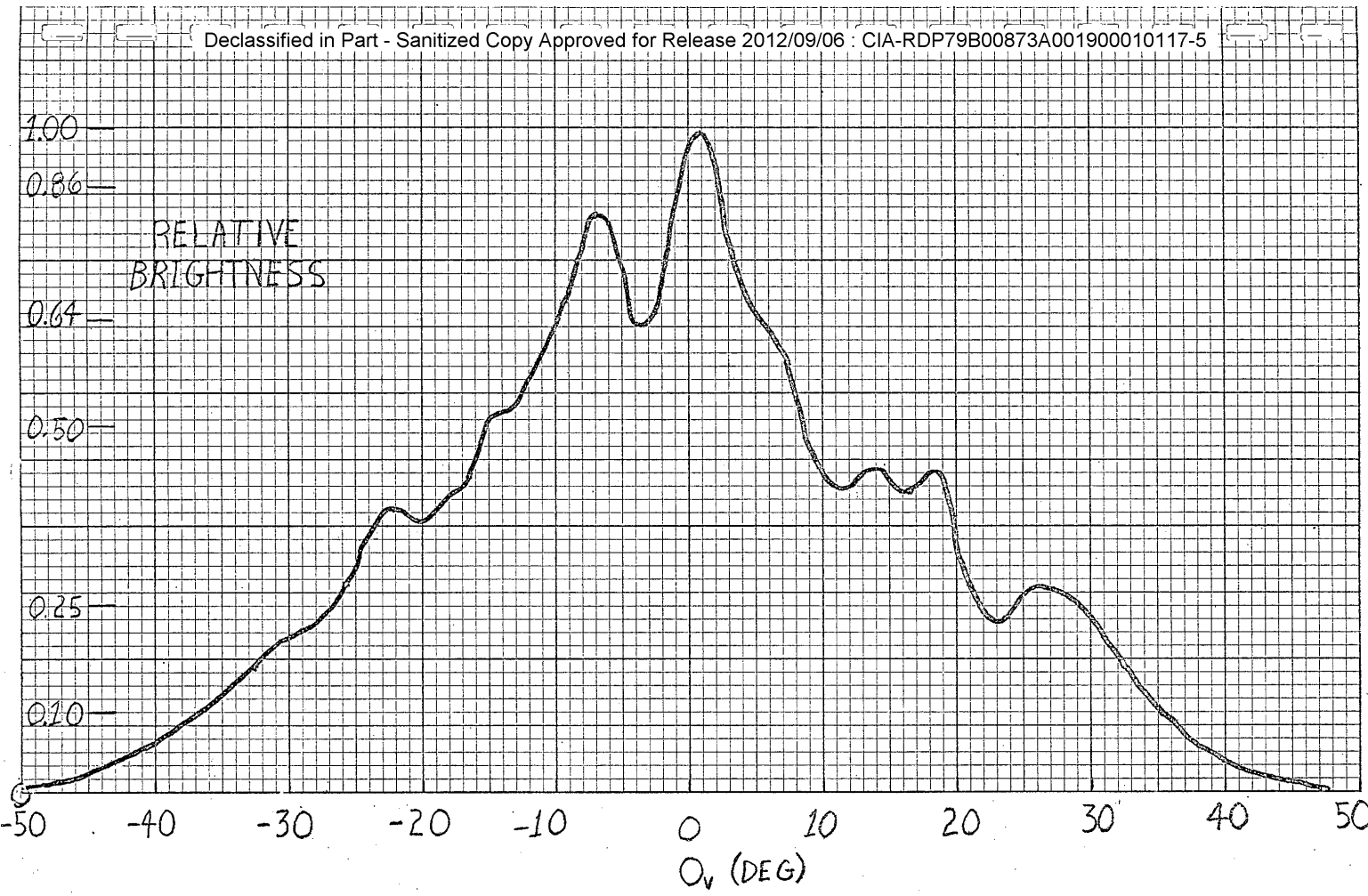

Figure 26: Angular distribution of brightness in horizontal plane. Projector angle zero. Center of screen.

P-19-53, 54, 55 and 56
July 17, 1970

of the lenticule cross section was performed but the imperfections were so small that it was not possible definitely to correlate them with the goniophotometer maxima and minima. Similar examination of diamond ruling point cross sections proved inconclusive also. Improved shaping of new diamond points is planned.

Figures 26 through 29 refer to measurements at the screen center. The sharper cutoffs at the edges of Fig. 27 are characteristic of the vertical distribution, which is produced by the lenticules facing the light source. These are the masked lenticules, and goniophotometer measurements on masked and unmasked sets of lenticules have shown that when the projector angle is zero, the presence of the masking does not change the distribution, i.e., substantially all the light is passing through the clear portion of the mask.

The diagonal scan of Fig. 28 shows a slightly greater angular spread than the vertical or horizontal, a characteristic which is advantageous for a rectangular viewing volume.

In Figure 29 the effect of horizontal projector angle is illustrated. Each curve is plotted versus viewing angle. The full angular width between 1/3 brightness points is actually slightly greater than for the case of zero projector angle. Total bend angle for any given point can be obtained by algebraically adding θ_p to θ_v. The curve for $\theta_p = -8.5^o$ is approximately symmetrical about $\theta_v = 8.5^o$ and similarly for $\theta_p = +8.5^o$. That is, in the horizontal plane the distribution is approximately symmetrical about the projector axis, as in scattering screens.

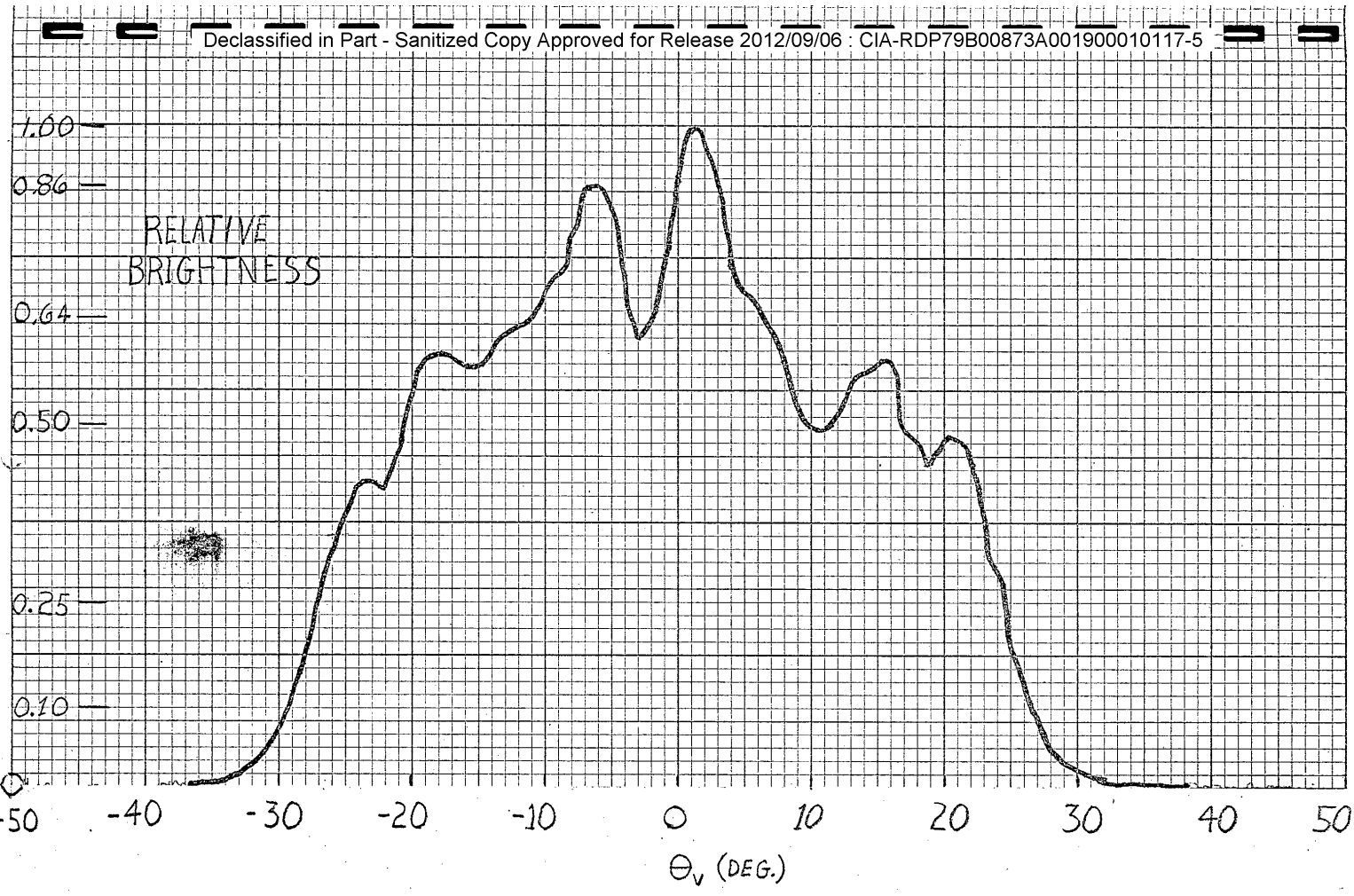

Figure 27: Angular distribution of brightness in vertical plane. Projector angle zero. Center of screen.

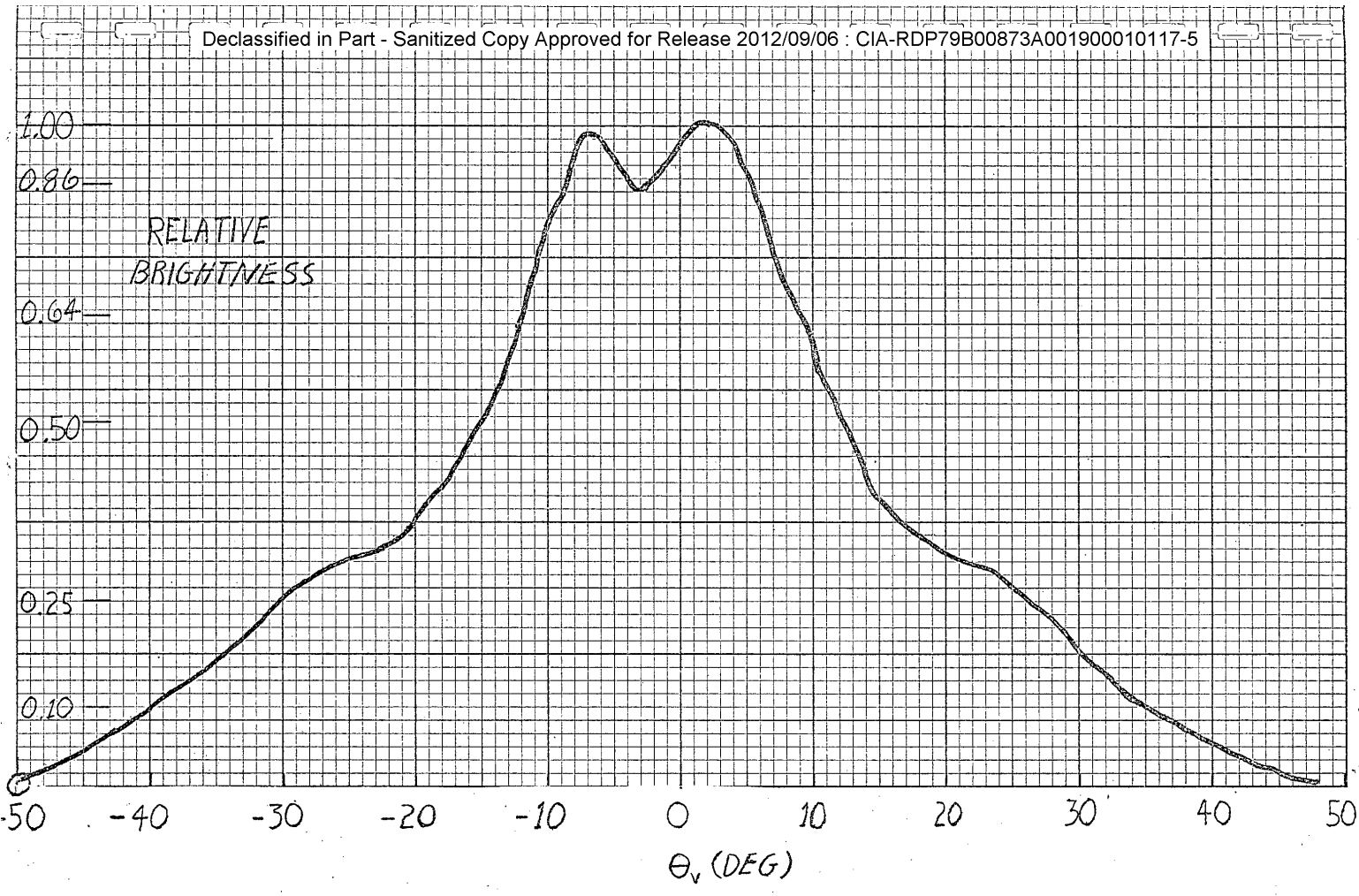

Figure 28: Angular distribution of brightness in diagonal plane. Projector angle zero. Center of screen.

P-19-53, 54, 55 and 56
July 17, 1970

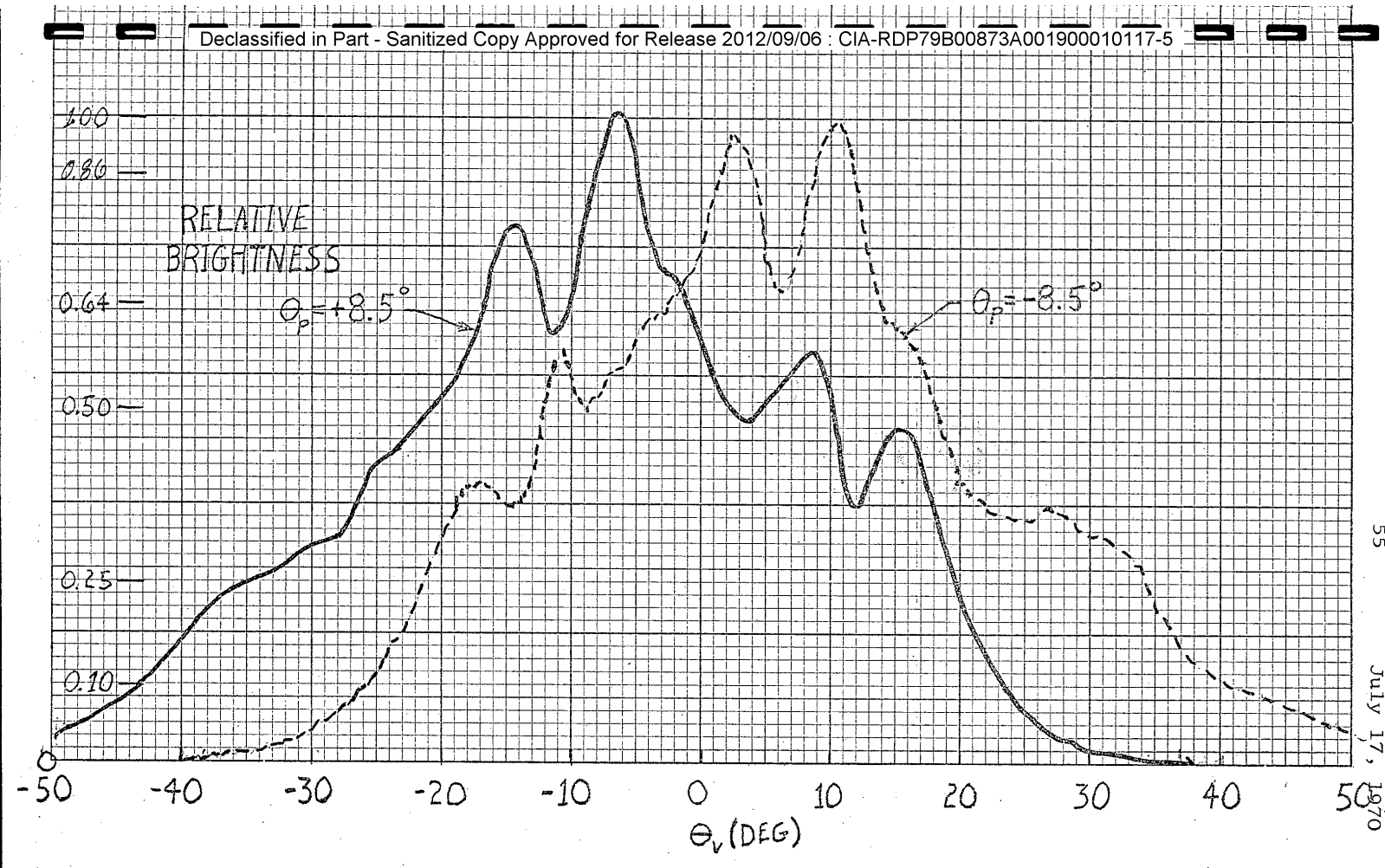

Figure 29: Angular distribution of brightness in horizontal plane. Projector angles $\pm 8.5^{\circ}$ in horizontal plane. Center of screen.

P-19-53, 54, 55 and 56
July 17, 1970

In the vertical plane, however, the distribution can be affected by the masking when the projector angle is changed vertically. The manner in which the mask was originally exposed was such as to simulate these projector angles, with sufficiently wide clear areas to allow some mismatch between projector angle and position on the screen. Figure 30 illustrates the degree to which this technique has succeeded. A vertical scan was made about a point 3" above the screen center with a projector angle of 8.5°. For this case the brightness is plotted versus bend angle θ_B to exhibit the approximate vertical symmetry about the projector axis. Similarly, Fig. 31 shows the diagonal case. Inasmuch as 8.5° is the maximum vertical and horizontal projector angle and 12° is the maximum diagonal projector angle for a 30" x 30" screen 100" distant from the projector lens, these results demonstrate the feasibility of the self-aligning masking technique for this case.

The brightness variation parameter $\theta_{3:1}$ can be defined as the bend angle at which the brightness falls to 1/3 its peak value. In view of the near-symmetry it is convenient to take half the full angle between 1/3 brightness points. Representative values taken from the curves of Figs. 26 through 33 appear in Table VI. The values for LS-60 are taken from Figure 8.

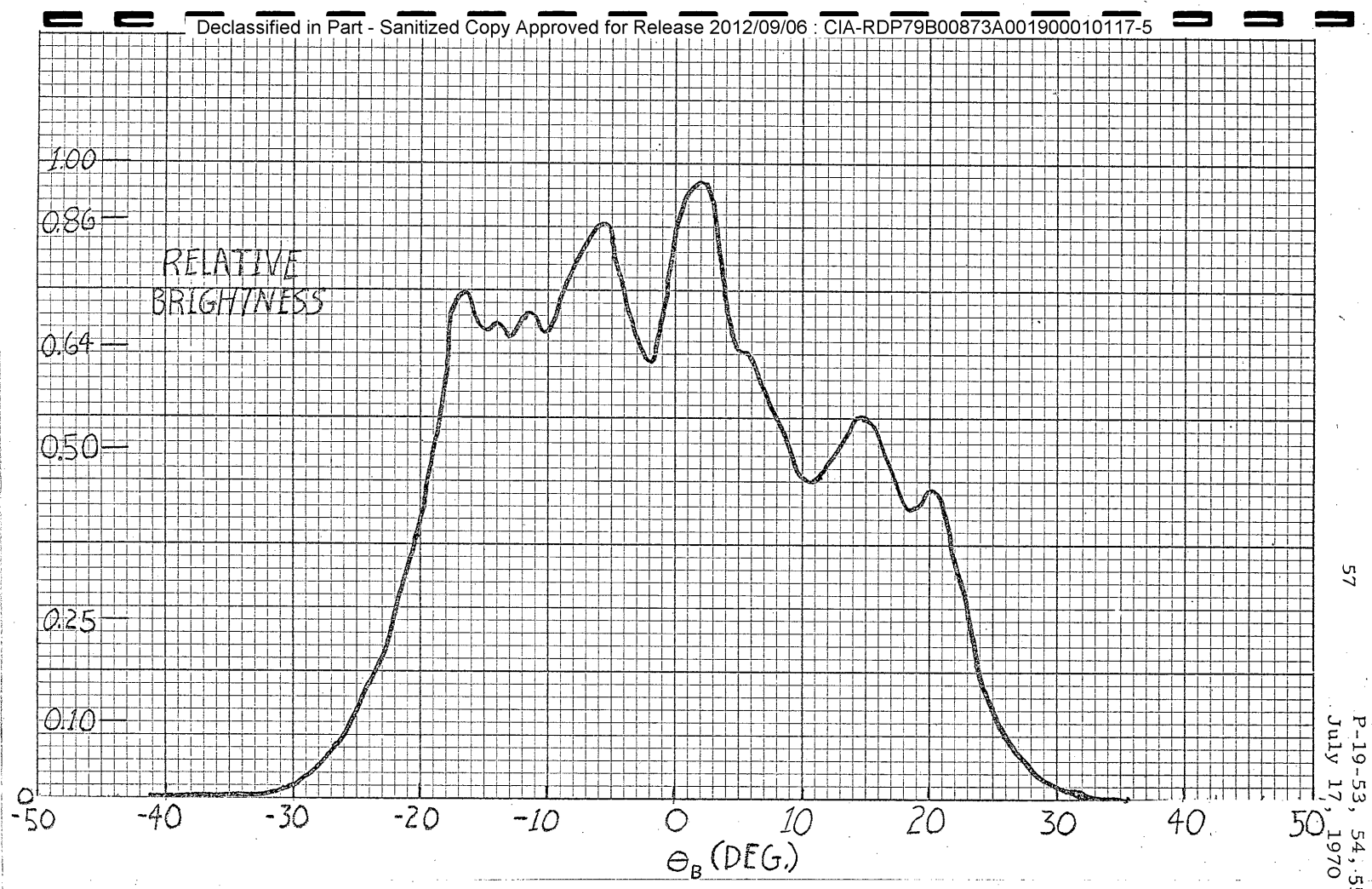

Figure 30: Brightness versus bend angle in vertical plane. Projector angle +8.5° in vertical plane. 3" above center of screen.

P-19-53, 54, 55 and 56
July 17, 1970

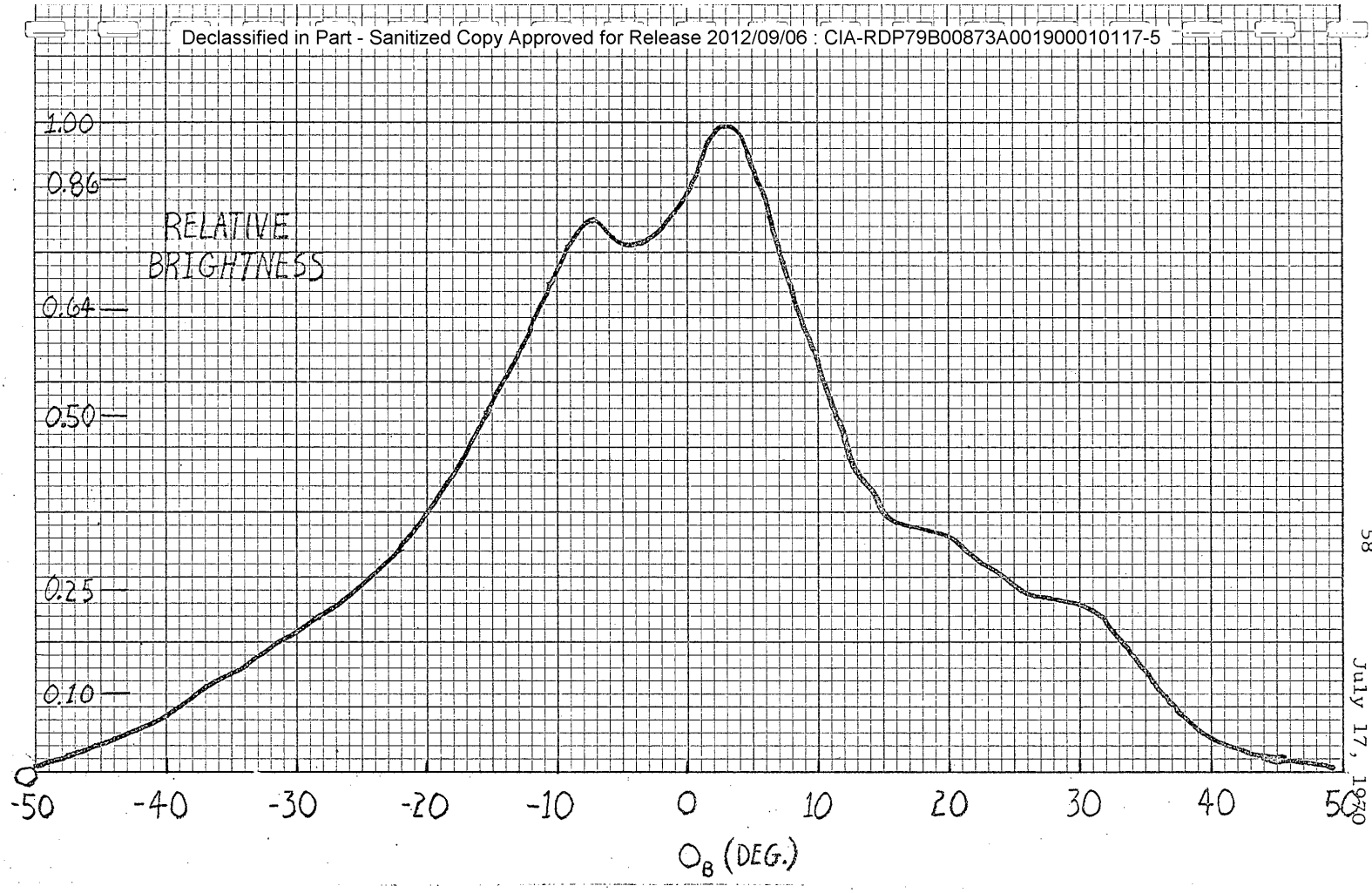

Figure 31: Brightness versus bend angle in diagonal plane. Projector angle 12° in diagonal plane. 4¼" from screen center along diagonal.

P-19-53, 54, 55 and 56
July 17, 1970

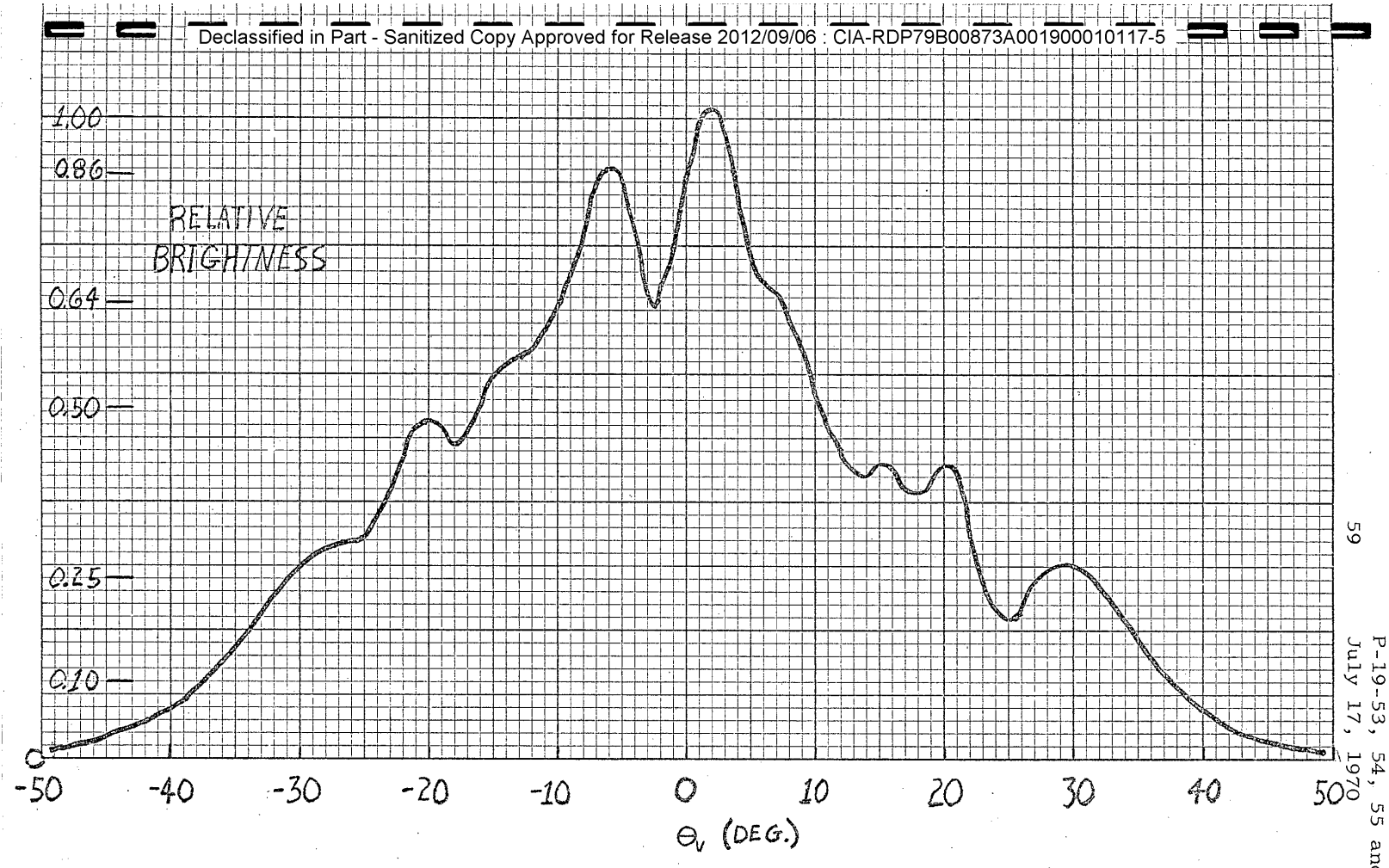

Figure 32: Angular distribution of brightness in horizontal plane. Projector angle zero. 2.8" from screen center along diagonal.

P-19-53, 54, 55 and 56
July 17, 1970

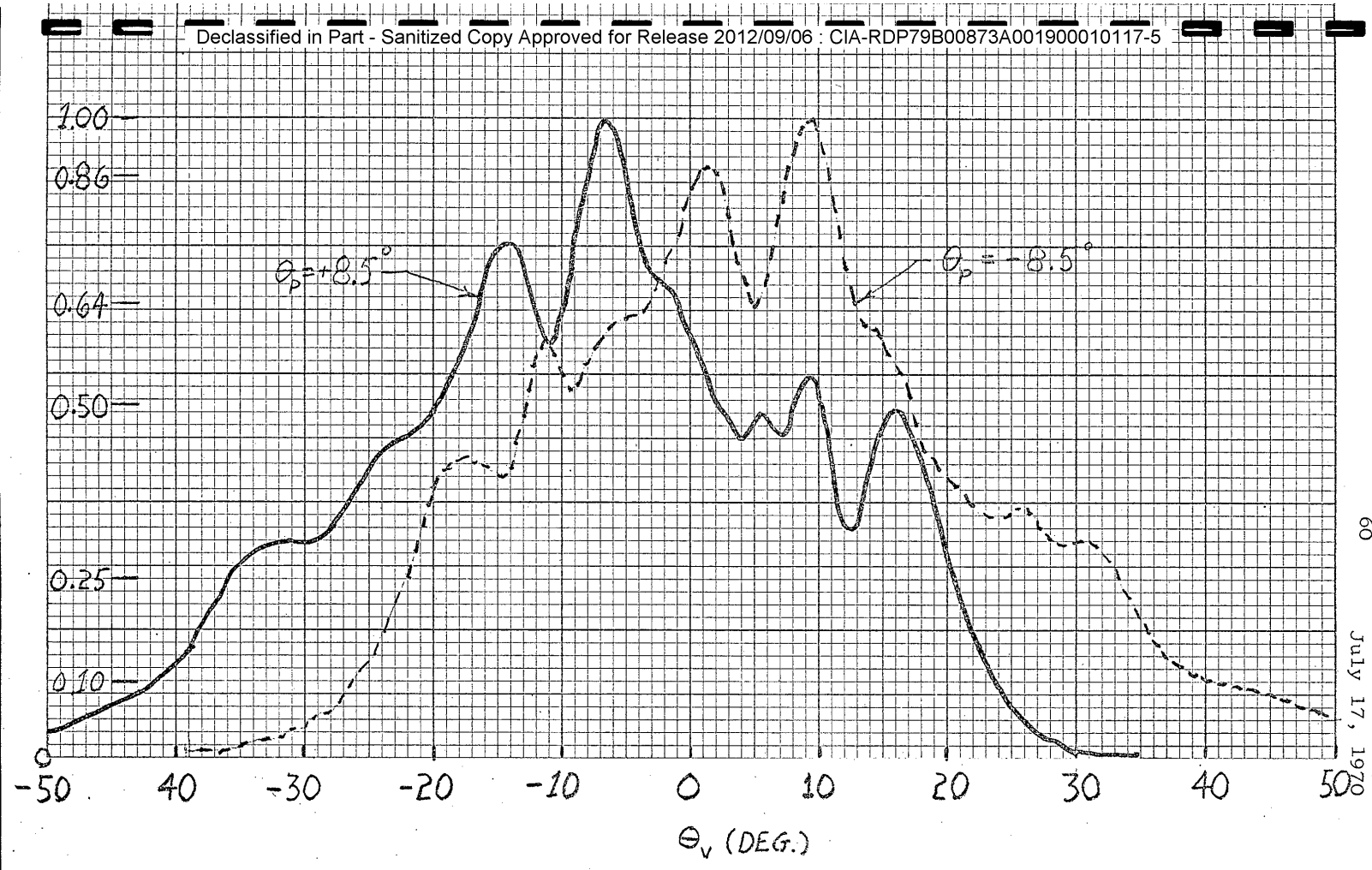

Figure 33: Angular distribution of brightness in horizontal plane. Projector angles $\pm 8.5^{o}$ in horizontal plane. 2.8" from center along diagonal.

P-19-53, 54, 55 and 56
July 17, 1970

4. Efficiency

Transmittances T_{90}, T_{45}, T_{30}, and T_P were measured by use of an integrating sphere, a Xenon arc lamp, with the system spectral response described previously. A very narrow beam of collimated incident light fell on the sample, which was placed at the appropriate distance from a circular or square aperture in the integrating sphere. Taking the thickness and refractive index of the substrate into account for each sample (the LS-60 screen was placed with scattering layer toward source, 1/4" glass substrate toward sphere), the distance to the circular sphere aperture was adjusted so that half-angle cones of $\pm 90^{\circ}$, $\pm 45^{\circ}$, and $\pm 30^{\circ}$ were collected by the sphere. The square aperture collected A $\pm 22^{\circ}$ (across flats) square pyramidal solid angle. The efficiency parameter T_P thus determined is most appropriate for the lenticular screen because of its rectangular light spreading characteristic.

5. Maximum Gain

A direct gain determination was made by measuring the ratio of the input illumination E to the output luminance L. The brightness gain[3] value is given by L/E if L is in fL and E in fc or by πL/E if L is in lm/ft^2 steradian and E in lm/ft^2. A small area A of the screen was illuminated by a measured value of E. The same detector was then used to measure the illumination E′ at a large distance r from the screen. Under these circumstances, the screen luminance is given by

$$L = E'A/r^2$$

and the brightness gain by

$$B = \frac{\pi r^2}{A} \cdot \frac{E'}{E} .$$

This definition of gain is based on a one-sided Lambertian diffuser model. The two-sided Lambertian model used in our previous work (P-19-30)[1] yields just twice this value. The maximum gain for the lenticular screen occurs slightly off axis. Table VI contains the numerical results.

6. Resolution

As mentioned previously, the discrete nature of the lenticules precludes the existence of a unique MTF except under dynamic scanning. However, a suitably standardized square-wave or sine-wave modulation measurement can be useful in comparing screens and serves as an objective analog to the more subjective limit-of-resolution determinations using Air Force resolution targets.

Contact square-wave modulation was measured using a test target, manufactured by Diffraction Limited, Inc., having for each spatial frequency a set of 15 clear bars alternating with 15 opaque bars of the same width. The bar aspect ratio was 10:1. Figure 34 shows the optical arrangement which was designed to simulate incident projector light and the acceptance angle of the eye pupil as nearly as practicable. L_1 was set at the f/22 stop which gave an actual convergence of f/44. L_2 was also set at the f/22 stop yielding an actual acceptance cone of f/25. A smaller acceptance cone reduced the detected power intolerably and produced diffraction spreading.

Under the f/44, f/25 conditions the image of the screen formed at the detector appeared as in Fig. 35, where the cross-hatched and clear bars represent the 6.7 mm^{-1} test target bars. The detector slit was parallel to the target bars and

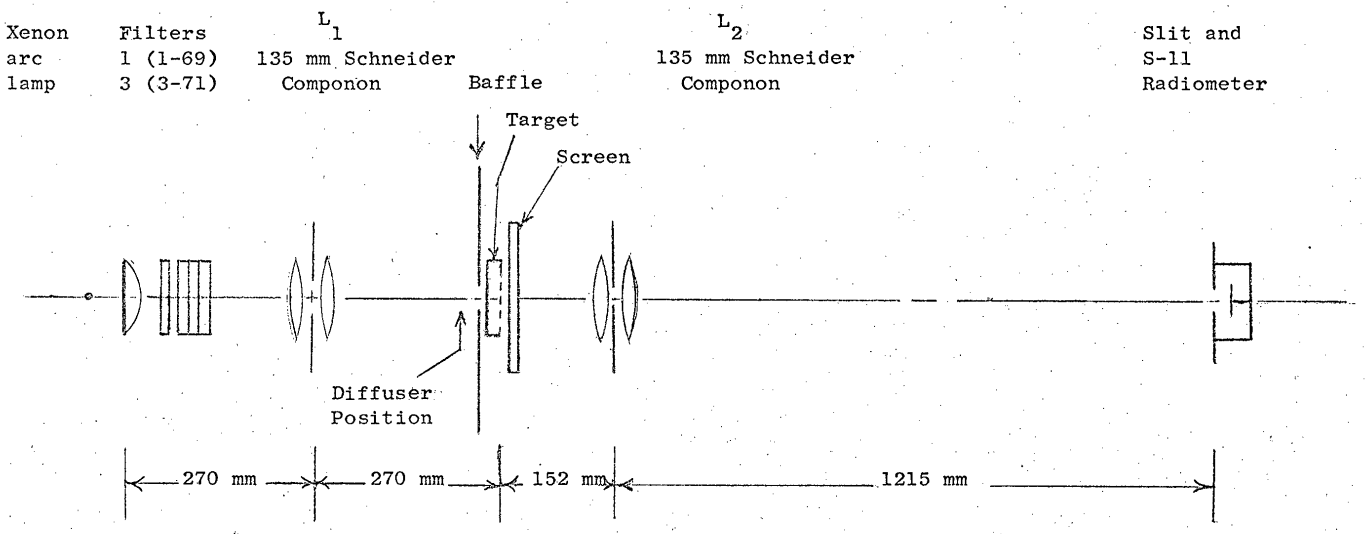

Figure 34: Optical arrangement for measurement of contact square-wave modulation.

P-19-53, 54, 55 and 56
July 17, 1970

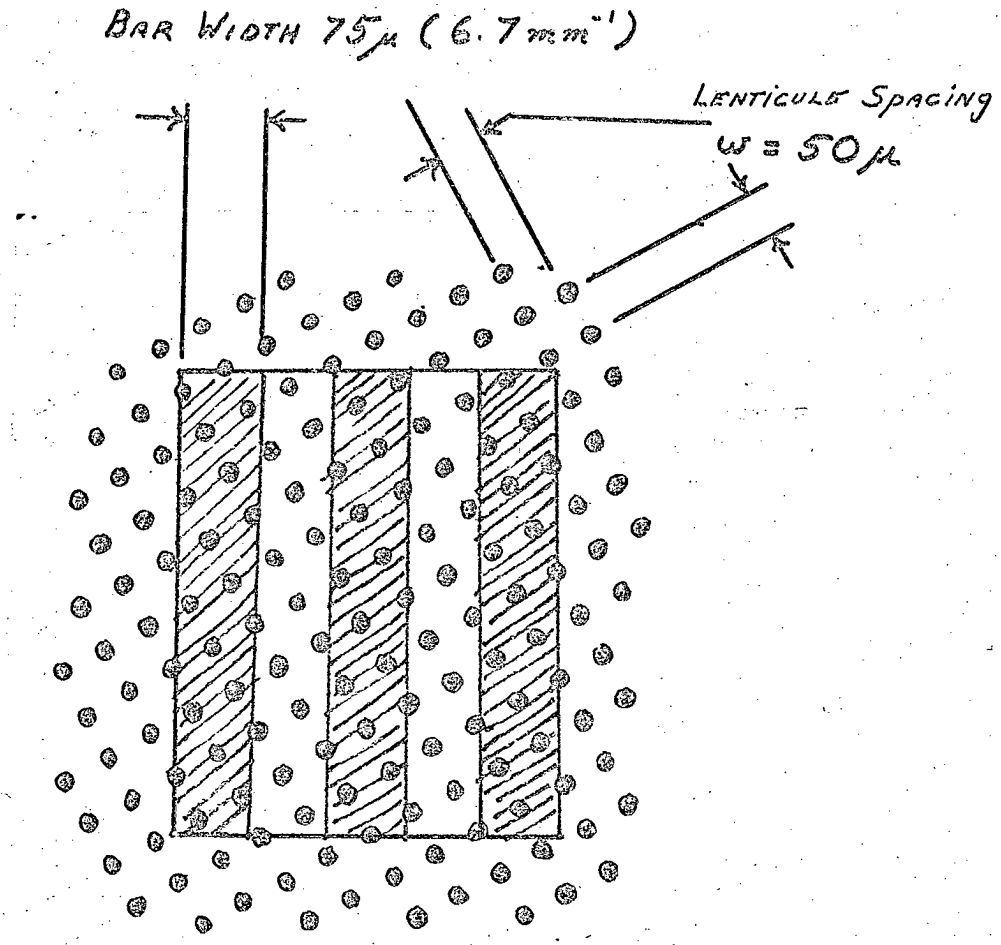

Figure 35. Superposition of test pattern on array of approximately point samples produced by screen.

scanned transversely. It will now be appreciated why the modulation depends on the slit width, the angle between lenticules and bars and the precise location of the test target with respect to the array.

Modulation values were obtained at 1, 5, and 10 mm^{-1} using narrow and wide slits. Although higher modulation values were obtained with narrow slits, the dependence on position and angle was stronger. Results which varied only a few percent upon translating the bar target were obtained using a slit width equal to one half the single bar width. These values are reported in Table VII for various target - lenticule angular orientations and representative combinations of projector angle and bend angle as previously defined in Fig. 25. Each modulation value is the average result for two translational positions of the target and for a given translational position modulation depths for 5 bar pairs were obtained and averaged. The modulation of the measuring system itself was determined by removing the screen and placing a diffuser behind the target in the position shown in Fig. 34. This was done in order to fill the aperture of L_2 in approximately the same manner with and without the sample. The baffle indicated in the Fig. minimized trapped and stray light. In all cases the modulation at 1 mm^{-1} was essentially unity both for S-5 and LS-60.

The minimum value of modulation at 45° orientation is probably a true trend, as it was more dramatic with narrow slits and at 10 mm^{-1} than for the 5 mm^{-1}, wide slit, data shown. The value

Table VII. Square-wave Modulation Values For The Lenticular Screen S-5

Spatial Frequency	Orientation	θ_P	θ_B	Modulation
5 mm^{-1}	0°	0	0	0.96
	5°	0	0	0.96
	20°	0	0	0.94
	30°	0	0	0.93
	45°	0	0	0.92
	60°	0	0	0.92
	90°	0	0	0.94
	20°	0	15°	0.95
	20°	12°	30°	0.94
10 mm^{-1}	0°	0	0	1.05
	45°	0	0	0.88 average
				0.91 maximum
				0.85 minimum

of 1.05 for 10 mm^{-1} at 0^{o} orientation is a symptom of the fact that all the details of this optical system are not yet fully understood. A value of 1.00 would not be unexpected for perfect alignment of mask with lenticules, but this apparent contrast enhancement must be a defect of the system.

With wide slits as above the LS-60 sample provided modulation of 0.98 at both 5 and 10 mm^{-1}. With narrow slits, values of 1.0 at 5 mm^{-1} and 0.95 at 10 mm^{-1} were obtained. Previous measurements (refer to Table V) using a 50 mm Westanar lens for L_2 and a narrow slit had yielded 0.96 and 0.92, respectively. These variations provide a rather accurate picture of the modulation measurement status: comparative results can be quite precise but the absolute values depend on measurement conditions, some controlled and some not controlled.

In connection with the last statement, it may be instructive to cite some projected, as contrasted with contact, square-curve modulation data obtained with the aid of the projector pictured in Fig. 21. A small portion of the Diffraction Limited test target was projected at 10X magnification onto the sample screen and a Westanar 50 mm camera lens was used to project the screen display at 10X magnification onto the slit plane. The slit was much narrower than a target bar. System modulation was determined with screen removed and the ratio of screen modulation to system modulation calculated.

Results for 533 mμ wavelength, 45° lenticule orientation, and an f/18 acceptance cone at L_2, are tabulated below. While it may not be strictly valid to divide by the no-screen modulation, it is reassuring to find projected modulation depths approaching the contact values.

	Modulation			screen mod./system mod.		
	1 mm^{-1}	5 mm^{-1}	10 mm^{-1}	1 mm^{-1}	5 mm^{-1}	10 mm^{-1}
System (no screen)	0.975	0.905	0.730			
S-5	0.975	0.770	0.330	1.00	0.85	0.45
LS-60	0.965	0.750	0.520	0.99	0.83	0.71

7. Contrast Retention

Specular reflectance R_{spec}, interpreted as the zeroth reflected diffraction order, was determined by using the lenticular screen as a reflection grating in an optical system which was equivalent to a grating spectrometer. The zeroth order was easily isolated and the power measured compared to the power detected when the screen was replaced by a mirror. The expected low ratios were obtained, 0.037% for the lenticules in the plane of incidence, 0.018% for lenticules perpendicular to the plane of incidence, and 0.02% for lenticules at 45° to the plane of incidence. LS-60 yielded the reasonable value of 4.6%. The angle of incidence in all cases was 33°.

Diffuse reflectance was measured in a Beckman DK-2 Spectroreflectometer and was 7% throughout the visible spectrum. A sample with no masking measured 12.5% diffuse reflectance.

Trapped light was investigated with the apparatus of Fig. 36. The principle of the measurement is the same as explained in detail in P-19-39. In the new setup the angular acceptance of the receiving lens is much smaller. The exceedingly low α_T value reported in Table VI for S-5 demonstrates that although trapped light can visually be seen to propagate within the screen, very little of it escapes in the axial direction. When the 1" disk was replaced by a 1 mm x 1 mm square and the 1/2" diameter hole by a 1 mm x 1 mm hole, the ratios rose to 0.2% for S-5 and 0.63% for LS-60. Thus in both screens there is evidently a strong dependence of α_T on spatial frequency. This suggests that a more systematic approach to the trapped and ambient light problem would be modulation measurements in the presence of controlled trapped and ambient light.

8. Color Fidelity

The material transmittance spectra of a small lenticular sample and a small LS-60 sample which could be accommodated by the Beckman DK-2 Spectro-reflectometer appear in Fig. 37.

The color variation with bend angle is revealed by two monochromatic goniophotometer scans in Fig. 38 for a single set of lenticules, curved surfaces facing the source. The shift in locations of the maxima and minima for the 400 mμ light as compared with the 589 mμ light are thought to give rise to observed broad color bands, although this has not yet been firmly established.

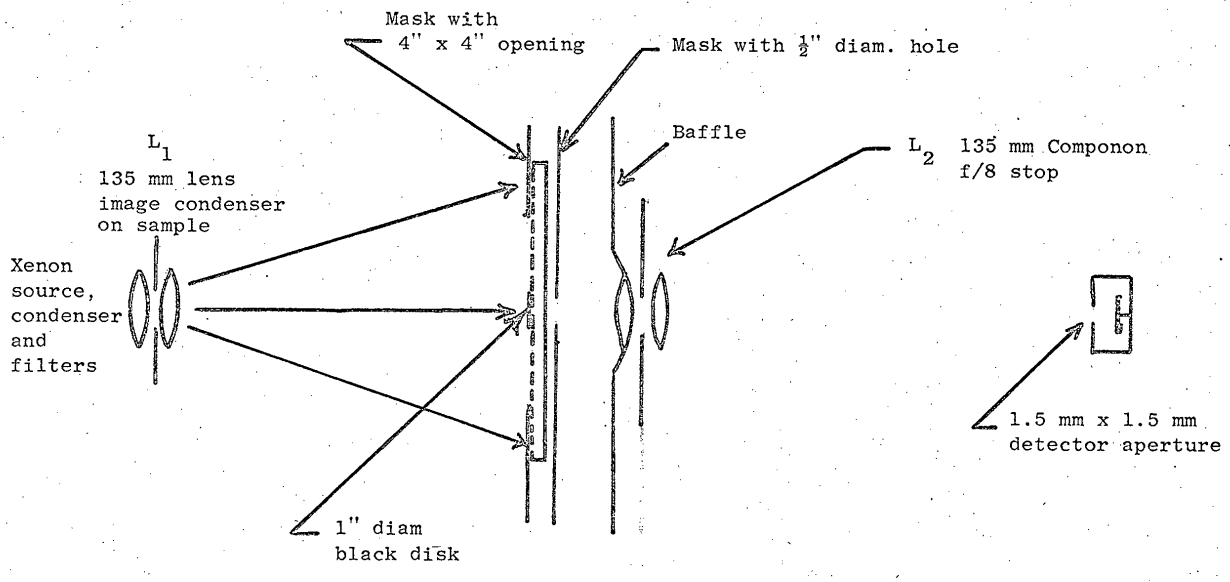

Figure 36: Optical arrangement for trapped light measurement.

P-19-53, 54, 55 and 56
July 17, 1970

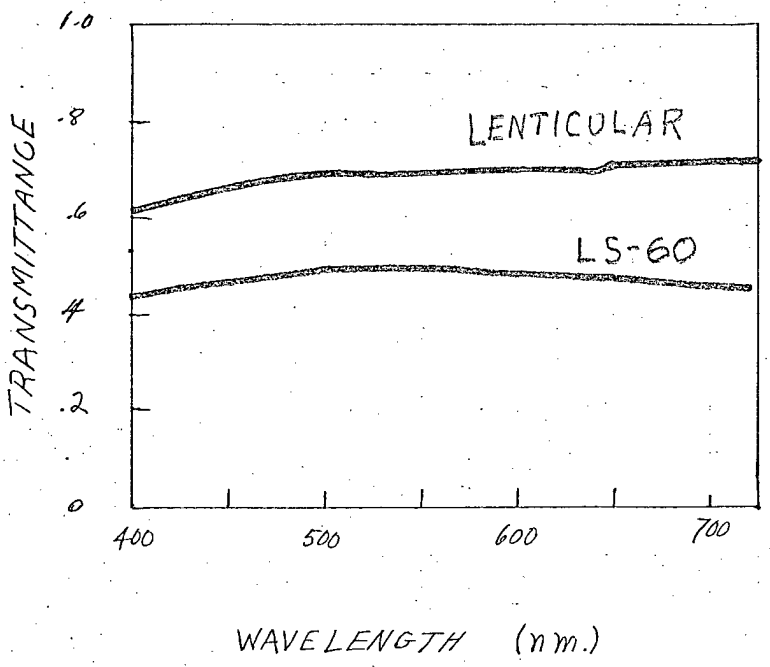

Figure 37. Material transmittance spectra of lenticular screen and Polacoat LS-60.

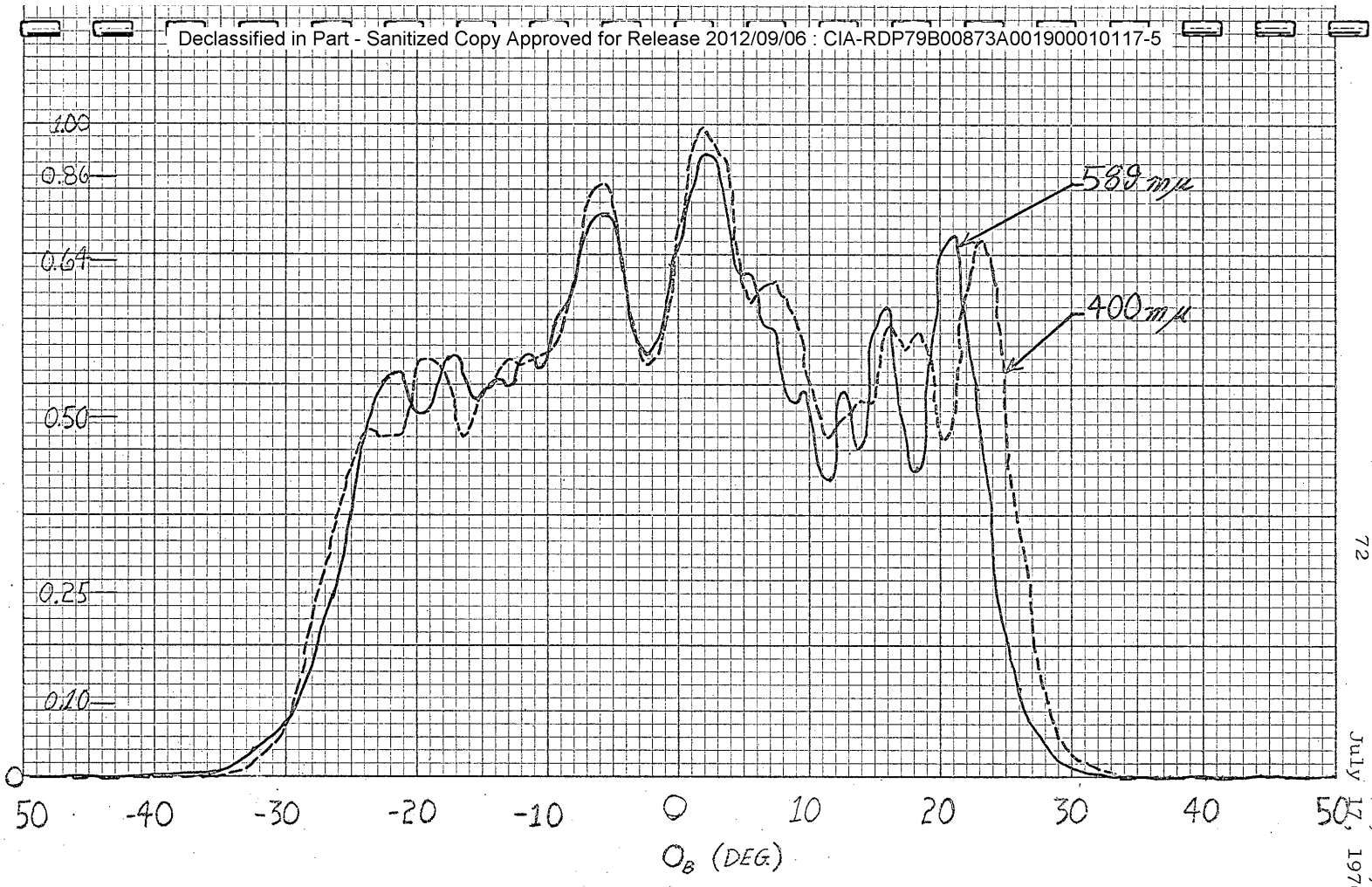

Figure 38: Brightness distribution versus bend angle for a single lenticular sheet with curved side facing source. 400 mμ and 589 mμ wavelengths.

P-19-53, 54, 55 and 56
July 17, 1970

9. Optical Quality and Extraneous Effects

The central several orders of the diffraction pattern were investigated to determine how the zeroth order compared in intensity with the others. An arrangement equivalent to a transmission grating spectrometer was set up with the lenticular screen as grating and sufficient resolution to distinguish the orders. Source filters, and detector were as in Fig. 24. The result of scanning across these orders can be seen in Fig. 39. The goniophotometer curve is shown for comparison. There is evidently no prominence of the zeroth order, which prominence might be considered as a type of specular transmittance.

Thus far, scintillation and optical uniformity have been observed only visually. However, scanning electron photomicrographs were made to determine what defects might be present in the epoxy lenticules and the polypropylene molds. Figure 40A shows the epoxy lenticule cross section. Figures 40B and C are photomicrographs taken along the lenticules or grooves at an angle of 75^{o}. This technique shows up on undulation in the groove depth (or lenticule height) which we believe to be associated with chatter of the diamond point during ruling of the aluminum master. Removal of these undulations in future rulings is expected to reduce scintillation.

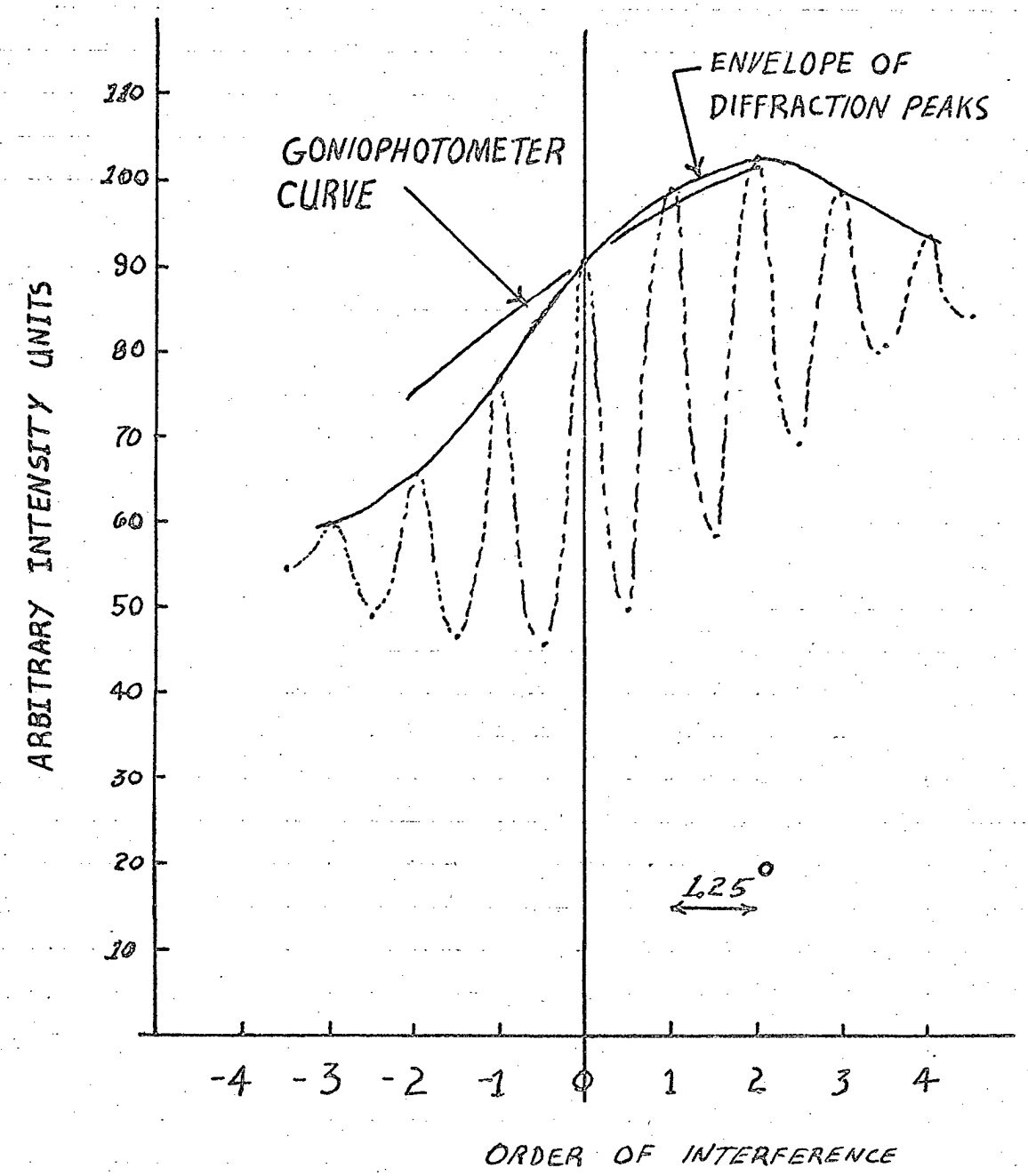

Figure 39. High resolution scan across central several orders of diffraction pattern.

A
100X

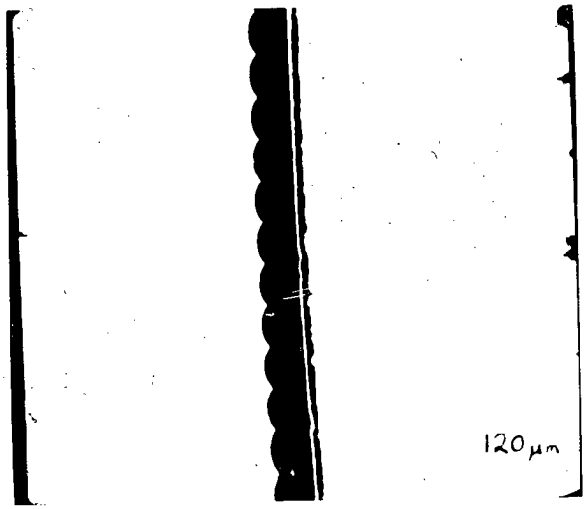

B
1000X

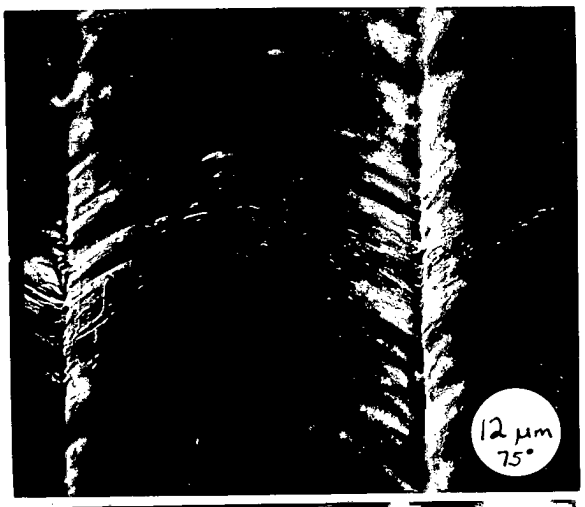

C
3000X

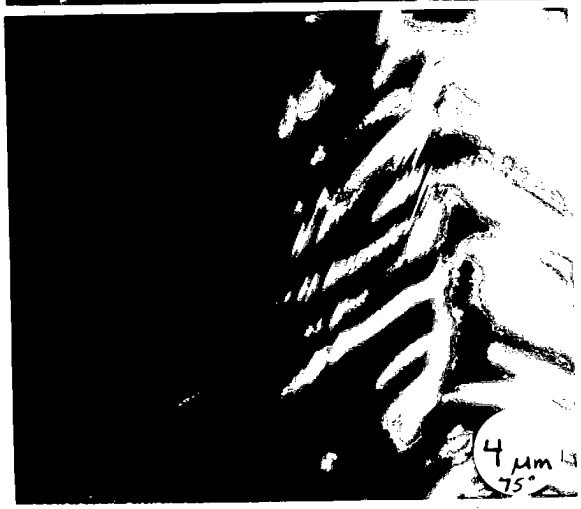

Figure 40: Scanning electron photomicrographs.
A. Cross section of epoxy lenticules on 2-mil polyester sheet.
B. Single epoxy lenticule viewed at 75° to the substrate normal.
C. Polypropylene mold near cusp, viewed at 75°.

V. POTENTIAL FOR IMPROVEMENT OF LENTICULAR SCREENS

While the feasibility and superior performance have been demonstrated, the feasibility sample exhibits some defects and design imperfections. Methods of overcoming the defects and improving the design have been conceived in most cases. The diffraction pattern is an obvious and serious defect. This pattern and its visibility under various viewing conditions is analyzed in some depth in Appendix A. The solution is to randomize the vertexes of the lenticules, as discussed and analyzed in Appendix B, and perhaps to slightly modify the shape of the projection lens pupil. There is no real doubt that the diffraction pattern can be sufficiently suppressed but data on the light distribution in the projection lens pupil and on color film that might be used is needed to ensure that sufficient suppression is provided. Considerable computation will be needed to select and verify a suitable "randomization" pattern. This pattern must be chosen for compatibility with the machine used to make the initial ruling. The machine used to make the feasibility sample can provide multiples of 10 microinches of depth control.

When the screen is illuminated by a projector with an empty gate a slight scintillation is apparent. This is due primarily to irregularities in the lenticules as seen in Fig. 40 . These irregularities originate in the ruling. Therefore improving the ruling by better shaped diamonds and lower cutting speeds will reduce the scintillation somewhat. Control of the thickness of epoxy between the mold cusps and photographic film will also help.

Careful photographic processing and reversing will prevent photographic graininess in the lenticule windows.

The angular coverage is less than desirable. More optical analysis of various shapes of lenticules, the two sets being of different shapes, is needed to provide a design to give the required coverage and degree of brightness variation and to give satisfactory masking. The optical design must be tailored to the projector and viewing geometry requirements for best results. Our current knowledge of these requirements indicates that an elliptical lenticule shape of minor to major axis diameter of 0.75:1 is required for the lenticules facing the projection lens. The sharp end of the ellipse faces the projection lens. Projector light is focused sharply at the second focus of the ellipse where the mask is located. For 0.002" lenticule pitch and to provide the required angular coverage a thinner film is needed. A suitable film on 0.0015" Estar® base is available from Kodak against a special order. A special machine to finish diamonds to shape is desirable and can be built. This machine should be able to finish the diamond to any smooth convex curve required. In general it is desirable to increase the refractive index of the lenticules, particularly the second set, to reduce the curvature needed to obtain the light spreading required. A tailored design will automatically minimize the trapped light as will the narrower windows permissible with the elliptically shaped lenticules which correct for spherical aberration.

Light transmission will be maximized by the tailored optical design and provision of anti-reflection coatings will both reduce surface reflection and increase transmission. Plastic lenticules will permit only soft coatings which require careful handling and cleaning.

The irregularities in the angular distribution curves, Figs. 26 through 33, are believed to be associated with minor imperfection in shaping of the diamonds. Shaping can be improved by building a special diamond finishing machine. The irregularities vary slightly with wavelength, Fig. 38 correlating with observed color bands. It is noticeable that the color bands due to the masked lenticule set are limited to the edge of the angular coverage whereas the bands due to the second set of lenticules extend over more of the total angular coverage. The exact origin of the bands is not known but if the origin is in the lenticule shape, improvements will eliminate the color bands. Another cure will have to be devised if the color band origin is not in the lenticule shape.

Methods of achieving a size of 30" x 30" are an important consideration. The maximum sized ruling area of 15" x 18" available from the existing machine limits the size of the current fabrication method to 15" x 15". Modified handling of the existing machine can result in 15" x 30" rulings. By parqueting two nickel replicas a nickel ruling of 30" x 30" can be generated. Further minor changes can produce 31" x 31" nickel rulings. Adequate width film can be ordered and no difficulty in locating a large heated platen

polypropylene molding machine is expected. It would be possible to build a version of the present ruling engine capable of ruling 31" x 31" at a practical cost in about one year. Thus, generally the present method can be stretched to 31" x 31". Because of the toughness and higher refractive index available with glass it is advisable to investigate the feasibility of glass lenticular screens. The advantages are most significant for the lenticules facing the viewer so that a plastic masked lenticule set combined with a glass unmasked lenticule set may be a good combination.

VI. CONCLUSIONS

Work on the 2-mil plastic crossed cylindrical lenticular screen approach has sufficiently progressed that we believe the fabrication and use of such screens in a 30" x 30" size to be practicable. Superior performance has been demonstrated in 6" x 6" feasibility samples. These screens are more than twice as bright as the best competing conventional diffusing-type screens, retain contrast, and therefore resolution, much better under ambient light, and have nearly as high resolution. Increasing the angular coverage, improving the optical quality, and eliminating the diffraction pattern and other spurious effects appears feasible. Glass should be investigated as an alternative material because of its versatility with respect to refractive index, durability and other physical properties.

References

1. R. B. Herrick and R. F. Adrion, Improved Screen for Rear-Projection Viewers, Final Technical Report P-19-30, January, 1968.

2. C. H. Graham, Vision and Visual Perception (John Wiley and Sons, Inc., New York, New York) p. 391.

3. H. R. Luxenberg and R. L. Keuhn, Display Systems Engineering (McGraw-Hill, New York, 1968) p. 294.

4. P-19-31 through P-19-55 are periodic technical reports written for the present contract under the title "Improved Screens For Rear-Projection Viewers." P-19-47 and P-19-48 include the Boeing report as an appendix.

APPENDIX A

Diffraction Effects in Lenticular Rear-Projection Screens

As a model for a two-dimensional lenticular rear-projection screen we consider a square opaque screen which contains a large number of identical and similarly oriented small apertures. The apertures are centered on a matrix of points (x_n, y_m), $n,m = 0,1, \ldots N-1$, so that the total number of apertures is N^2, and the spacing between adjacent points is d. (See Fig. A1). Light of wavelength λ from a monochromatic point source at $P_o(x_o,y_o,z_o)$ is incident on the screen, which is in the x-y plane, and the diffracted light is observed at the point $P(x,y,z)$. Each small aperture has an amplitude diffraction pattern which we denote by $U_a(p,q,\lambda)$, where $p=1-1_o$, $q=m-m_o$, and the first two direction cosines for P_o and P are $1_o=\cos\alpha_o$, $m_o=\cos\beta_o$, $1=\cos\alpha$, and $m=\cos\beta$. Now when light from P_o is incident on the screen, the field amplitude at point P due to light diffracted by a small aperture at (x_n, y_m) is[1]

$$U_{nm}(p, q, \lambda) = U_a e^{ik(px_n + qy_m)} \qquad (1)$$

where $k = 2\pi/\lambda$. In eq. (1) we have assumed Fraunhofer diffraction and have omitted constant phase terms, since these will not affect the field intensity. To get the total amplitude at point P we sum over all the small apertures:

$$U(p,q,\lambda) = U_a \sum_{n=o}^{N-1} \sum_{m=o}^{N-1} e^{ik(px_n+qy_m)} \qquad (2)$$

1. For numbered references see page VII - 9.

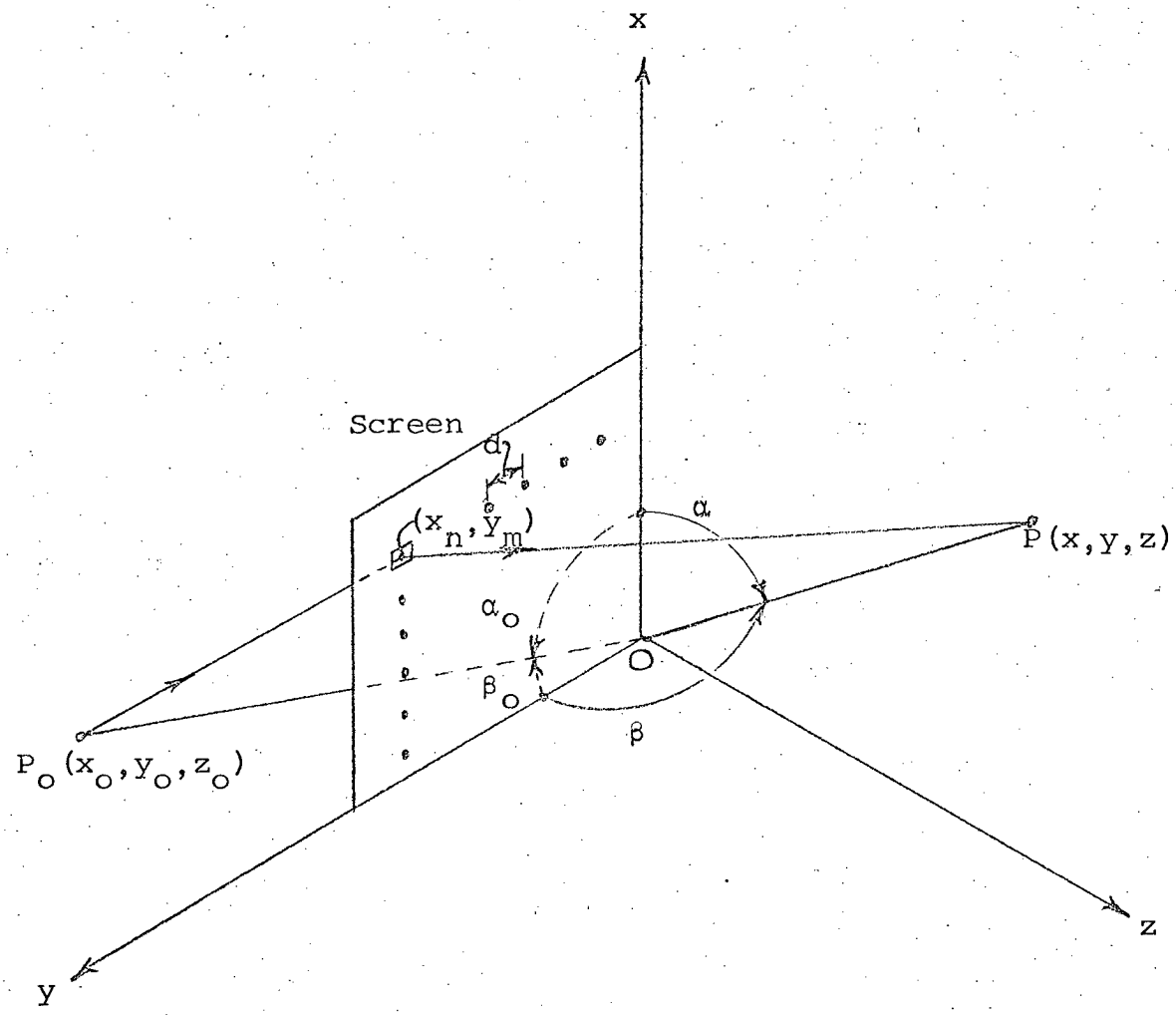

Figure A1. Model for calculating the diffraction pattern of a lenticular screen.

Now we have $x_n = nd$ and $y_m = md$, so that eq. (2) becomes

$$U(p,q,\lambda) = U_a \sum_{n=o}^{N-1} e^{inkdp} \sum_{m=o}^{N-1} e^{imkdq} \qquad (3)$$

If the sums are performed in eq. (3), the definitions of p and q used, and the modulus of U is taken, we get the field intensity as

$$I(1,m,1_o,m_o,\lambda) = I_a(1-1_o, m-m_o, \lambda) \frac{\sin^2\left|\frac{1}{2}Nkd(1-1_o)\right| \sin^2\left|\left(\frac{1}{2}Nkd(m-m_o)\right|\right.}{\sin^2\left|\frac{1}{2}kd(1-1_o)\right| \sin^2\left|\left(\frac{1}{2}kd(m-m_o)\right|\right.} \qquad (4)$$

Eq. (4) gives the field intensity in direction (1,m) due to a monochromatic point source (wavelength λ) located by $(1_o, m_o)$. The field intensity I is in fact the Fraunhofer diffraction pattern of a two-dimensional diffraction grating consisting of N x N apertures, each of which has diffraction pattern I_a. In general I_a is broad in angular extent so that it serves as the envelope of the diffraction pattern I and determines the maximum viewing angle of the screen.

The principal maxima of I occur at observation directions (1,m) which satisfy both

$$1-1_o = k_1 \frac{\lambda}{d}, \; k_1 = 0,1,2, \ldots .$$

and (5)

$$m-m_o = k_2 \frac{\lambda}{d}, \; k_2 = 0,1,2, \ldots .$$

The angular width of these maxima is approximately

$$\Delta\theta \simeq \frac{\lambda}{Nd} \qquad (6)$$

and is very small for large N and d. From eq. (4) we find that the height of these maxima is about $N^4 I_a|_{max}$, and the remainder of the pattern is only a few percent of this, so that the pattern modulation is large.

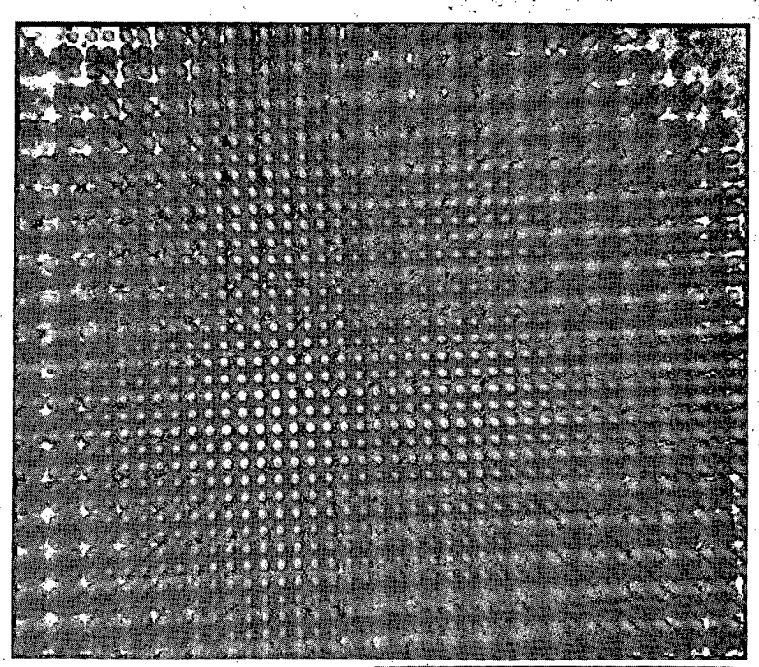

Figure A2

Lenticular screen diffraction pattern with small projection lens pupil and narrow-band light.

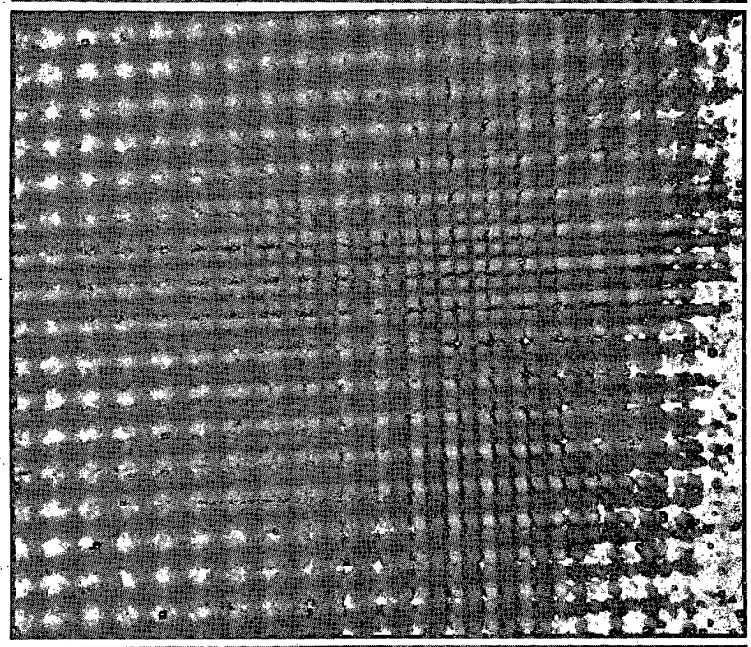

Figure A3

Lenticular screen diffraction pattern with small square projection lens pupil.

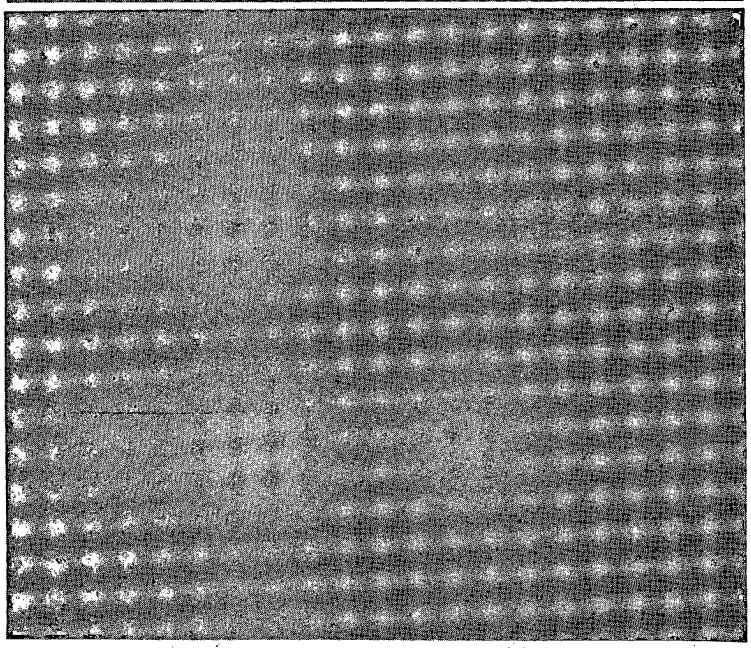

Figure A4

Lenticular screen diffraction pattern smoothed by a large projection lens pupil.

A photograph of the diffraction pattern I of a lenticular screen with $d \sim 50$ microns and $N \sim 3000$ is shown in Fig. A2. This photograph is essentially a visual representation of eq. (4). The diffraction pattern is a virtual image that appears to emanate from the vicinity of the "point" source, which was obtained by inserting a small aperture in the exit pupil of the projection lens in a conventional projection system. Narrow-band light centered at $\lambda = 0.53$ microns was obtained by using an interference type bandpass filter. Each spot in the pattern may be considered as a separate image of the point source.

Now under normal conditions of use, the screen will be illuminated by a broadband, extended virtual source which appears in the exit pupil of the projection lens. First, consider the effect on the diffraction pattern of an extended, incoherent source. The source may be viewed as composed of a large number of point sources, each of which generates a diffraction pattern given by eq. (4). The total intensity is just a superposition of the intensities due to each of the point sources. Therefore if we let $B_s(l_o, m_o, \lambda)$ represent the intensity distribution of the virtual source in the projection lens exit pupil, the total intensity is

$$I_1(l,m,\lambda) = \iint_{\substack{\text{proj. lens} \\ \text{pupil}}} dl_o \, dm_o \, B_s(l_o, m_o, \lambda) \; I\,(l, m, l_o m_o, \lambda) \qquad (7)$$

where I is given in eq. (4). The integral in eq. (7) can be evaluated numerically, but for our purposes the general features of the result are adequate. Study of eqs. (5) indicates that as

the location of the point source (l_o, m_o) changes to $(l_o+\delta, m_o+\delta)$, then the location of the maxima in the diffraction pattern shift from (l,m) to $(l+\delta, m+\delta)$. Thus if (l_o, m_o) ranges over the lens exit pupil, we see that each of the maxima maps out an image of the exit pupil. So we expect the diffraction pattern to consist of an array of images of the projection lens exit pupil. Figure A3, a photograph of the diffraction pattern when a square aperture was inserted in the exit pupil, verifies this. This is a useful result because now we see that by increasing the angular size of the lens exit pupil, we can begin to fill in the dark areas between the principal maxima. If the exit pupil is made large enough, the various images of the pupil overlap, smoothing out the intensity variations in the diffraction pattern and thus decreasing the modulation. This is shown in Fig. A4.

Next, the effect of a broadband source can be computed in principle by multiplying I_1 by the source spectral distribution $S(\lambda)$ and integrating over λ:

$$I_2(l,m) = \int d\lambda \; S(\lambda) \; I_1 \; (l,m,\lambda) \qquad (8)$$

As before, we can obtain the general features of this result without actual evaluation. From eqs. (5), when λ changes by $\delta\lambda$, the maxima of the diffraction pattern move from (l,m) to $(l + \frac{k_1}{d}\delta\lambda, \; m + \frac{k_2}{d}\delta\lambda)$. Thus each wavelength component of the source gives rise to a diffraction pattern which is angularly displaced compared to the patterns due to other wavelengths. Thus for a broadband, extended source, the diffraction pattern

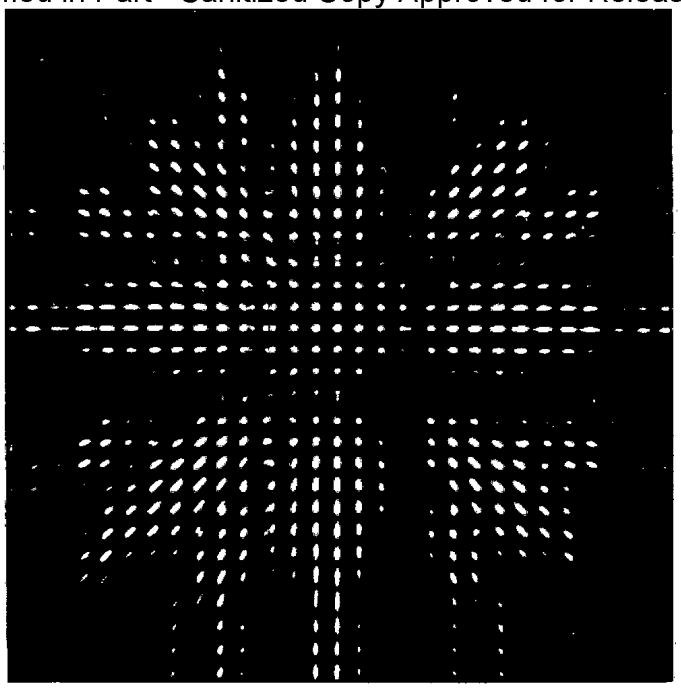

Figure A5

Lenticular screen diffraction pattern due to white light with a small projection lens pupil.

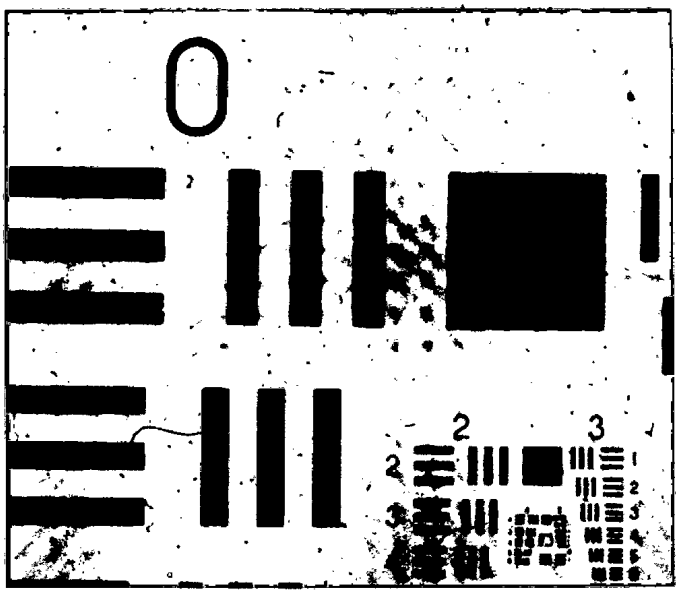

Figure A6

The diffraction pattern due to white light and small pupil is out of focus when the camera is focused on imagery.

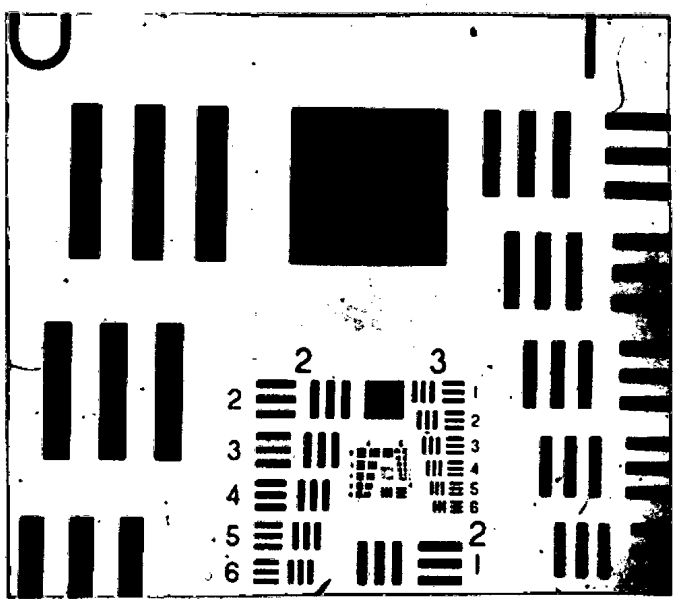

Figure A7

The diffraction pattern is not visible when a large pupil and white light are used and the camera is focused on imagery.

consists of the superposition of many arrays of exit pupil images, with one array for each wavelength component of the source. Also from eqs. (5), we see that the spacing of the pupil images increases with λ and that long wavelength images should be located farther from the center of the pattern than corresponding short wavelength images. At the pattern center $k_1 = o = k_2$ [(see eq. (5)], the wavelength dependence vanishes, and a single white image of the exit pupil appears. All this is verified by the photograph in Fig. A5 which shows the screen diffraction pattern for a broadband source with a small circular aperture placed in the lens exit pupil. No attempt was made to match the film spectral response to that of the eye, but the general trends are evident.

The photographs in Figs. A2, A3, A4 and A5 were made with no imagery on the lenticular screen and with the camera focused on the diffraction pattern. Since the diffraction pattern appears as a virtual image near the projection lens exit pupil, the diffraction pattern and any screen imagery cannot in general be simultaneously focused by any imaging instrument such as a camera or the eye. Figure A6 is a photograph of a lenticular screen with imagery. This is a worst case, since a <u>small</u> aperture was placed in the projection lens exit pupil to generate a diffraction pattern identical to that shown in Fig. A5. However, in Fig. A6 the camera was focused on the screen imagery, and so the diffraction pattern was defocused considerably.

Figure A7 is a color photograph made under similar conditions, except that the lens exit pupil was made large so that considerable overlapping of the pupil images in the diffraction pattern occurred. Figure A7 shows that the combined effect of pupil image overlap and defocusing of the diffraction pattern is that the modulation and color in the diffraction pattern are much less noticeable.

We can get an estimate of the amount of defocusing of the diffraction pattern, as seen by an observer, by utilizing the geometrical optics expression for the modulation transfer function (MTF) of a defocused, ideal lens[2]:

$$\text{MTF}\ (v) = \frac{2J_1\ (\pi Bv)}{\pi Bv} \qquad (9)$$

where J_1 is the first order Bessel function, B is the diameter of the blur circle produced by defocusing, and v is the spatial frequency. In our case the lens under consideration is that of the human eye. Newton's formula for the conjugate points of a compound lens is[3]

$$xx' = f_1 f_2 \qquad (10)$$

where f_1 = first focal length, f_2 = second focal length, x = object distance measured from first focal plane, and x′ = image distance measured from second focal plane. For the human eye we have f_1 = 17 mm and f_2 = 23 mm, approximately[4]. Also, the pupil diameter of the eye is D = 4 mm typically, and the image space refractive index is n = 1.33, the refractive index of the vitreous humor.

For an observer with eyes focused on screen imagery at a distance of x_i = 254 mm (10"), we calculate from eq. (10) that x'_i = 1.5 mm. Assuming that the distance from the observer to the projection lens exit pupil is x_d = 3 m, then for the diffraction pattern eq. (10) gives x_d' = 0.1 mm. The defocusing distance is then $\delta = x_i' - x_d'$ = 1.4 mm. The distance δ is large enough so that the optical path difference to different regions of the blur circle exceeds one wavelength, thereby justifying our geometrical optics approach. The blur circle diameter is given by

$$B \simeq \delta \frac{D}{f_2} = 0.24 \text{ mm} \qquad (11)$$

If the screen has lenticule spacing $d \simeq 50\ \mu$, and we take light wavelength $\lambda \simeq 0.5\ \mu$, then the diffraction pattern maxima are angularly spaced by $\delta\theta = \frac{\lambda}{d}$ radians. The spatial frequency of the diffraction pattern image in the eye is then

$$v = \frac{n}{f_2\, \delta\theta} = \frac{nd}{f_2 \lambda} = 5.9 \text{ cycles/mm} \qquad (12)$$

The MTF of the eye for this defocused diffraction pattern is then

$$\text{MTF } (5.9) = \frac{2J_1 \left|(\pi)\ (0.24)\ (5.9)\right|}{(\pi)\ (0.24)\ (5.9)} = -\ 0.10 \qquad (13)$$

Thus defocusing reduces the perceived diffraction modulation to only 10% of its actual value, and so the pattern modulation is much less noticeable in Figs. A6 and A7. The minus sign in eq. (13) indicates that the defocused image has undergone contrast reversal.

As a second example, suppose the observer is farther from the screen, say 508 mm (20"). Then using eqs. (9) — (12) we get

$$MTF\ (5.9) = 0.51 \qquad (14)$$

For this case the perceived modulation remains at 51% of its actual value. This indicates that the farther the observer is from the screen, the more noticeable the diffraction pattern will be. It will also be appreciated that the use of a magnifier to inspect imagery will suppress the diffraction pattern.

References

1. Born & Wolf, Principles of Optics, Pergamon Press, 1964, p. 400.

2. Smith, Modern Optical Engineering, McGraw-Hill, 1966, p. 320.

3. Rossi, Optics, Addison-Wesley, 1957, p. 82.

4. Military Standardization Handbook, Optical Design, 5 Oct. 1962, p. 4-4.

APPENDIX B

Analysis of Lenticule Periodicity

The necessity of randomizing a fine lenticular array in order to break up the diffraction spectrum was recognized early in the lenticular screen program. Practically it is easier, and may be sufficient, merely to modify the periodicity of the array. We found that a 250-micron spacing produced no observable diffraction effects and a 50-micron spacing did produce an observable diffraction pattern. The absence of the pattern in the 250-micron case results mainly from its wide lenticule spacing, which produces orders of diffraction too closely spaced for visual observation except under highly coherent conditions. If a suitable 250-micron periodicity can be superimposed on the 50-micron periodicity of the fine lenticular array, the diffraction orders become five times more closely spaced.

A simple way of increasing the period of the array is to vary the lenticule height, keeping the shape and spacing constant. For example, a sequence of five different heights, repeated across the array yields a five-fold increase in period. In the parlance of diffraction grating theory, height variation is superior to spacing variation because spacing variation alone allows a strong zeroth order, or "central image", to remain, while height variation allows its control along with the other orders.

The multiply periodic lenticular array thus fashioned can be thought of as a superposition of five identical lenticular

gratings, each of period 5 w as shown in Fig. B1. Each grating is suitably displaced both along z and along the normal. The spacing of lenticules is uniformly w and we neglect the small differences in lenticule width. To simplify the analysis, we treat the case of a one-dimensional grating with normally incident light, under Fraunhofer conditions. That is, the incident light is collimated and the diffracted light is observed in the focal plane of a lens placed near the grating.

In Fig. B2 are illustrated the optical paths traversed by rays refracted at the same angle θ at corresponding positions of two lenticules separated by a distance mw. The difference in optical path is given by

$$\Delta p_m = \frac{mw}{\cos \alpha} \sin \beta + n a_m, \text{ which reduces to}$$
$$\Delta p_m = mw \sin \theta + (n - \cos \theta)\, a_m \qquad (1)$$

where n is the refractive index of the lenticular material with respect to air, a_m is the difference in lenticule height, and m = 0, 1, 2, 3, 4. The phase difference is then

$$\varphi_m = \frac{2\pi}{\lambda} \left[mw \sin \theta + (n - \cos \theta)\, a_m \right] \text{ radians.} \qquad (2)$$

The 0th lenticule of Figure B2 is one element of a 0th grating of period 5 w and the mth lenticule is one element of an mth order grating of period 5 w. The path difference given by Eq. (1) applies also to the entire 0th and mth gratings. For a given value of θ, the mth grating amplitude transmission

function can be represented by

$$T_m(z) = \sum_{q=-\infty}^{\infty} \delta\ (z - 5wq) \quad , \tag{3}$$

which is a good approximation when many lenticules are included. The amplitude distribution in the mth diffraction pattern is

$$A_m(y) = \int_{-\infty}^{\infty} T_m(z)\ e^{-2\pi iyz}\ dz$$

$$= \frac{1}{5w} \sum_{q=-\infty}^{\infty} \delta\ (y - \frac{q}{5w}) \quad , \tag{4}$$

$$\text{where } y = \frac{\sin\theta}{\lambda} \quad . \tag{5}$$

The resultant amplitude distribution for all 5 gratings is the sum, with appropriate phase shifts from Eq. (2):

$$A(y) = \sum_{m=o}^{4} A_m(y)\ e^{-i\varphi_m} \tag{6}$$

Since $A_m(y)$ is the same for all m, this can be written

$$A(y) = A_m(y)\ B(y) \quad , \tag{7}$$

$$\text{where } B(y) = \sum_{m=o}^{4} e^{-i\varphi_m} \quad . \tag{8}$$

The dirac comb $A_m(y)$ results from the periodicity of the gratings and restricts the pattern to the discrete directions satisfying $y = q/5w$. The phase differences then become

$$\varphi_m = 2\pi \left[\frac{mq}{5} + (n - \cos\theta)\ \frac{A_m}{\lambda} \right] \quad . \tag{9}$$

The calculation of the relative amplitude for a given angle θ amounts to the evaluation of $|B(y)|$ for $y = \frac{\sin \theta}{\lambda} = q/5w$, using phases given by Eq. (9). The relative intensity is then proportional to $|B(y)|^2$ multiplied by the geometrical optics intensity envelope provided by goniophotometer measurements. Obviously this analysis can be applied to any periodicity desired. Conveniently, a computer program can be written to evaluate $|B(y)|^2$. This evaluation can be performed as a function of wavelength to determine color effects. Generally equal intensity for all diffraction orders and little variation with wavelength is desired.

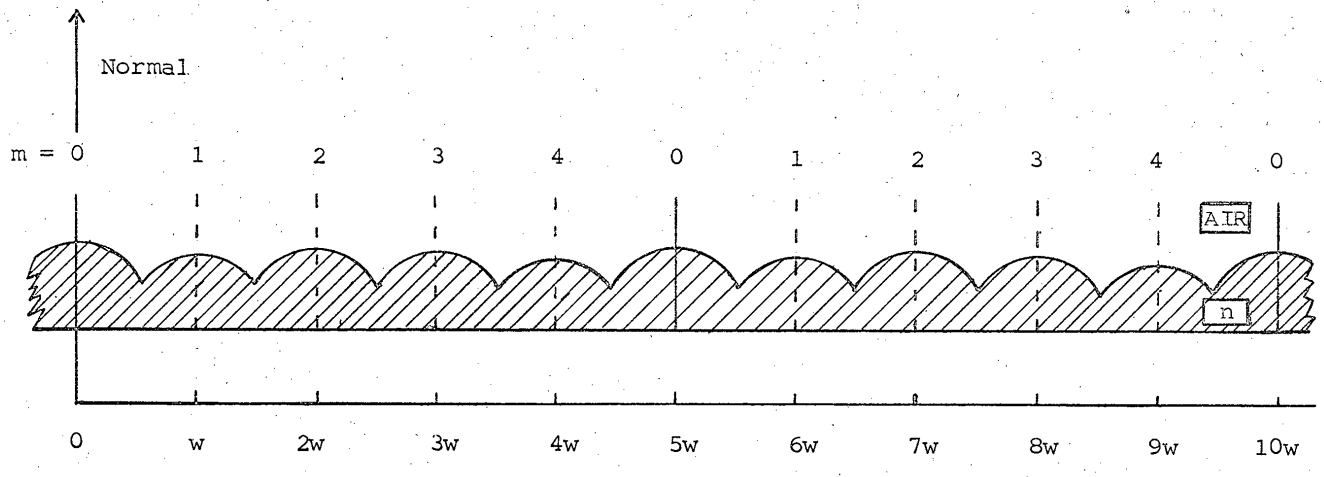

Figure B1. Cross section of multiply periodic cylindrical lenticular array. Height variations exaggerated.

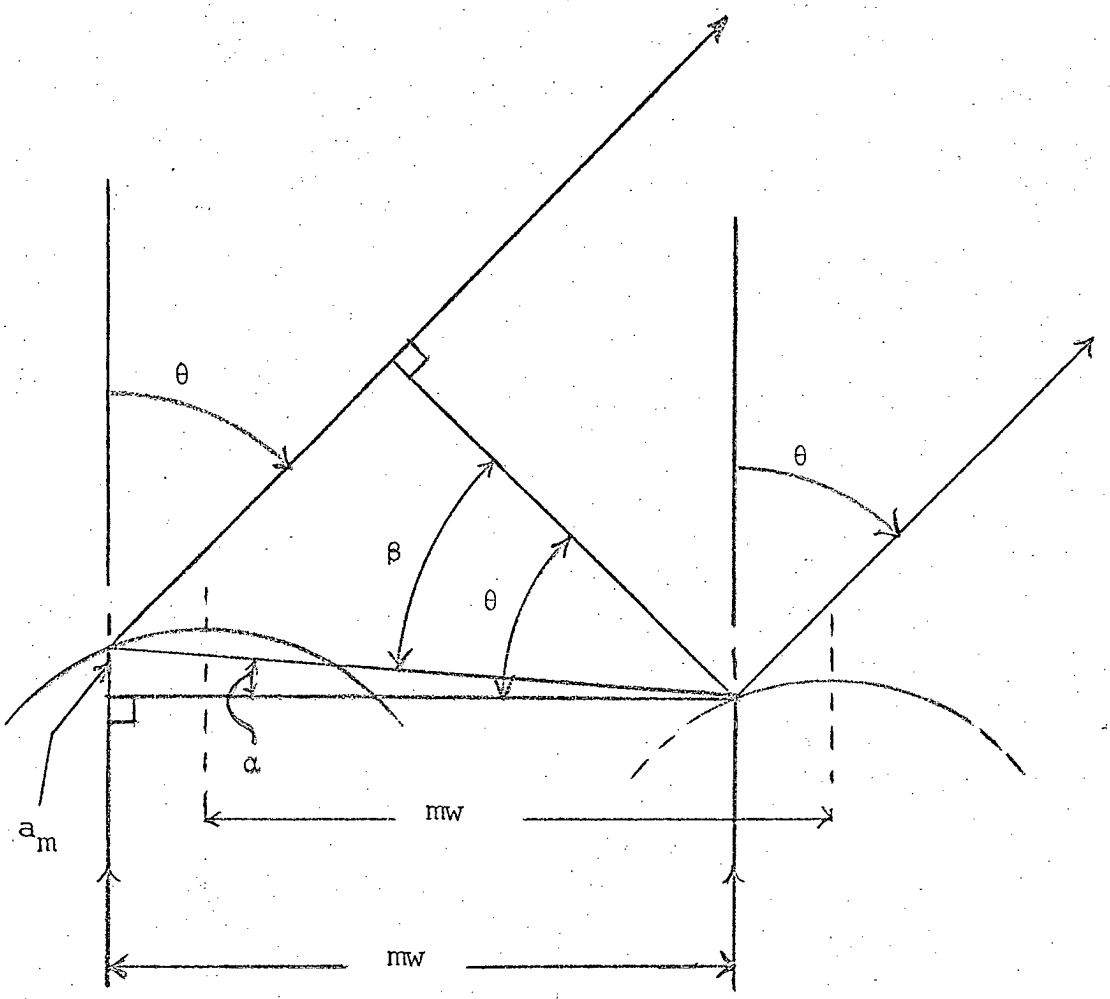

Figure B2. Geometry for determining optical path differences between 0th and mth lenticules.